MOLECULAR CHARACTERIZATION OF PHOTORECEPTOR PERIPHERIN-2 AND ROM-1 COMPLEXES AND ROLE IN DISC MORPHOGENESIS AND RETINAL DEGENERATION

by

Christopher Jereme Ronald Loewen

B.Sc. (Honours), University of British Columbia, 1995

A THESIS SUBMITTED IN PARTIAL FULFILLMENT OF

THE REQUIREMENTS FOR THE DEGREE

Doctor of Philosophy

in

THE FACULTY OF GRADUATE STUDIES

Department of Biochemistry and Molecular Biology

We accept this thesis as conforming

To the required standard

THE UNIVERSITY OF BRITISH COLUMBIA

July 2001

In presenting this thesis in partial fulfilment of the requirements for an advanced degree at the University of British Columbia, I agree that the Library shall make it freely available for reference and study. I further agree that permission for extensive copying of this thesis for scholarly purposes may be granted by the head of my department or by his or her representatives. It is understood that copying or publication of this thesis for financial gain shall not be allowed without my written permission.

Department of Biochemistry & Molecular Biology

The University of British Columbia
Vancouver, Canada

Date Sept 20, 2001

ABSTRACT

Peripherin-2 and rom-1 are homologous integral membrane proteins of the tetraspanin superfamily that form multisubunit complexes in the rims of photoreceptor outer segment discs. Peripherin-2 is critical for formation and maintenance of rod and cone discs, while rom-1 is involved in regulation of this process. Mutations in peripherin-2 cause various forms of human retinal degeneration including retinitis pigmentosa (RP) and macular degeneration (MD). Peripherin-2 and rom-1 contain seven highly conserved cysteines in the intradiscal loop region, two of which in peripherin-2 are linked to RP.

Each of these cysteines in peripherin-2 has been individually replaced by serine to determine its role in folding and subunit assembly. Six of the seven conserved cysteine residues in the intradiscal loop of peripherin-2 are essential for proper core tetramer formation with rom-1. They likely constitute three intramolecular disulfide bonds crucial to the proper folding of the subunits. Mutations at C165 and C214 cause RP. The remaining cysteine, C150, is not involved in tetramer formation, but is solely responsible for disulfide-mediated oligomerization of tetramers into higher order complexes. Core tetramer formation is required for disulfide-mediated oligomerization and for targeting to rod outer segments. RP-causing mutations in peripherin-2 prevent tetramer and higher-order oligomer formation and cause mistargeting to rod inner

segments. Disulfide-mediated oligomerization plays a role in disc rim and incisure formation and involves both noncovalent and covalent (disulfide bonds) interactions. Rom-1 functions in the regulation of disulfide-mediated oligomerization by inhibiting disulfide-linking of tetramers. Human RP caused by mutations in peripherin-2 results from (1) having decreased levels of protein in the outer segments, and (2) by interference with the function of WT protein in outer segments in a dominant-negative manner.

TABLE OF CONTENTS

LIST OF TABLES

LIST OF FIGURES

LIST OF ABBREVIATIONS

ADRP .....autosomal dominant retinitis pigmentosa

AMD .....age-related macular dystrophy

ARRP .....autosomal recessive retinitis pigmentosa

BEM.....Bull's-eye maculopathy

BME.....β-mercaptoethanol

bp .....base pairs

BPD .....butterfly-shaped pigment dystrophy

BSA .....bovine serum albumin

c .....conserved

C2-3 .....cytoplasmic loop joining transmembrane segments 2 and 3

CaM.....calmodulin

cc.....connecting cilium

CD.....cone dystrophy

cDNA .....DNA reverse transcribed from an mRNA template (coding DNA)

cGMP .....guanosine 3′,5′ –cyclic monophosphate

CRD.....cone-rod dystrophy

CSNB .....congenital stationary night blindness

del.....deletion

DNA.....deoxyribonucleic acid

dpf .....days post fertilization

DTT .....dithiothreitol

ECL.....enhanced chemiluminescence

EM.....electron microscopy

EMBL .....European Molecular Biology Laboratory

ER .....endoplasmic reticulum

ERG .....electroretinogram

Fs.....frameshift

FTIR .....Fourier transform infrared spectroscopy

GAP .....GTPase activating protein

GARP .....glutamic acid rich protein

GC.....guanylate cyclase

GCAP .....guanylate cyclase activating protein

GDP.....guanosine 3′-diphosphate

GFP .....green fluorescent protein

GST .....glutathione S-transferase

GTP .....guanosine 3′-triphosphate

Ig.....immunoglobulin

IS.....inner segment

kDa .....kilodalton

l.....lens

L1-2 .....intradiscal loop joining transmembrane segments 1 and 2

L3-4 .....intradiscal loop between transmembrane segments 3 and 4

LCA .....Leber's congenital amaurosis

LUV .....large unilamellar vesicle

M II .....metarhodopsin II

M1.....transmembrane segment 1

M2.....transmembrane segment 2

M3.....transmembrane segment 3

M4.....transmembrane segment 4

MAb.....monoclonal antibody

MBP.....maltose binding protein

MD .....macular dystrophy

mi .....mitochondrion

M_r.....relative molecular weight

mRNA .....messenger RNA

n.....nucleus

nc.....nonconserved

NEM.....N-ethyl maleimide

OS.....outer segment

PAGE .....polyacrylamide gel electrophoresis

PBS .....phosphate buffered saline

PCR .....polymerase chain reaction

PD.....pattern dystrophy

PDE .....phosphodiesterase

PDI.....protein disulfide isomerase

phag.....phagosomes

PMSF .....phenyl methyl sulfonyl fluoride

pp .....pseudopodia

r.....retina

RCD.....rod-cone dystrophy

rds .....retinal degeneration slow

REMI.....restriction endonuclease mediated integration

RK.....rhodopsin kinase

RNA.....ribonucleic acid

ROS.....rod outer segment

RP .....retinitis pigmentosa

RPA .....retinitis punctata albescens

RPE .....retinal pigment epithelium

S.....Svedberg ($\times 10^{-13}$ s)

$s_{20,w}$.....standardized velocity sedimentation coefficient

SDS.....sodium dodecyl sulfate

stop.....stop codon

T.....transducin

TM4SF.....transmembrane four superfamily

TR .....Texas red

Tris.....Tris [hydroxymethyl]aminomethane

w/w.....weight per weight

WGA.....wheat germ agglutinin

WT.....wild type

ACKNOWLEDGEMENTS

I would like to give my sincerest gratitude to Bob Molday for his excellent supervision throughout the course of my PhD and for allowing his lab to be such a dynamic and enjoyable place to work. I remember one of the first things you said to me, Bob, as a young man of twenty thinking about a career in science, during that first interview. It was that science is not a nine-to-five job and that hard work is not necessarily a substitute for smart work. Taking that to heart I set my work schedule, ten to three, always keeping in mind how clever my experiments were. Alas, I learned soon enough that what you really meant was that science is *at least* a nine-to-five job. I'm glad I figured it out (and just in time) because here I am today, a PhD. Nevertheless, it has been a truly great experience. A little advice from a fellow PhD, if you're still giving that speech to students like me – stress the *at least* part! It will certainly do them some good! Thanks Bob, you have been a great mentor.

...and of course my thanks go to the rest of the Molday lab, past and present, for keeping things interesting, to say the least. I apologize (again) for the dishes, the timer, and the Ramones (Laurie). It has been a pleasure working with all of you. I want to especially thank Andy Goldberg and Orson Moritz for their guidance and patience and for all the effort they put into this project. We've had a lot of fun. A big thank you to Laurie Molday for doing so much (everything) to keep the lab running smoothly and for teaching me many of the techniques I know today. Also thanks to Jinhi Ahn, my papers and thesis have far fewer typographical and grammatical errors – thank you.

I would like to thank my friends and family, who have been and will continue to be a large force in my life, for all their support. You know who you are. So many wonderful people, I'm glad we could all meet (likely at 1846 W12th Ave.). I want to especially thank my parents, Agnes, Gary, and Paul, and my siblings Simone, Shane, and Nicole, for giving love and encouragement along the way, and for always remembering to ask, "So are you still working on those eyeballs?". Yes.

Lastly, to my beautiful wife Sarah, I dedicate this thesis. You have given me unconditional love and support, and for that you have my heart. Grow old along with me, the best is yet to be. Thank you for everything my love, you are an inspiration.

CHAPTER 1 - INTRODUCTION

1.1 THE EYE

The vertebrate eye is a sophisticated optical device designed by evolution over millions of years. It functions to project and focus the images from our universe onto a delicate disc of neural tissue called the retina (**Fig 1**). Light focused by the lens onto the retina at the back of the eye is captured chemically by the rod and cone photoreceptors. The vertebrate retina consists of three layers of cells and two layers of synapses (**Fig 1**). The photoreceptors transmit their information (colour, intensity, contrast) to the bipolar, amacrine, and horizontal cells of the inner retina. These cells integrate the signals from the entire retina and transmit them to the ganglion cells which comprise the optic nerve. As many as fifty photoreceptors can synapse with a single bipolar cell in the complex process of image coding. A single ganglion cell can receive input from up to 75,000 rod photoreceptors. It is then the responsibility of the visual cortex of the brain to decode these integrated signals and recreate the image originally focused on the retina (reviewed by Kolb, 1994).

1.1.1 Rod and cone photoreceptors

The two major classes of photoreceptors, rods and cones, are responsible for vision in dim light and colour vision, respectively. There

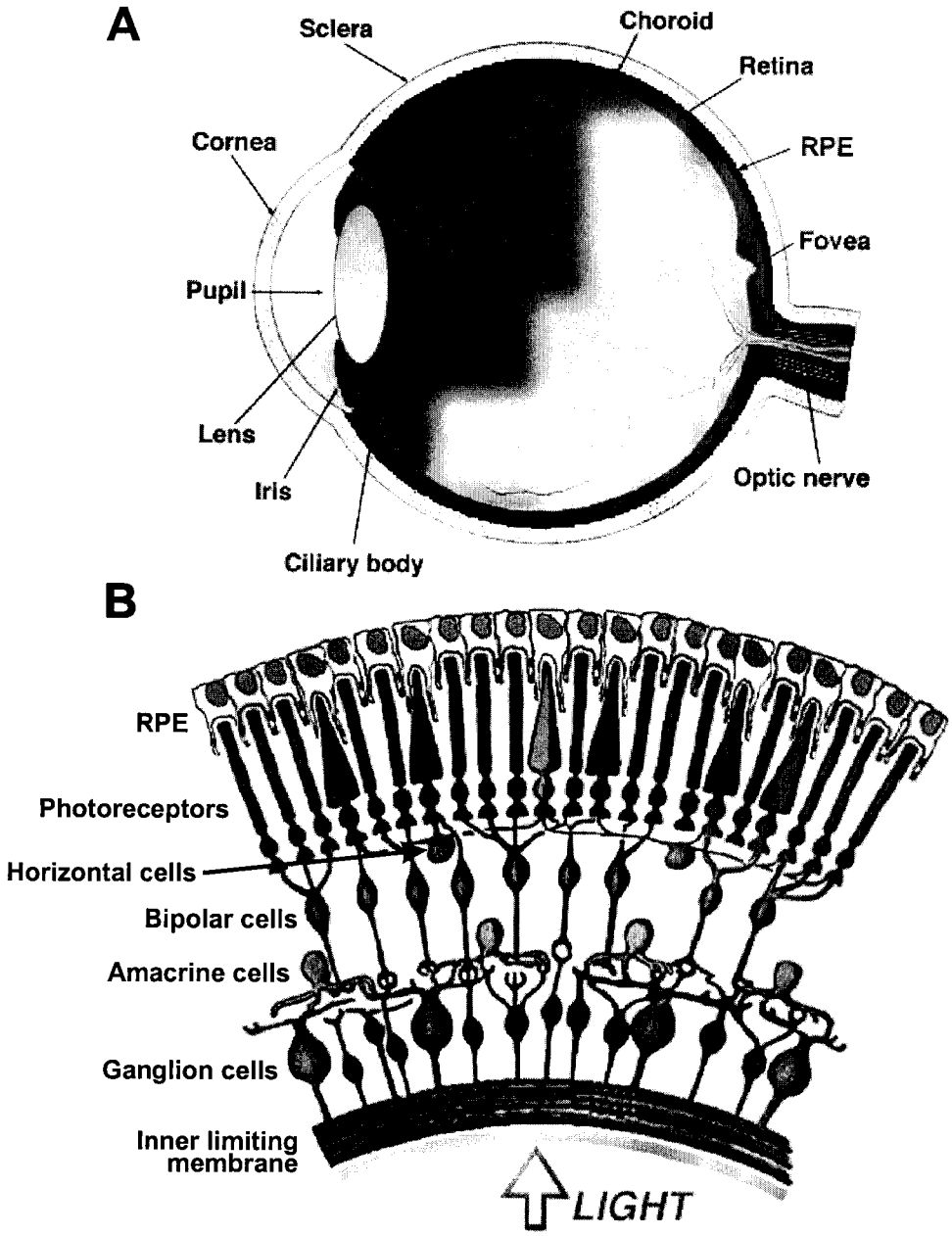

Fig 1. **Structure of the vertebrate eye and retina.** (A) Light enters the eye by passing through the transparent tissue called the cornea and is focused by the lens onto the retina at the back of the eye. There, the photoreceptor cells detect the light and transmit a signal via the optic nerve to the brain. The choroid, the vascular layer which provides nutrients to the retina, lies adjacent to the sclera, a hard protective outer layer, and the retinal pigment epithelium (RPE) which is in intimate contact with the photoreceptors. (B) The RPE is responsible for maintenance of the rod (dark blue) and cone (red, green, and blue) photoreceptors which comprise the outer nuclear layer. Photoreceptors synapse with the neurons of the inner nuclear layer (horizontal, bipolar, and amacrine cells) which in turn synapse with ganglion cells whose axons comprise the optic nerve. Modified from Webvision (www.webvision.med.utah.edu).

are three sub-classes of cones in humans that respond to red, green and blue wavelengths of light. Rods dominate the peripheral retina and are absent in the fovea, a small region of the central retina which is the focal point of the lens. Cones are thinly dispersed throughout the peripheral retina and are concentrated in the fovea, which is responsible for high visual acuity. The ratio of rods to cones in the human retina is 20:1 (Osterberg, 1935).

Although rods and cones vary in shape and size (and are hence called rods and cones), they have a similar cellular organization. They contain a synaptic terminal, cell body, inner segment, and outer segment region (**Fig 2**). The outer segment contains 500 - 2000 membraneous discs that are separate from the plasma membrane in rods but continuous with the plasma membrane in cones. Discs are comprised of rim and lamellar regions, each of which has its own complement of proteins. In rods, large invaginations of the disc rim produce incisures which align with the long axis of the photoreceptor. The number of incisures varies from species to species. The opsin photopigments are located in the lamellar regions. The outer segment is supported by the connecting cilium, which isolates it from the mitochondria, Golgi, and endoplasmic reticulum of the inner segment. The cell body contains the nucleus, and the synaptic terminus is the site of glutamate release and nerve transmission (reviewed by Massey & Maguire, 1995).

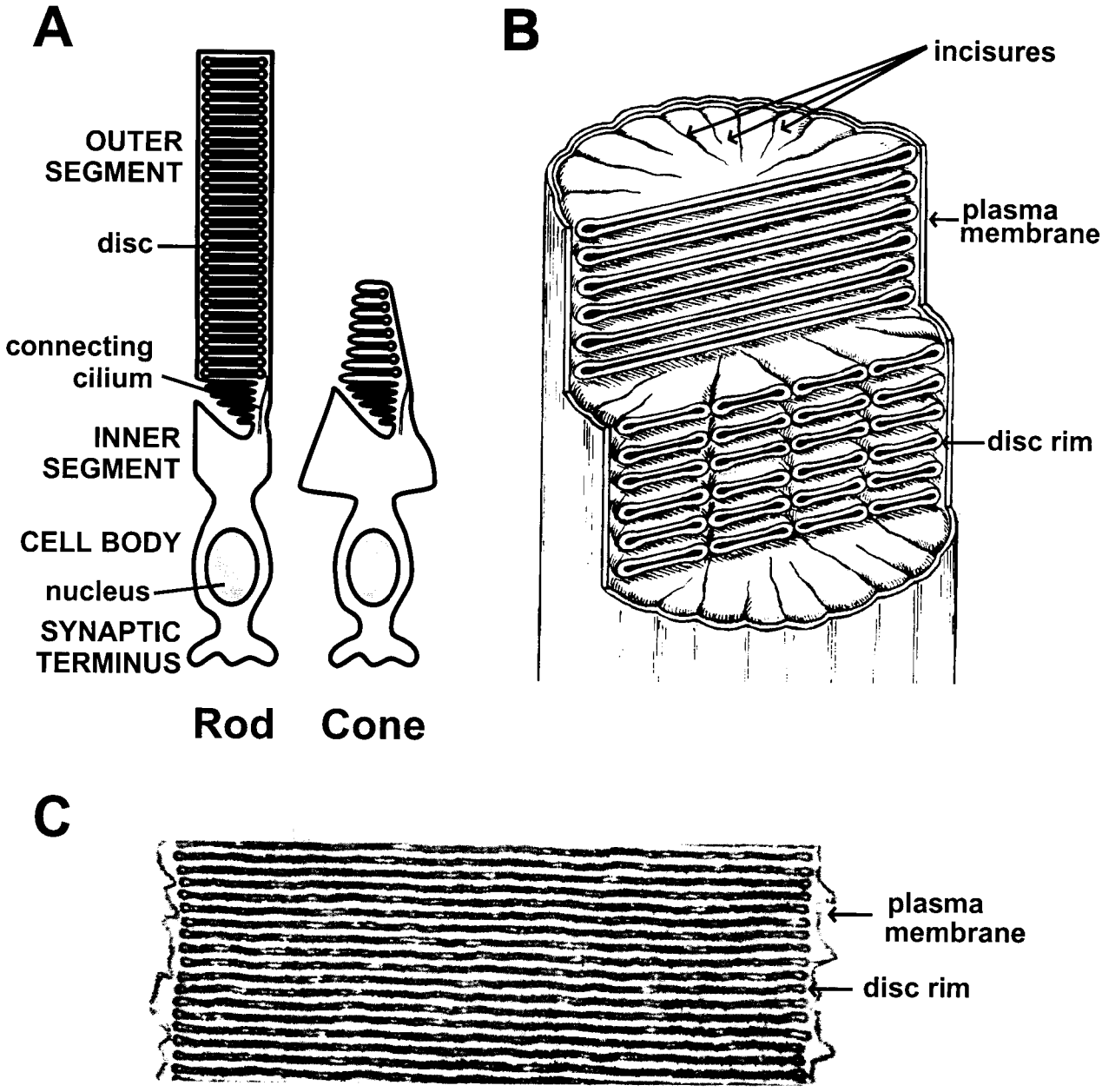

Fig 2. **Vertebrate photoreceptor cells.** (A) Rod and cone neurons are comprised of an outer segment which contains a stack of membranous discs. These discs are separate from the plasma membrane in rods and continuous with it in cones. The outer segment is separated from the inner segment by a non-motile connecting cilium. The inner segment contains the organelles, the cell body contains the nucleus, and the synaptic terminus is the site of neurotransmitter release and signalling. (B) Diagram of a frog rod outer segment illustrating the shape and organization of discs and the presence of incisures. (C) Electron micrograph of a longitudinal section of a rhesus monkey rod outer segment; X 75,600. Modified from Dose (1996) (A); Steinberg (1980) (B&C).

1.1.2 Phototransduction

Phototransduction occurs in the outer segments of rod and cone cells (**Fig 3**). In rods it begins when a photon of light isomerizes the 11-*cis*-retinal chromophore of rhodopsin to its *all-trans* isomer. This leads to a conformational change in rhodopsin and the production of metarhodopsin II (M II) (reviewed by Koch, 1995; Palczewski, 1994; Polans, Baehr & Palczewski, 1996; Pugh & Lamb, 1993). This signal is amplified through the activation of the G-protein transducin ($T_{\alpha\beta\gamma}$), which exchanges bound GDP for GTP and dissociates into T_α and $T_{\beta\gamma}$ subunits. A single metarhodopsin II molecule can activate between 100 and 500 molecules of transducin (Gray-Keller, Biernbaum & Bownds, 1990). The activated T_α subunit binds phosphodiesterase (PDE) stoichiometrically and stimulates the conversion of cGMP to GMP. One activated PDE-T_α complex can catalyze the hydrolysis of up to 1000 cGMP molecules resulting in an amplification of $1 - 5 \times 10^5$ molecules of cGMP per second per rhodopsin molecule (Yee & Liebman, 1978). Decreased levels of cGMP result in closing of the cGMP-gated channels and reduced conductance of the plasma membrane to sodium and calcium. The hyperpolarization of the cell results in the inhibition of neurotransmitter (glutamate) release at the synaptic terminal.

Mechanisms exist to reset the photoreceptors to allow for a fast physiological response to light. Active metarhodopsin II is inactivated by

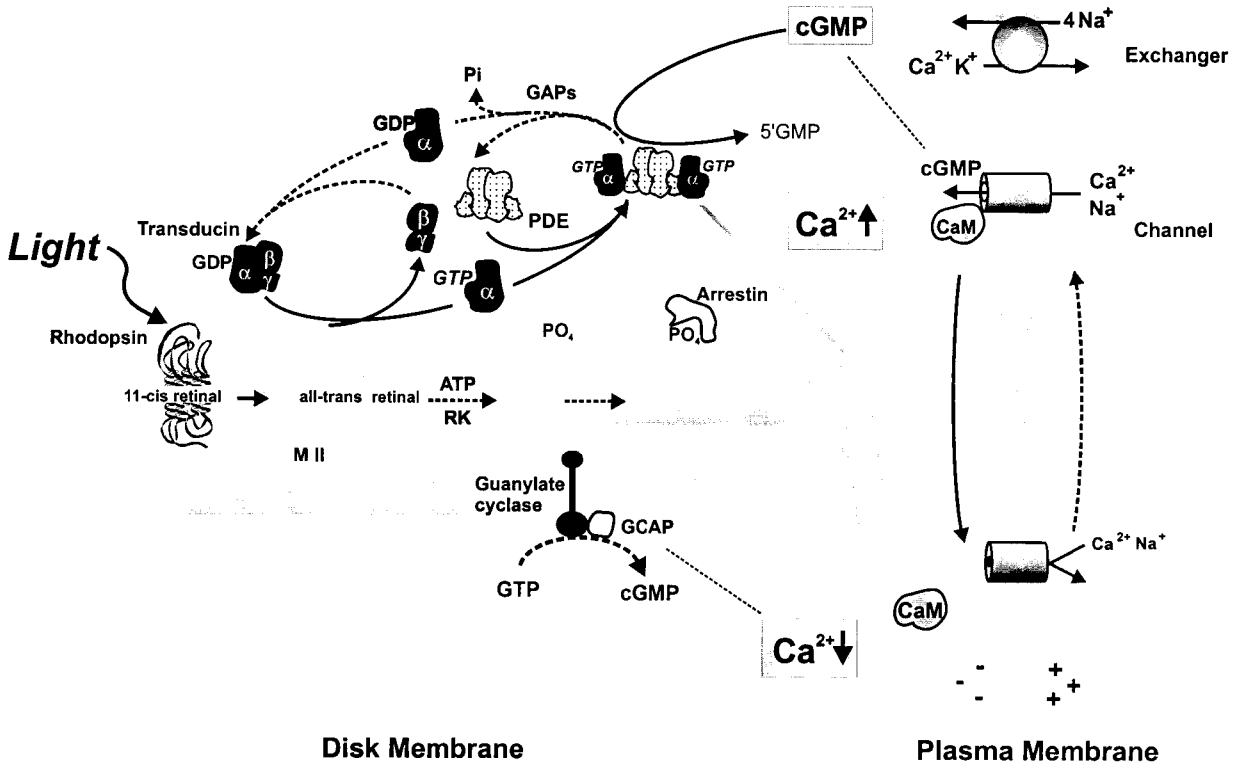

Fig 3. **Phototransduction.** Light initiates the isomerization of 11-*cis* retinal to all-*trans* retinal which converts rhodopsin into the activated metarhodopsin II state (M II). Transducin exchanges bound GDP for GTP and Tα activates PDE which converts cGMP to GMP. Decreased levels of cGMP result in closing of the channel and hyperpolarization of the rod cell. Photorecovery is initiated by shutting off the visual cascade by (1) phosphorylation of rhodopsin and binding of arrestin, (2) GAP assisted hydrolysis of GTP by Tα and dissociation from PDE, and (3) reassociation of Tα with Tβγ to form the inactivated transducin heterotrimer. Low intracellular calcium resulting from channel closure leads to (1) GCAP assisted activation of guanylate cyclase and an increase in cGMP concentration, (2) dissociation of calmodulin (CaM) from the channel and increased channel sensitivity to cGMP. As cGMP levels increase, the channels reopen and the rod cell is returned to the depolarized state. The increase in calcium results in inactivation of guanylate cyclase and dephosphorylation of rhodopsin. *Solid arrows* show the photoexcitation process and *dashed arrows* show the photorecovery process. Modified from Molday (1998).

rhodopsin kinase (RK) catalyzed phosphorylation and the subsequent binding of arrestin. This reaction in turn is regulated by calcium concentrations through the interaction of RK with the calcium-activated protein recoverin. The all-*trans*-retinal chromophore is reduced to all-*trans*-retinol by retinal dehydrogenase and is released from the inactive phosphorylated rhodopsin. This prevents the binding of transducin, RK, or arrestin to opsin. Rhodopsin is regenerated upon dephosphorylation by protein phosphatase 2A and rebinding of 11-*cis*-retinal.

The stimulation of PDE by T_α is regulated by the intrinsic GTPase activity of T_α and by GTPase-activating proteins (GAPs). Binding of T_α to PDE or GAPs significantly increases its intrinsic GTPase activity and results in the hydrolysis of GTP, dissociation from PDE, and rebinding of $T_{\beta\gamma}$. Transducin and PDE are returned to their resting states and are ready for subsequent activation.

Photoactivation results in a decrease in intracellular calcium. The closing of the cGMP channels due to low levels of cGMP prevents the influx of calcium into the outer segment. A Na/Ca-K exchanger however, continues to extrude calcium from the cell resulting in a decrease in calcium from 500 to 50 nM. The enzyme guanylate cyclase (GC), which is inactive at high calcium concentrations (dark state), is activated by guanylate cyclase activating proteins (GCAPs) in low calcium. GCAPs are calcium binding proteins that activate GC in their unliganded state.

Guanylate cyclase converts GTP into cGMP thereby increasing the level of cGMP in the cell. This in turn reopens the channels and restores the resting membrane potential. The cGMP-gated channel is also regulated by the calcium-binding protein calmodulin (Hsu & Molday, 1993). In low calcium concentrations (and low cGMP concentrations), calmodulin dissociates from the channel. This increases the apparent affinity of the channel for cGMP and allows it to open at low cGMP concentrations. These concerted effects result in the fast recovery of the cell to the dark state and cessation of the neural signal.

1.1.3 Disc morphogenesis and shedding

Rod and cone photoreceptors continually renew the photosensitive membranes of their outer segments (Young, 1976). Completely new outer segments are generated on average every ten days at a rate of one hundred discs per day or maximally one new disc every 9 min (Besharse & Defoe, 1998; Besharse, Hollyfield & Rayborn, 1977). Disc morphogenesis occurs at the base or proximal end of the outer segment and discs migrate distally towards the tip where disc shedding and phagocytosis by the retinal pigment epithelium (RPE) occurs. A close relationship exists between disc morphogenesis and shedding that is dependent upon the intimate interaction of the RPE with the photoreceptors (Kaplan, Iwata & Sterrett, 1990). A single rat RPE cell

can phagocytize as many as 30,000 discs per day, a prodigious effort. Generally, disc shedding is a diurnal process that occurs at the onset of light after a period of darkness and involves the actions of melatonin, dopamine, and a photoreceptor circadian clock (Besharse & Defoe, 1998).

Why then do photoreceptors and RPE cells expend so much energy on membrane synthesis and renewal? It has been known since antiquity, in Plato's Phaedo, that Socrates advised against staring directly into the sun because of acute light damage to the eye (Duke-Elder, 1954). In fact, damage to the photoreceptors and RPE cells of the retina by acute and chronic light exposure has been shown to occur in animal models and varies with wavelength (Lanum, 1978; Oranisciak & Winkler, 1994; Reme *et al.*, 1998). There is also a positive correlation between light exposure and the occurrence of age-related macular degeneration in humans, the most common form of blindness in the elderly (Cruickshanks, Klein & Klein, 1993; Taylor *et al.*, 1990; Taylor *et al.*, 1992). Very recently, it has been shown for the first time that light causes retinal-catalyzed photo-oxidation and aggregation of a number of photoreceptor disc proteins including ABCR, peripherin-2 and rom-1 (Sun & Nathans, 2001), thus providing a molecular rationale for light damage. It therefore seems quite clear that outer segment membranes and their constituent proteins are highly susceptible to light-damage and must be rapidly regenerated to maintain proper vision.

An elegant model for the mechanism of vertebrate disc morphogenesis has been proposed based on electron microscopic observations of rods and cones in the rhesus monkey and squirrel (Steinberg, Fisher & Anderson, 1980). At the base of the outer segment adjacent to the connecting cilium, membraneous evaginations occur in a sequential manner growing radially as they are displaced distally along the outer segment (**Fig 4**). A second process, rim formation, is initiated at nodes between evaginations on the connecting cilium and proceeds outward along the plane of the disc circumscribing it. At the opposite end of the disc to the connecting cilium, a membrane fusion event occurs in rods that seals the disc and separates it from the plasma membrane. The precise molecular mechanisms of disc morphogenesis have yet to be determined, however. Studies examining the effects of cytochalasin D on disc morphogenesis have revealed that membrane evagination and disc formation are dependent on the activity of filamentous actin in the cilium, but disc displacement is not (Hale, Fisher & Matsumoto, 1996; Kaplan, 1998). Breaking the photoreceptor RPE cell contact by retinal detachment also prevents membrane evagination and disc formation, but not displacement (Hale, Fisher & Matsumoto, 1991; Kaplan, Iwata & Sterrett, 1990). This suggests that displacement of discs towards the RPE is an active process independent of disc formation. A role for microtubules in disc displacement has been suggested. Also, membrane-

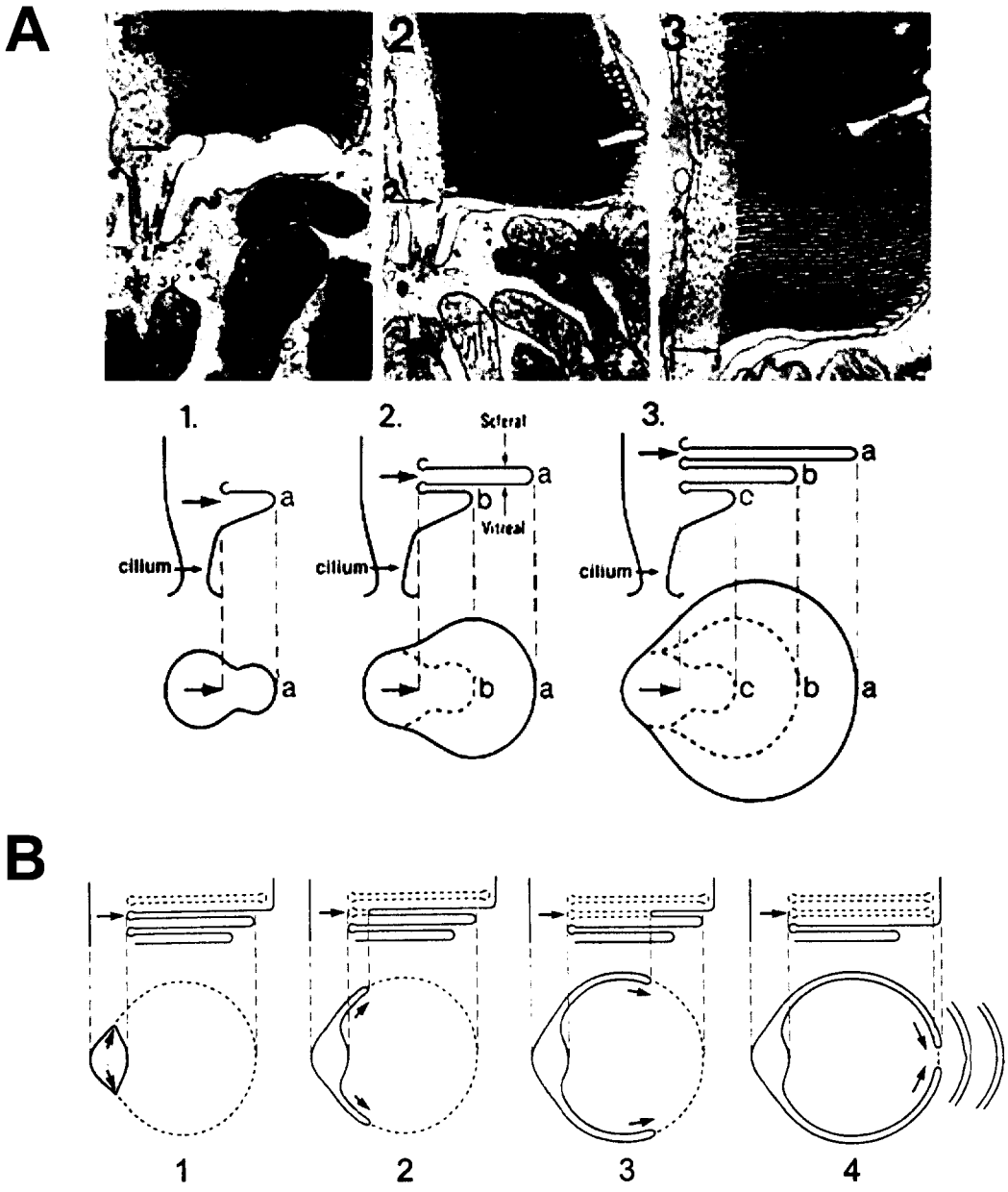

Fig 4. **Disc morphogenesis.** (A) The sequence of membrane evagination as observed by electron microscopy and in diagram. The continuous process of budding and displacement results in a steady supply of nascent discs to the rim forming region. (B) A diagram of rim formation illustrating discs in both longitudinal and cross section. The rim forming region (1) between the vitreal and scleral faces of nascent discs grows outward (2-3) around the circumference of the disc. Meeting of the two sides of the growing rim (4) results in membrane fusion and separation of the disc from the plasma membrane. Modified from Steinberg (1980).

impermeable sulfhydryl modifying reagents inhibit disc formation and suggest a role for disulfide bonding in disc morphogenesis (Wetzel, Parsons & Besharse, 1994).

The current model for disc shedding and phagocytosis involves two inter-related processes (Besharse & Defoe, 1998). Discs located near the distal tip of the outer segment in close contact with the RPE undergo membrane fusion events presumably with the plasma membrane. This culminates in the shedding of packets of discs (**Fig 5**). At the same time, actin-filled processes from RPE cells called pseudopodia penetrate into the outer segment in regions of fusion and engulf the disc packets. What follows is a sequence of ingestion and digestion of the ROS membranes within the RPE cell and the recycling of some of the membrane components, including retinal and docosahexanoic acid, to the photoreceptor. It is unclear at the present time which of these cells initiates this process since both disc shedding and phagocytosis seem to occur concomitantly. Because RPE cells in contact with photoreceptors do not constitutively phagocytize discs, and photoreceptors in contact with RPE cells defective for pseudopodia outgrowth do not undergo shedding, there must be a delicate interplay governing initiation of these processes. During disc shedding, adhesion between RPE and photoreceptor cells is significantly increased. It is unclear what receptors are responsible for this, but there is evidence for roles of an F_c -immunoglobulin receptor

A

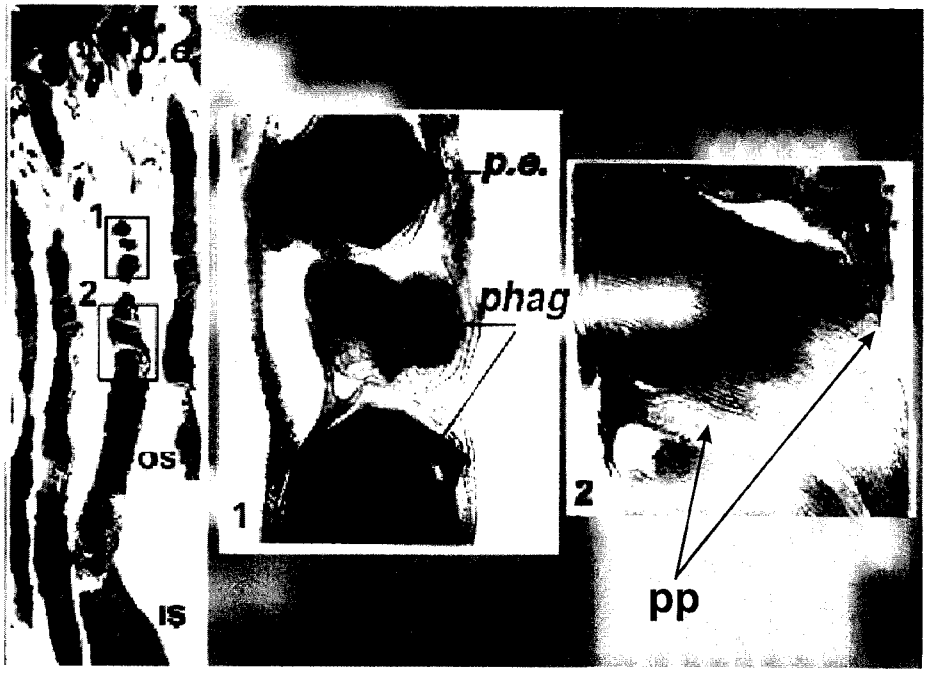

B

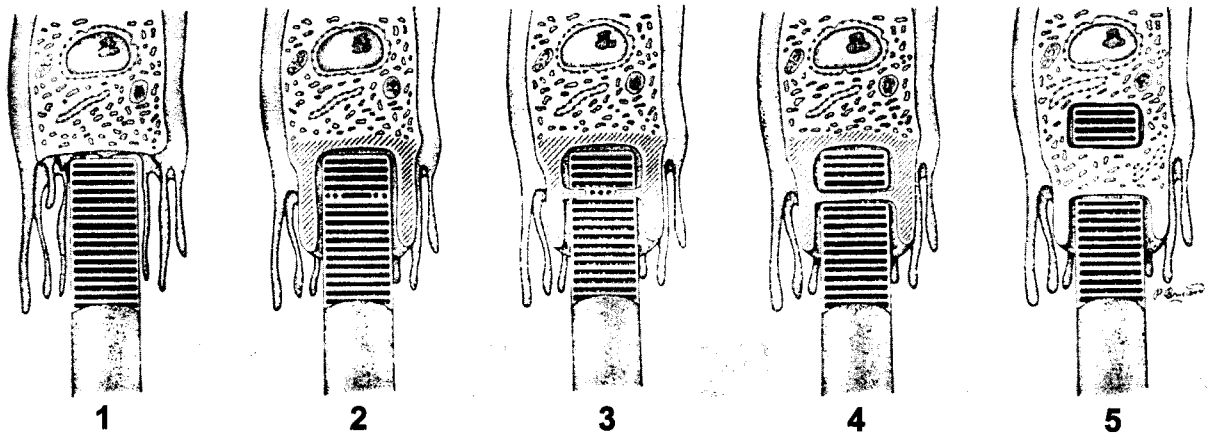

Fig 5. **Disc shedding and phagocytosis.** (A) Electron micrographs of rod photoreceptors showing (1) RPE phagosomes (phag) containing discs and (2) penetration of the outer segment by pseudopodia (pp) of the RPE (IS, inner segment; OS, outer segment). (B) Diagram of the events occuring in phagocytosis of discs. Initiation of pseudopodia growth occurs concomitantly with photoreceptor disc-plasma membrane fusion (1-2). Penetration of the disc stack (3-4) results in release and internalization of a packet of discs (5) by the RPE. Modified from Steinberg (1977) (A); Matsumoto (1987) (B).

System (Elner *et al.*, 1981; Laird & Molday, 1988), a mannose receptor system (Boyle *et al.*, 1991), and a CD36-integrin receptor system (Ryeom, Sparrow & Silverstein, 1996).

1.2 IDENTIFICATION OF PERIPHERIN-2 AND ROM-1

Peripherin-2 (formerly known as peripherin/rds) and rom-1 are homologous tetraspanning integral membrane proteins that form multisubunit complexes at the rims of rod and cone outer segments discs (Molday, 1998). Roles for these complexes in disc morphogenesis and membrane fusion have been proposed (Arikawa *et al.*, 1992; Boesze-Battaglia *et al.*, 1998; Wrigley *et al.*, 2000). Mutations in peripherin-2 are responsible for autosomal dominant retinal dystrophies (Farrar *et al.*, 1991a).

1.2.1 Initial characterization of peripherin-2

Peripherin-2 was identified using biochemical and immunochemical approaches (Connell & Molday, 1990; Molday, Hicks & Molday, 1987). The protein was first identified on Western blots of bovine ROS using two monoclonal antibodies (Per2B6 and Per3B6) produced in mice immunized with total ROS membranes (Molday, Hicks & Molday, 1987). Since peripherin-2 co-migrates with rhodopsin (approx. 35 kDa) on SDS-PAGE, it was not detected on Coomassie or silver stained gels even though it

constitutes approximately 3% of total ROS membrane protein (Goldberg & Molday, 1996b). Further biochemical analysis of peripherin-2 revealed that it forms disulfide linked dimers and is glycosylated (Connell *et al.*, 1991; Molday, Hicks & Molday, 1987). Coomassie stained SDS gels of purified peripherin-2 showed that it also migrates as a doublet, indicating the possibility of an interaction with another protein. Immunoelectron microscopy of bovine retinas using these monoclonal antibodies (**Fig 6**) showed specific disc rim and incisure labeling similar to what had been observed for a 290 kDa protein from frog photoreceptors (Papermaster *et al.*, 1978). Peripherin was named for its unique location at the periphery of discs. This localization is very different than the localization of rhodopsin along the flattened lamellar region of the disc (Molday, Hicks & Molday, 1987).

Peripherin-2 was cloned by two different laboratories using different approaches. In our lab, a λgt11 expression library was screened with anti-peripherin monoclonal antibodies (Connell & Molday, 1990). The cDNA encodes a protein of 346 amino acids and hydropathy plots predict four transmembrane segments. A large 141 amino acid intradiscal loop connects transmembrane segments three and four and a 60 amino acid C-terminal tail extends from the fourth transmembrane segment (**Fig 7**). The membrane topology was confirmed in-part using the pre-embedding labeling of isolated ROS for analysis by electron microscopy. Labeling

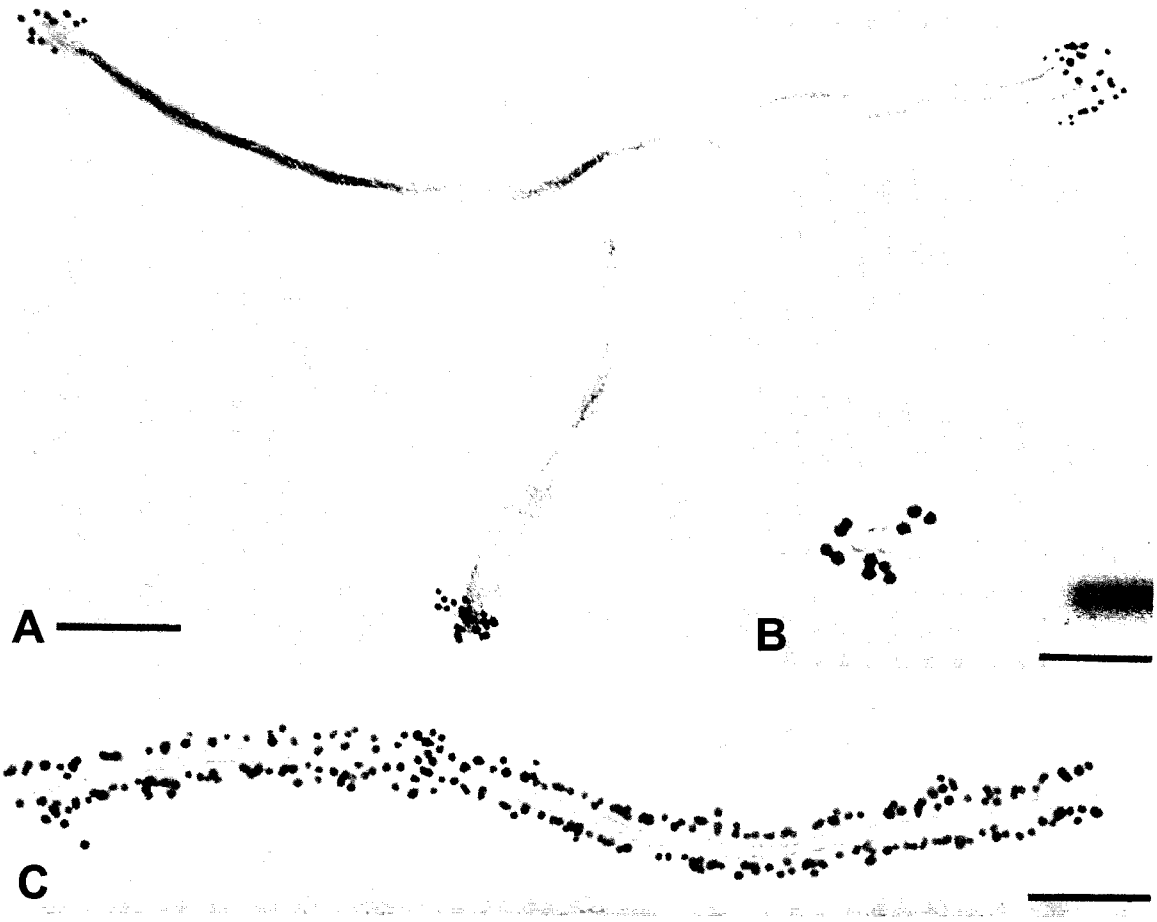

Fig 6. **Immunolocalization of peripherin-2 to the disc rim.** (A&B) Electron micrographs of isolated ROS discs showing immunogold labeling of peripherin-2 specifically at the disc rim. (C) Immunogold labeling of rhodopsin shows lamellar but not rim localization. Bars: A&C = 0.1 μm, B = 0.05 μm. Modified from Molday (1987).

with the Per2B6 monoclonal antibody showed that the epitope contained in the C-terminus was located on the cytoplasmic side of the membrane (Connell & Molday, 1990). Peripherin-2 contains 13 cysteines, six which are not conserved, and seven which are highly conserved among species and with rom-1 (Molday, 1994). All conserved cysteines are located in the intradiscal (extracellular equivalent) loop. A consensus sequence for N-linked glycosylation is also present within the intradiscal loop at N229. No homology with any existing sequences in the EMBL database was found at the time, but peripherin-2 has since been included in the *tetraspanin* family of proteins to which it shares only limited homology.

Using a subtractive genetic approach, Travis et al. (1989) identified the gene defect responsible for the phenotype of the retinal degeneration slow (*rds*) mouse at approximately the same time. The homozygous *rds* mouse is characterized by the absence of rod and cone outer segments and the heterozygous *rds* mouse exhibits whorls of disorganized disc membranes (Sanyal & Jansen, 1981). A slow degeneration of the retina occurs such that after a year only a few photoreceptors remain.

The *RDS* gene was found to be 92.5% identical to bovine peripherin and therefore represents the mouse ortholog (Connell *et al.*, 1991). The same gene appears to encode for peripherin-2 in rods and cones since (1) in the *rds* mouse neither rod nor cone outer segments develop, (2) monoclonal antibodies to the C-terminus of bovine peripherin label both

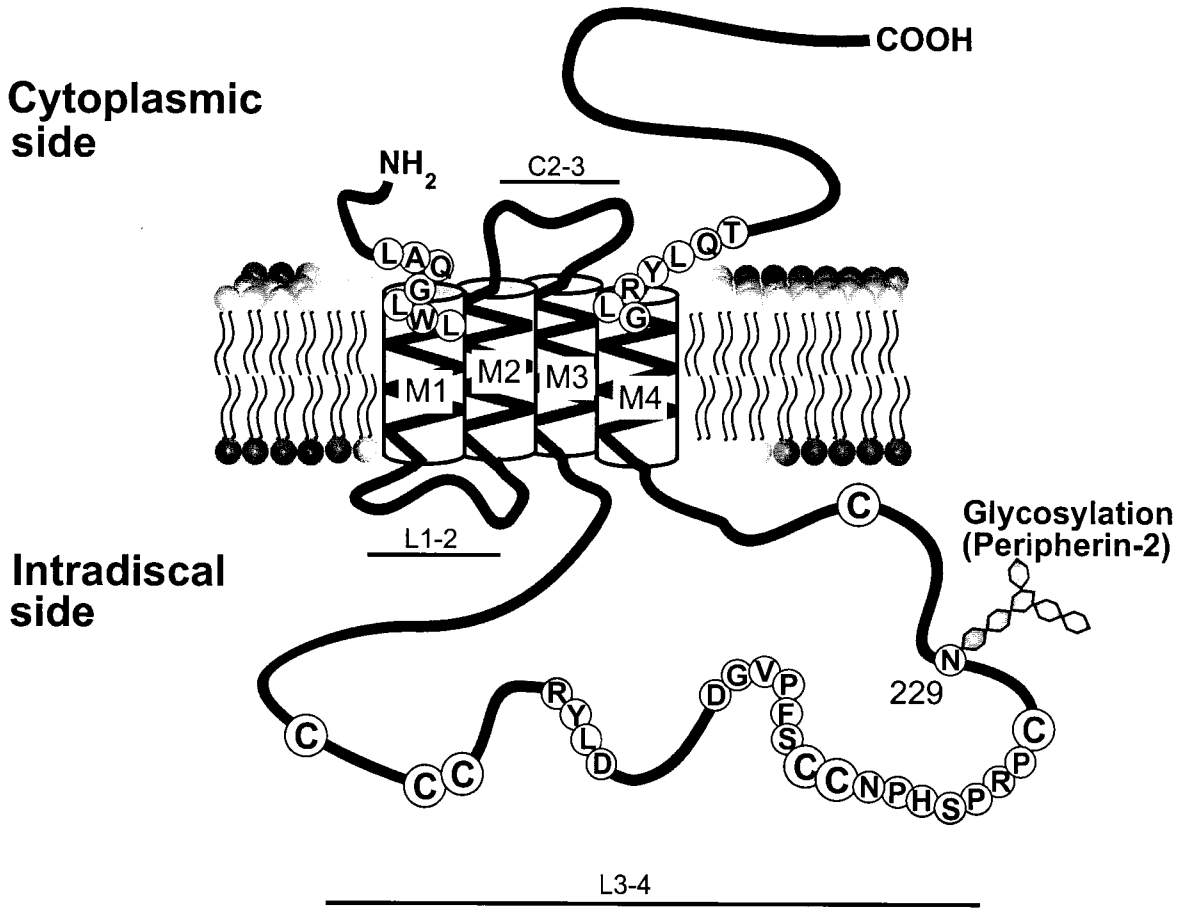

Fig 7. **Topological model for peripherin-2 and rom-1.** Both proteins contain four transmembrane segments (M1-M4), cytoplasmic N and C termini, and a large intradiscal loop (L3-4) of approx. 140 amino acids. Peripherin-2 contains an N-linked oligosaccharide chain (hexagons) that is not present in rom-1. Conserved cysteines and stretches of conserved amino acids between peripherin-2 and rom-1 are indicated. Modified from Molday (1994).

rods and cones (Arikawa *et al.*, 1992), and (3) the cDNA for rod peripherin labels cones by *in situ* hybridization (Uehara *et al.*, 1993). Since these efforts, peripherin-2 orthologs have been identified in human, rat, cat, dog, chicken, and frog, but not in the fruit fly, the worm, or yeast (BLAST search). The human gene has been localized to chromosome 6p12 by in situ hybridization (Travis *et al.*, 1991) and contains three exons (Kajiwara *et al.*, 1991).

1.2.2 Initial characterization of rom-1

The human rom-1 cDNA was initially cloned by genetic methods using a differential screening approach (Bascom *et al.*, 1992b). It encodes a protein of 351 amino acids. The rom-1 sequence was found to be 35% identical to bovine peripherin-2 and hydropathy plots predict a topology similar to peripherin-2 with four transmembrane segments, an intradiscal loop, and a long C-terminal tail (**Fig 7**). The intradiscal loop regions of peripherin-2 and rom-1 are more highly conserved exhibiting 47% identity. The seven cysteines within this loop are also conserved. Several sequences are identical in peripherin-2 and rom-1 including RYLD and DGVPFSCCNPXSPRPC (Bascom, Schappert & McInnes, 1993). Rom-1 differs from peripherin-2 in that it lacks an N-linked glycosylation consensus sequence and has more acidic residues (pI 5.2 vs 8.2 for peripherin-2).

Rom-1 was localized to the rim region of ROS discs by immunoelectron microscopy with polyclonal antibodies, but no labeling of cones was observed (Bascom *et al.*, 1992b). Rom-1 was found to coprecipitate with peripherin-2 when purified using the anti-peripherin-2 monoconal antibody Per2B6. Like peripherin-2, it migrated as disulfide-linked homodimers when analyzed by two-dimensional SDS-PAGE (Bascom *et al.*, 1992b). Disulfide-linked heterodimers of peripherin-2 and rom-1 were not observed and as a result it was concluded that the two proteins associated noncovalently to form a multisubunit complex. The human rom-1 gene localizes to chromosome 11q13 (Bascom *et al.*, 1992a).

The presence of rom-1 in cones and the predicted membrane topology for rom-1 were confirmed in studies using antibodies generated to specific sequences of bovine rom-1 (Moritz & Molday, 1996). Bovine rom-1 was found to be 84% identical to human rom-1 and was localized to rod and cone outer segment disc rims by immunoelectron microscopy. Pre-embedding immunoelectron labeling of isolated ROS discs with polyclonal antibodies to the C-terminal tail of rom-1 confirmed that this region is located on the cytoplasmic side of the disc. Proteolytic studies in conjunction with antibodies generated to the cytoplasmic C-terminus and to the intradiscal loop region of rom-1 verified the topological organization of rom-1 (Moritz & Molday, 1996). Co-immunoprecipitation

experiments demonstrated the presence of a peripherin-2:rom-1 complex in bovine ROS.

1.2.3 Tetraspanin superfamily

Peripherin-2 and rom-1 are members of a family of proteins known as the tetraspanin or transmembrane four superfamily (TM4SF). These proteins are characterized by the presence of four transmembrane domains and an extended extracellular (or intradiscal in the case of peripherin-2 and rom-1) loop connecting transmembrane segments three and four (reviewed by Wright & Tomlinson, 1994). There is little homology between peripherin-2 and rom-1 and the tetraspanin group beyond the overall topology and the existence of three short motifs in the loop region involving cysteines. In contrast, peripherin-2 and rom-1 have extended cytoplasmic C-terminal regions that are absent in most other tetraspanin proteins. No structural information is available on any of these proteins at this time (BLAST conserved-domain database search). However, it is known that other members of the tetraspanin family form oligomeric structures similarly to peripherin-2 and rom-1.

The tetraspanin family comprises a group of at least 19 cell-surface proteins. It includes the leukocyte cell surface markers CD9, CD37, CD53, CD63, CD81, CD82, and CD151 which are thought to be involved in B-cell maturation, signal transduction, cell adhesion, fusion, and cell motility.

CD63 and CD81 have been identified on the surface of some melanoma and leukemia cells, respectively, and may be involved in proliferation (Atkinson *et al.*, 1984; Oren *et al.*, 1990). Some of these proteins have been shown to modulate integrin signaling. This suggests that they play a role in the regulation of cell motility (Berditchevski & Odintsova, 1999; Yauch & Hemler, 2000). Other tetraspanins have been suggested to interact with Ig superfamily proteins, the neural protein L1, and MHC I and MHC II molecules, among others (Yauch & Hemler, 2000).

The function of one tetraspanin protein, latebloomer from *Drosophila*, has been defined (Kopczynski, Davis & Goodman, 1996). Latebloomer is expressed at the growth cone of developing motor neuronal axons and is involved in forming contacts between the axons and their efferent muscles. Fruit flies that lack this protein display slowed nervous system development, although these contacts do eventually form.

1.3 HUMAN DISEASE

1.3.1 Retinal diseases and disease genes

Retinal diseases encompass a heterogenous group of dystrophies and are diagnosed by clinicians according to their hereditary pattern and clinical symptoms. Autosomal dominant, autosomal recessive, and X-linked forms have been identified and involve a number of different genes

(**Table 1**). Clinical symptoms are described by fundoscopic examination in which an ophthalmoscope is used to observe anatomical abnormalities in the retina, the pigment epithelium and the retinal blood vessels, and by electroretinography which utilizes a contact lens electrode to record electroretinograms (ERGs) which monitor the responses of rods and cones to flashes of light. By clinical diagnosis, the most common forms of retinal degenerations are retinitis pigmentosa (RP) and macular degeneration (MD). Few treatments are currently available.

Retinitis pigmentosa affects approximately 1 in 3700 people (Boughman, Conneally & Nance, 1980). It is characterized by onset in the second or third decade of life, night blindness, a progressive loss in the peripheral visual field, subsequent gradual loss in central visual function, abnormal electroretinograms, and development of retinal pigmentary patches (reviewed by (Henkenlively, 1988; Kajiwara *et al.*, 1993)). In the later stages of the disease (patients in their fifties and sixties) ERG responses are absent, severe attenuation of retinal blood vessels has occurred, and patients are usually completely blind. RP is further classified genetically as autosomal dominant, recessive, or X-linked, and based on the rate of onset (rapid or slow).

Macular degeneration is characterized by loss of central vision resulting from degeneration of cones in the macular region of the retina (Bressler, Bressler & Fine, 1988). Age-related MD, which affects up to

Table 1
Proteins Involved in Retinal Diseases

Protein	Cellular localization	Disease[a]
cGMP-gated channel (α)	rods	ARRP
rhodopsin	rods	ADRP, ARRP, CSNB
phosphodiesterase (α,β)	rods	ARRP, CSNB
arrestin	rods	CSNB
rhodopsin kinase	rods	CSNB
transducin (α)	rods	CSNB
RPGR	rods	X-linked RP
peripherin-2	rods and cones	ADRP, digenic ADRP, MD, PD
rom-1	rods and cones	Digenic ADRP
ABCR	rods and cones	Stargardt's MD, AMD, ARRP, CRD
guanylate cyclase	rods and cones	LCA, CRD
GCAP1	rods and cones	Cone dystrophy
CRX	rods and cones	LCA, CRD
XLRS1	rods and cones, extracellular	X-linked retinoschisis
myosin VIIA	rods and cones, RPE	Usher syndrome
CRALBP	RPE and Müller	ARRP
bestrophin	RPE	Best's MD
RPE65	RPE	LCA, ARRP
TIMP3	Bruch's membrane	Sorby's MD

[a] ARRP - autosomal recessive retinitis pigmentosa, ADRP - autosomal dominant retinitis pigmentosa, CSNB - congenital stationary night blindness, MD - macular dystrophy, PD - pattern dystrophy, AMD - age-related macular dystrophy, CRD - cone-rod dystrophy, LCA - Leber's congenital amaurosis; table modified from Molday (1998).

10% of people over fifty (11 million North Americans) is divided into two groups, a *dry* form with a defined hereditary component, and a *wet* form. The dry form accounts for 80% of cases and is characterized by the presence of drusen (proteo-lipid deposits in Bruch's membrane), irregularities in the RPE, and geographic atrophy. The wet form is characterized by serious detachment of the RPE resulting from neovascularization of the underlying choroid (Spalton, Hitchings & Hunter, 1994). In children, Stargardt's disease and fundus flavimaculatus, which are rare autosomal recessive forms of macular degeneration, are characterized by central visual dysfunction, the presence of perimacular yellow deposits, and atrophy of the RPE (Spalton, Hitchings & Hunter, 1994). Mutations in ABCR have been linked to both of these diseases as well as the dry form of AMD (Allikmets *et al.*, 1997a; Allikmets *et al.*, 1997b).

1.3.2 Mutations in peripherin-2 that cause retinal disease

After determining that a mutation in the gene for peripherin-2 resulted in retinal degeneration in the rds mouse, many researchers turned their efforts to identifying mutations in peripherin-2 responsible for human retinal disease. To date over thirty mutations have been found and are summarized in **Table 2**. These mutations are responsible for a heterogeneous group of autosomal dominant diseases which include RP,

Table 2

Peripherin-2 Mutations Associated with Human Retinopathies

Mutation[a]	Location[b]	Disease[c]	Reference
Trp25*fs*	M1	RPA	(Kajiwara *et al.*, 1993)
Ser27Phe	M1	CD	(Fishman *et al.*, 1997)
Arg46*stop*	L1-2	ADRP	(Meins *et al.*, 1993)
ΔMet67	M2	PD	(Jacobson *et al.*, 1994)
ΔCys118/119	M3	ADRP	(Farrar *et al.*, 1991b; Wells *et al.*, 1993)
Leu126Arg	L3-4	ADRP	(Kajiwara *et al.*, 1992)
Tyr140*fs*	L3-4	MD	(Keen *et al.*, 1994; Kim *et al.*, 1995)
Tyr141Cys	L3-4	ADRP	(Sohocki *et al.*, 2001)
Tyr141His	L3-4	MD	(Trujillo *et al.*, 2001)
Arg142Trp	L3-4	MD	(Hoyng *et al.*, 1996)
Lys153Arg	L3-4	ADRP, RCD, PD	(Jacobson *et al.*, 1994)
ΔLys153/154	L3-4	ADRP, MD	(Weleber *et al.*, 1993)
Cys165Tyr	L3-4	ADRP	(Souied *et al.*, 1998)
Gly167Asp	L3-4	BPD	(Nichols *et al.*, 1993b)
Arg172Glu	L3-4	MD	(Wells *et al.*, 1993)
Arg172Trp	L3-4	MD	(Jacobson *et al.*, 1994; Wells *et al.*, 1993)
Asp173Val	L3-4	ADRP	(Gruning *et al.*, 1994)
Gln178Arg	L3-4	ADRP	(Sohocki *et al.*, 2001)
Trp179Arg	L3-4	ADRP	(Bareil *et al.*, 2000)
Tyr184Ser	L3-4	CRD	(Wada *et al.*, 1995)
Leu185Pro	L3-4	ADRP	(Kajiwara, Berson & Dryja, 1994; Kajiwara *et al.*, 1991)
ΔLys193	L3-4	RCD	(Jacobson *et al.*, 1994)
Val200Gly	L3-4	CRD	(Nakazawa *et al.*, 1996)
Gly208Asp	L3-4	ADRP	(Trujillo *et al.*, 1998)
Pro210Arg	L3-4	ADRP	(Gorin *et al.*, 1995)
Pro210Ser	L3-4	ADRP	(Kemp *et al.*, 1994)
Phe211Leu	L3-4	ADRP	(Ekstrom *et al.*, 1998)
Ser212Gly	L3-4	ADRP	(Farrar *et al.*, 1992)
Cys214Ser	L3-4	ADRP	(Saga *et al.*, 1993)
Cys214Tyr	L3-4	MD	(Trujillo *et al.*, 2001)
Pro216Leu	L3-4	ADRP	(Kajiwara *et al.*, 1991)
Pro216Ser	L3-4	ADRP	(Fishman *et al.*, 1994)
ΔPro219	L3-4	ADRP	(Kajiwara *et al.*, 1991)
Asn244Lys	L3-4	ADRP, BEM	(Kikawa *et al.*, 1994)
Asn244His	L3-4	ADRP, BEM	(Nakazawa *et al.*, 1994)
Tyr258*stop*	L3-4	MD	(Wells *et al.*, 1993)
Gly266Asp	M4	ADRP	(Kajiwara *et al.*, 1992)
Ser299*fs*	C-term	BPD	(Nichols *et al.*, 1993a)
Leu307*fs*	C-term	ADRP	(Gruning *et al.*, 1994)

[a] *fs* – frameshift, *stop* - stop codon; [b] see Fig 7; [c] RPA - Retinitis punctata albescens, CD – cone dystrophy, ADRP - autosomal dominant retinitis pigmentosa, PD - pattern dystrophy, MD - macular dystrophy, RCD - rod-cone dystrophy, BPD - Butterfly-shaped pigment dystrophy, CRD - cone-rod dystrophy, BEM - Bull's-eye maculopathy

MD, and pattern dystrophies like butterfly-shaped pigment dystrophy, fundus flavimaculatus, cone-rod dystrophy, and Bull's Eye maculopathy (reviewed by Molday, 1998). Mutations in peripherin-2 account for approximately 5% of individuals with autosomal dominant RP.

The majority of disease-causing mutations are located within the large highly conserved intradiscal loop of peripherin-2. Most of these are of the missense type and result in proteins containing amino acid substitutions. However, mutations have also been found that result in amino acid deletions and protein truncations. Since decreased levels of peripherin-2 result in photoreceptor degeneration in the *rds* mouse, it is likely that some of these mutations, especially the truncations, also result in decreased levels of functional protein in the outer segment. A dominant-negative effect resulting from the presence of mutant protein in the outer segments, however, may also contribute to the heterogeneity in disease type and age of onset.

It is interesting that some peripherin-2 mutations primarily affect cones, while others affect rods. A mutation at Arg172, for example, results in MD where cones but not rods are affected, but a mutation at Asp173 primarily affects rods and results in RP. Since the same gene is likely present in both rods and cones, this means that rods can tolerate the 172 mutation, but not the 173 mutation, and vice versa for cones. These mutations either must affect the protein's structure differently in

rods and cones, or disrupt protein interactions specific for these cell types.

The only mutations found in rom-1 conclusively linked to retinal disease have been involved in a novel form of digenic RP that requires a L185P mutation in peripherin-2 in addition to a null or G113E mutation in rom-1 (Bascom *et al.*, 1993; Dryja *et al.*, 1997; Kajiwara, Berson & Dryja, 1994). Individuals who inherit both mutant alleles (double heterozygotes) display the autosomal dominant RP phenotype, while individuals who inherit only the peripherin-2 or rom-1 mutant allele (single heterozygotes) are essentially normal. Even though rom-1 forms an oligomeric complex with peripherin-2 and is similar in its subcellular localization, topology, and sequence conservation, its lack of involvement in retinal disease implies a different, possibly non-dominant role for this subunit in outer segment morphogenesis.

1.4 MOLECULAR CHARACTERIZATION OF PERIPHERIN-2 AND ROM-1

1.4.1 Oligomeric structure and size

To further characterize the molecular properties of the peripherin 2:rom-1 complex, Goldberg et al. (1996) employed the technique of velocity sedimentation to define the size and stoichiometry of these complexes. Experiments were performed under mildly disulfide-reducing

conditions (1 mM DTT) to prevent secondary oxidation of the protein. Immunoaffinity-purified, detergent-solubilized peripherin-2:rom-1 complex from bovine ROS sedimented as a single peak indicating that these proteins form a complex of a discrete size (Goldberg, Moritz & Molday, 1995). Hydrodynamic characterization of this complex, which combines velocity sedimentation measurements in H_2O and D_2O and gel exclusion chromatography to determine molecular mass, gave an estimated molecular mass of 135,000 kDa. This value is in reasonable agreement with a tetrameric protein (152,000 kDa calculated from the primary sequences).

A heterologous expression system was developed to examine the assembly of peripherin-2 and rom-1 subunits into oligomeric complexes. When individually expressed in COS-1 cells, peripherin-2 and rom-1 formed disulfide-linked dimers, but did not associate when solubilized cell extracts were mixed prior to immunoprecipitation. In contrast to rhodopsin which targets to the plasma membrane when expressed in COS-1 cells, peripherin-2 and rom-1 localized to internal membranes and were absent from the plasma membrane of these cells. When co-expressed in COS-1 cells, peripherin-2 and rom-1 did associate specifically to form a heteromeric complex thus showing that the information required for subunit assembly is contained in the amino acid

sequence of these proteins and that co-assembly in the endoplasmic reticulum of cells is required for association.

When individually expressed in COS-1 cells, or when co-expressed and purified, peripherin-2 and rom-1 sedimented similarly to the tetrameric protein from ROS under reducing conditions. These results indicate that peripherin-2 and rom-1 can form homotetrameric complexes in the absence of the other subunit and that oligomeric assembly of these proteins can occur in COS-1 cells. Based on these results and on previous studies by Bascom et al. (1992), a model was developed for native peripherin-2:rom-1 complex in which a disulfide-linked homodimer of peripherin-2 associates noncovalently with a disulfide-linked homodimer of rom-1 to form a heterotetrameric protein (**Fig 8**). In the absence of rom-1, peripherin-2 disulfide-linked homodimers associate to form a homotetrameric protein.

1.4.2 Molecular basis for digenic RP

Using the heterologous expression system described above, the effects of the L185P mutation in peripherin-2 on its structure, subunit assembly and interaction with rom-1 were determined (Goldberg & Molday, 1996a). The authors found that the L185P mutation prevented homotetramer formation and resulted in a protein that sedimented at a slower rate than WT. The protein did form disulfide-linked dimers. When

co-expressed with rom-1, L185P peripherin-2 co-assembled and co-sedimented as a tetrameric protein. These results indicate that in the presence of rom-1, L185P peripherin-2 can assemble into a heterotetrameric protein similarly to WT. Based on these results a subunit assembly model for digenic RP was developed to correlate molecular interactions with genotype and phenotype (**Fig 8**). This model stresses the functional importance of having sufficient levels of peripherin-2 containing tetramers in ROS and predicts that homotetramers of peripherin-2 function normally. This study demonstrated for the first time how disease-causing mutations in peripherin-2 affect its structure.

1.4.3 Role for peripherin-2 in membrane fusion

A potential role for peripherin-2 in disc-plasma membrane fusion has been examined *in vitro* (Boesze-Battaglia *et al.*, 1997; Boesze-Battaglia *et al.*, 1998 2000). When peripherin-2-enriched large unilamellar vesicles (LUVs) were incubated with ROS plasma membrane vesicles, fusion occurred in a calcium dependent manner, and was increased with phosphorylated peripherin-2. Fusion was decreased upon trypsinization of peripherin-2. A peptide (PP-5) corresponding to amino acids 311-325 of the cytoplasmic C-terminal region of peripherin-2 inhibited fusion between disc and plasma membranes and promoted

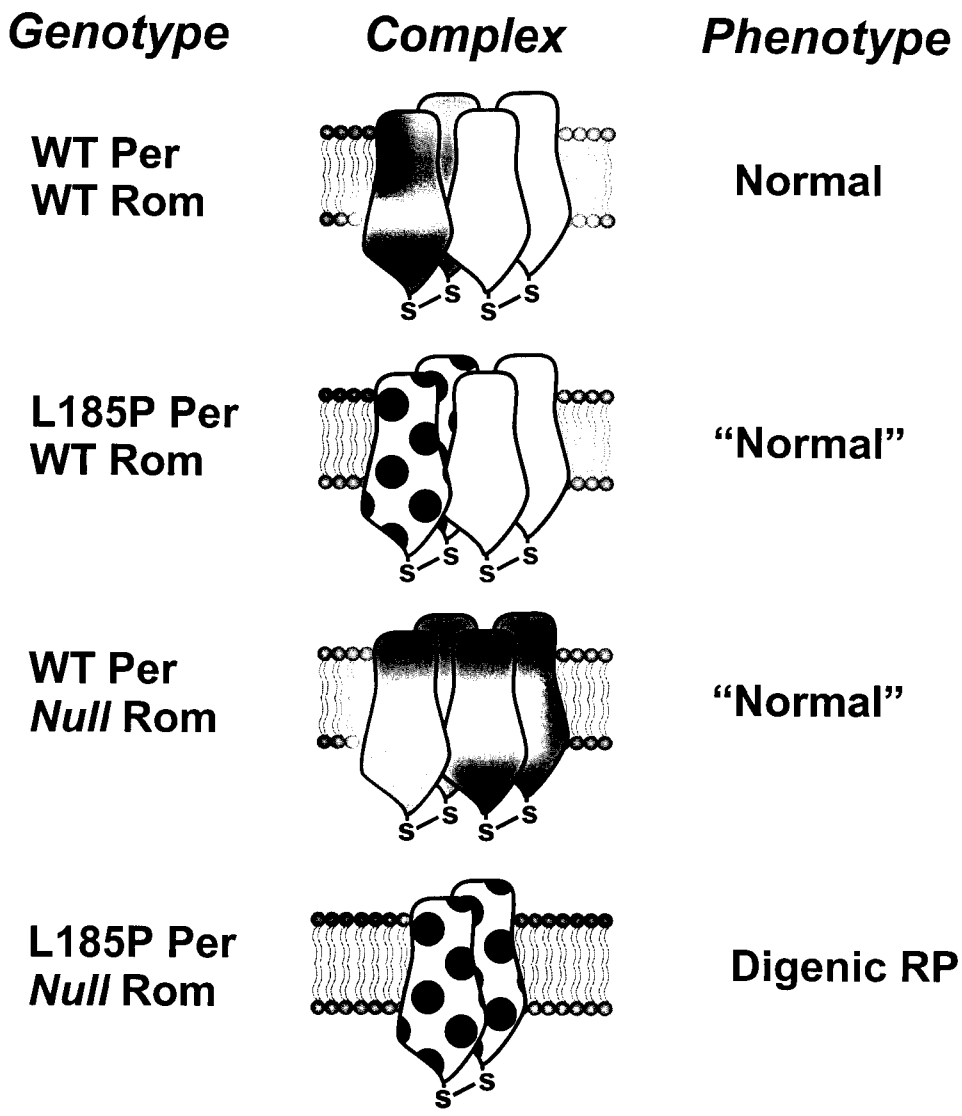

Fig 8. **Subunit assembly model for digenic RP.** Normal individuals have a full complement of WT peripherin-2 (dark fill)-rom-1 (light fill) tetramers. Those with only an L185P mutation in peripherin-2 are borderline "normal" because L185P peripherin-2 (spotted fill) is predicted to assemble into functional tetramers with rom-1. Those with only a null mutation in rom-1 are "normal" because peripherin-2 homotetramers are predicted to compensate for reduced levels of rom-1. Only individuals with an L185P peripherin-2 mutation and a rom-1 null exhibit the disease phenotype because L185P peripherin-2 is incapable of supporting ROS morphogenesis. Therefore decreased levels of tetramers are predicted to contribute to the RP disease phenotype. Modified from Molday (1998).

vesicle aggregation and membrane depolarization. Other peptides from the N- and C-termini had no effect. This peptide can be modeled as an amphipathic alpha helix and shares similarities to other fusogenic peptides. FTIR studies confirm its alpha helical nature and gel exclusion chromatography experiments suggest that it may exist as a tetramer. Mutation of PP-5, which disrupts its amphipathic nature, inhibited membrane depolarization, but not vesicle aggregation, and disruption of its alpha helical nature had no effects.

It is therefore possible that in photoreceptors, a tetrameric C-terminal region of peripherin-2 promotes fusion between disc and plasma membranes at the distal tip and is regulated through phosphorylation. This process must be highly regulated since disc shedding occurs in specific cells at specific times and only in the distal tip region of rods and cones. Peripherin-2 may also be involved in fusion events that result in disc closure during disc morphogenesis. These hypotheses have yet to be tested *in vivo*. Mutations that affect the C-terminus of peripherin-2 are known to cause RP.

1.4.4 Role for peripherin-2 in flattening membrane vesicles

In a recent study by Wrigley *et al.* (2000), the effect of peripherin-2 on the shape of pancreatic microsomal vesicles was examined by electron microscopy. When peripherin-2 is expressed *in vitro* under disulfide

reducing conditions in the presence of microsomal vesicles, typical round vesicles are observed. When expressed under nonreducing conditions a significant fraction of the vesicles exhibit a flattened appearance with regions of high curvature similar to disc rims of ROS. Rhodopsin expressed under the same conditions did not result in vesicle flattening. Expression of the RP-causing C165Y and P216L mutants prevented flattening of vesicles as did expression of the C150S mutant which prevents disulfide-dimerization of peripherin-2 (Goldberg, Loewen & Molday, 1998).

It appears, therefore, that a function of peripherin-2 may also be to bind membranes in a disulfide-dependent manner. This function may serve to bring adjacent membrane evaginations together at the base of the outer segment during disc rim formation and may be responsible for the high degree of curvature associated with the rim region of discs. The inability of the disease-causing mutations, which are located in the intradiscal region, to flatten membranes supports a role for peripherin-2 in membrane adhesion in photoreceptors. It is important to note however that these experiments have been conducted in a cell-free system and that the presence of peripherin-2 in the flattened vesicles was not verified.

1.5 ANIMAL MODELS

1.5.1 The rds mouse

A role for peripherin-2 in photoreceptor disc morphogenesis and human retinal disease originated from studies in the *rds* mouse, a natural peripherin-2 gene knock-out. Mice homozygous for the *rds* mutation fail to develop photoreceptor outer segments and the photoreceptors undergo slow degeneration over the period of about a year (Jansen & Sanyal, 1984; Sanyal & Jansen, 1981). Heterozygous *rds* mice exhibit shortened, highly disorganized outer segments consisting of whorls of membranes. The gene responsible for the *rds* phenotype was identified in the *rds* mouse and it was found to contain a large insertion of foreign DNA that results in a premature stop codon (Travis *et al.*, 1989). The normal gene was shown to encode for the peripherin-2 protein (Connell *et al.*, 1991). Therefore, reduced levels of peripherin-2 result in photoreceptor degeneration and death. Adding back a WT transgene restores normal photoreceptor morphogenesis and rescues the *rds* phenotype (Travis *et al.*, 1992). These results and the unique location of peripherin-2 at the disc rims indicate that peripherin-2 plays an essential role in disc morphogenesis, a process that is necessary for photoreceptor viability.

1.5.2 Rom-1 knockout mouse

To examine the function of rom-1 in photoreceptors, Clarke *et al.* (2000) inactivated the gene by replacing the first exon with a neomycin resistance gene, and examined the effects in both homozygous and heterozygous mice. A marked contrast between the phenotype of rom-1 null mice and homozygous *rds* mice is observed. Photoreceptor outer segments develop in rom-1 null mice and appear fairly normal, except for occasional disc disorganization and the presence of longer discs at 18 months. These abnormalities disappear at later ages. Also, the length of the outer segment is decreased and the thickness of the photoreceptor nuclear layer is reduced. Heterozygous mice appear normal. Therefore, rom-1 appears to play a minor regulatory role in disc morphogenesis, unlike peripherin-2 which is absolutely required for outer segment formation. This result is consistent with the lack of involvement of rom-1 in human disease.

Biochemical analysis of rom-1 null mice revealed that the absence of rom-1 had no effect on the expression level or subcellular localization of rhodopsin, ABCR, or peripherin-2. Interestingly, in the absence of rom-1, peripherin-2 formed homotetramers similarly to what is observed in transfected COS-1 cells. This supports the importance of peripherin-2 homotetramer formation in disc morphogenesis. These results were predicted in the molecular model for digenic RP by Goldberg *et al.* (1996)

where individuals with a null mutation in rom-1 are normal because of peripherin-2 homotetramerization (**Fig 8**).

1.5.3 P216L peripherin-2 transgenic mouse

To develop a mouse model for human RP, Kedzierski *et al.* (1997) examined the effect of expression of the P216L mutant protein on WT, *rds* heterozygous, and *rds* homozygous mouse backgrounds. P216L peripherin-2 was unable to rescue the *rds* phenotype in the homozygous or heterozygous backgrounds. Interestingly, the phenotype in the *rds* heterozygous state is more severe with the P216L transgene than without. This implies that the P216L mutation exerts a dominant negative effect. The P216L transgene also caused photoreceptor degeneration on a WT background providing further evidence for the dominant-negative effect of this mutant. The authors did not tag the transgene and therefore could not distinguish it from endogenous peripherin-2. Thus the effects of this mutation on its subcellular localization and biochemical properties were not examined.

1.5.4 Peripherin-2:rom-1 chimeric mouse

To isolate the functions of the C-terminal and intradiscal loop regions of peripherin-2, Kedzierski *et al.* (1999) constructed a chimeric rom-1 molecule that contained the intradiscal loop region of peripherin-2.

The ability of this molecule to restore photoreceptor function was addressed *in vivo* by transgenic expression in the *rds* mouse background. In the heterozygous *rds* background, the chimera rescued the photoreceptor defect completely; however, no difference was observed between homozygous *rds* mice expressing the chimera and those not expressing it. Biochemical analysis of transgenic mice revealed that the ratio of peripherin-2 to rom-1 in ROS is approximately 2.5, that the transgene is glycosylated and interacts with both peripherin-2 and rom-1, but does not form disulfide-linked heterodimers. The authors claim that peripherin-2 homo-oligomerization is stronger than hetero-oligomerization with rom-1, and that peripherin-2 and rom-1 are quantitatively associated.

This study highlights the functional importance and independence of both the intradiscal loop region and the C-terminal region to photoreceptor disc morphogenesis. The inability of the chimera to rescue the homozygous *rds* phenotype identifies the importance of the C-terminal region and supports *in vitro* data suggesting a role for this region in membrane fusion during disc formation (Boesze-Battaglia *et al.*, 1998). The authors did not extensively characterize the morphology of the membranes in these animals. It is possible that the C-terminus of peripherin-2 functions in protein targeting to the outer segment, a function that may not be not present in rom-1. Rescue of the

heterozygous *rds* mouse by the chimera highlights the dominant function of the intradiscal loop of peripherin-2 and further implicates the importance of loop-mediated peripherin-2 subunit interactions in disc morphogenesis.

1.5.5 Gene therapy on the rds mouse

To investigate the possibility of treatment of retinal diseases by gene therapy, Ali *et al.* (2000) examined the effects of intraocularly injected recombinant adeno-associated virus carrying the gene encoding peripherin-2 in the null background of the *rds* mouse. The authors observed a 30% rod transduction efficiency. Photoreceptors expressing peripherin-2 re-established outer segment structures which contained stacks of discs similarly to WT. Expression of rom-1 and rhodopsin was also restored and localization of these proteins to outer segments was established. The presence of phagosomes in RPE cells and restoration of ERG responses in treated animals indicate a reconstitution of photoreceptor metabolism and phototransduction. This study demonstrates for the first time that function can be restored in fully differentiated mature photoreceptor cells by re-introduction of a photoreceptor specific gene. Hence, gene therapy to treat peripherin-2-linked retinal disease may be possible, but other factors need to be

defined including the stability of long term expression and the effects on cone photoreceptors.

1.6 THESIS INVESTIGATIONS

At the beginning of this project, very little was known about the role of cysteine residues and disulfide bonds in the structure of peripherin-2 and rom-1 complexes. It was known that each protein formed disulfide-linked homodimers and contained seven conserved cysteine residues in the intradiscal loop region. Mutations in two of the intradiscal cysteines had been linked to human RP. Hence, the initial goal of this thesis work was to determine the importance of the cysteine residues in peripherin-2 on its oligomeric structure. The results presented in this thesis provide compelling evidence for a central and unique role of disulfide-mediated oligomerization of peripherin-2 core complexes in photoreceptor disc morphogenesis, and identify a differential regulatory role for rom-1 in this process. The hypothesis that human disease results from decreased levels of peripherin-2 complexes in rod outer segments has been confirmed *in vivo*.

Chapter 2 of this thesis describes a mutational study in which each of the thirteen cysteine residues of peripherin-2 was replaced by serine. The ability of these proteins to form disulfide dimers, assemble into core

tetramers, and interact with rom-1 was examined. This work has been published elsewhere (Goldberg, Loewen & Molday, 1998).

Chapter 3 describes the characterization of peripherin-2 and rom-1 complexes under nonreducing conditions using a novel two-dimensional velocity sedimentation technique. The importance of disulfide dimer formation is determined. This work has been published elsewhere (Loewen & Molday, 2000).

Chapter 4 examines the structural determinants of core tetramer formation and disulfide-mediated oligomerization by analyzing the L185P mutation in peripherin-2 responsible for digenic RP. A role for these oligomers in preventing disease is proposed. This work has been published elsewhere (Loewen, Moritz & Molday, 2001).

Chapter 5 presents the results of a collaborative work with David Papermaster's group at the University of Connecticut which examines the effects of expression of RP-causing mutations in peripherin-2 on rod photoreceptors in transgenic *Xenopus laevis*. The subcellular localization of the transgenes and the effects on rod morphology are determined. This manuscript is in preparation.

CHAPTER 2 – ROLE OF CYSTEINES IN PERIPHERIN-2 STRUCTURE

2.1 INTRODUCTION

Peripherin-2 contains thirteen cysteine residues. Six are not conserved among species or with rom-1 and are located in the cytoplasmic and transmembrane regions (**Fig 9**). Seven are completely conserved among species and with rom-1 and are located in the intradiscal loop region of the molecule. Mutations in two of the conserved cysteines (C165Y and C214S) are responsible for autosomal dominant RP (see Table 2 in Introduction).

In this study, the importance of the cysteine residues on the structure and subunit assembly of peripherin-2 has been examined. Each of the 13 cysteine residues in bovine peripherin-2 was individually replaced with a serine residue by site-directed mutagenesis, and the resulting mutants were expressed individually or together with rom-1 in COS-1 cells. SDS-polyacrylamide gel electrophoresis, immunoprecipitation, and velocity sedimentation were carried out to evaluate the ability of these mutants to form disulfide-linked homodimers, associate with rom-1, and assemble into tetramers.

The results of this study suggest that (1) the conserved C150 residue is required for intermolecular disulfide bonding but not subunit assembly; (2) the six other conserved cysteine residues are crucial for

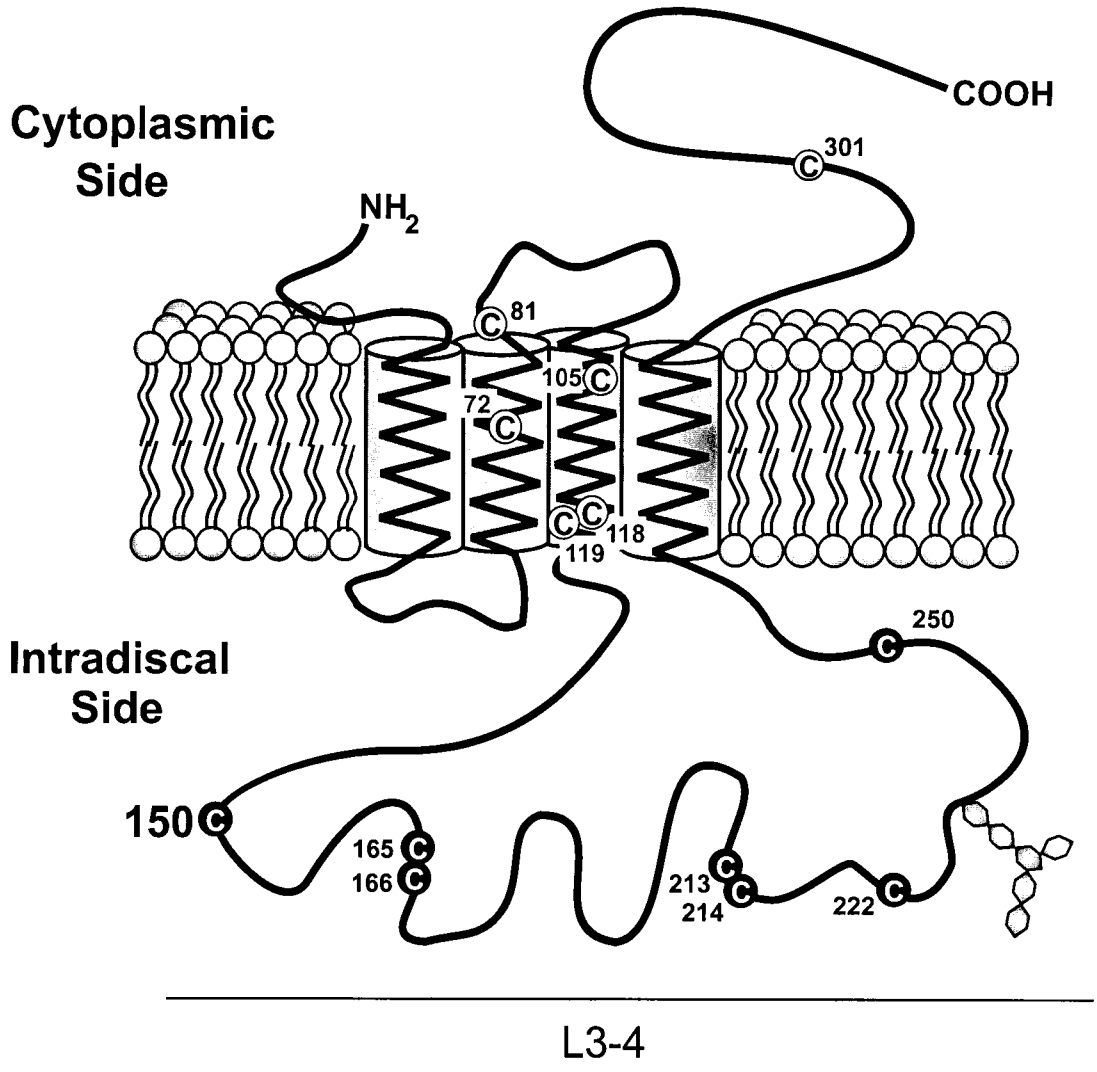

Fig 9. **Location of cysteines in bovine peripherin-2.** Nonconserved cysteines (open circles) are at amino acid positions 72, 81, 105, 118, 119, and 301; conserved cysteines (shaded circles) are present within the intradiscal L3-4 loop at positions 150, 165, 166, 213, 214, 222, and 250.

proper folding and subunit assembly, possibly through formation of intramolecular disulfide bonds; and (3) the misfolding and defective subunit assembly of the C165S and C214S mutants is responsible for a form of monogenic autosomal dominant retinitis pigmentosa.

Most of these results are published elsewhere (Goldberg, Loewen & Molday, 1998). All experiments described in this chapter were performed by the author except: (1) site-directed mutagenesis; (2) analysis of cysteine mutants by reducing and nonreducing SDS-PAGE (Fig 10).

2.2 MATERIALS AND METHODS

2.2.1 Site-directed mutagenesis

Plasmids composed of the pcDNAI/AMP vector (Invitrogen, San Diego, CA) and the full-length coding regions for bovine peripherin-2 (pcPER) or rom-1 (pcROM) were used for heterologous (COS-1) cell expression as previously described (Goldberg, Moritz & Molday, 1995). A PCR-based method of primer-directed mutagenesis (Nelson & Long, 1989) was used to generate missense mutations in which individual cysteine residues were replaced with serine residues; subcloned portions of the WT pcPER were used as templates.

Plasmid pHindbg was constructed by ligating a 260 base-pair (bp) *Hind*III/*Bgl*II fragment of the peripherin-2 coding region (5' region) into a *Hind*III/*Eco*RI-digested Bluescript II KS+ plasmid (Stratagene, La Jolla,

CA) using a synthetic *Bgl*II/*Eco*RI adapter (5'-GATCTGGTCACCG-3', 5'-AATTCGGTGACCA-3'). Plasmid pBgSks was constructed by ligating a 416 bp *Bgl*II/*Sac*II fragment of the peripherin-2 coding region (central part) directly into the Bluescript II KS+ plasmid polylinker. Plasmid pScXho was constructed by ligating a 521 bp *Sac*II/*Xho*I fragment of the peripherin-2 coding region (3' region) directly into the Bluescript II SK+ plasmid polylinker. Sense-strand synthetic oligonucleotides (NAPS, Vancouver, BC) and the templates used for the corresponding mutagenesis reactions are shown in **Table 3**.

PCR products obtained essentially as described (Nelson & Long, 1989) were digested with the appropriate restriction enzymes, purified from agarose gels, and cloned into their respective template vectors (see above and **Table 3**). The desired mutations were selected by complete (single-strand) dideoxy-sequencing with a Sequenase T7 kit (USB). The mutagenized regions were subsequently subcloned back into the WT peripherin-2 gene and final expression constructs were confirmed by restriction mapping.

2.2.2 Heterologous expression

COS-1 cells (ca. 2×10^5/ 60 mm dish) were singly transfected with expression plasmid (12 μg) or cotransfected with a mixture of two

Table 3
Synthetic Oligonucleotides Used for PCR Mutagenesis

Subclone	Mutation	Synthetic oligonucleotide
pHindBg	C72S	5′-CTGTCC**TCT**GTCTTCAATTCTCTGG-3′
pBgSks	C81S	5′-GGCAAGATC**TCT**TACGACGCCC-3′
	C105S	5′-GCCGTG**TCT**GTCCTCTTCAACG-3′
	C118S	5′-GGCCCTC**AGC**TGCTTCCTCCTGC-3′
	C119S	5′-GCCCTCTGC**AGC**TTCCTCCTGCG-3′
	C150S	5′-CCAGGCCGG**TCT**TTCATGAAG-3′
	C165S	5′-GATCGAATTCAAG**AGC**TGCGG-3′
	C166S	5′-CGAATTCAAGTGC**AGC**GGCAAC-3′
	C213S	5′-CCCTTCAGC**TCC**TGCAACCC-3′
	C214S	5′-TTCAGCTGC**AGC**AACCCCAAC-3′
pScXho	C222S	5′-CCGCGGCCC**TCG**ATCCAGTACC-3′
	C250S	5′-CTGCGTGGC**AGC**AGGGCC-3′
	C301S	5′-GACCCTGAG**TCC**GAGAGTGAGG-3′

expression plasmids (6 μg each) using the calcium phosphate method essentially as described (Chen & Okayama, 1987; Goldberg, Moritz & Molday, 1995). At 72 h post-transfection, one dish of cells was washed twice with PBS and solubilized with 300 - 500 μl of 1% Triton X-100 in PBS buffer containing PMSF (pH 7.4). For velocity sedimentation studies, 1mM DTT was included in the solubilization buffer. Cell extracts were centrifuged at 90,000 × g for 30 min at 4° C in a Beckman TLA-45 rotor and the supernatants (detergent solubilized fraction) were retained on ice until used. Typically 15 - 30 μl of extract was subjected to SDS-PAGE under reducing and nonreducing conditions (presence or absence of 4% 2-mercaptoethanol), and peripherin-2 expression was detected on Western blots.

2.2.3 Immunoprecipitation and velocity sedimentation

Homomeric peripherin-2 and heteromeric peripherin-2:rom-1 complexes were isolated from COS-1 cell extracts by an immunoprecipitation procedure (Goldberg & Molday, 1996a). Triton X-100-solubilized cell extracts (100 μl) were incubated with 25 - 50 μl of anti-peripherin-2 MAb Per2B6 coupled to Sepharose beads. The matrix was washed three times with excess buffer to remove unbound proteins, and the bound peripherin-2 complex was eluted with an excess of 2B6

peptide corresponding to the C-terminal nine amino acids of bovine peripherin-2.

For velocity sedimentation studies, the purified peripherin-2 complex was applied to 5-20% (w/w) sucrose gradients in PBS buffer containing 0.1% Triton X-100, PMSF and 1 mM DTT and centrifuged in a Beckman TLS-55 rotor for 16 h at 50,000 rpm and 4° C. Four-drop fractions were collected from the tube bottom and equivalent volumes were subjected to SDS-PAGE under reducing conditions. Sedimentation profiles of fractionated sucrose gradients were determined by western blotting with Per2B6 MAb and laser densitometry, according to Goldberg *et al.* (1995).

2.2.4 Calculation of sedimentation coefficients

Estimates of $s_{20,w}$ values were made as described originally (Goldberg, Moritz & Molday, 1995), but with the following modifications: all partial specific volume values were assumed to be 0.83 ml/g (determined for the bovine peripherin-2:rom-1 complex (Goldberg & Molday, 1996b)), initial sample radius (r_{min}) was taken as 47.5 mm (Beckman TLS-55 rotor r_{min} corrected for sample and gradient volume), and gradient height was measured as 29 mm. For a review of velocity sedimentation analysis see Clarke & Smigel (1989).

2.2.5 SDS-PAGE and Western blotting

25 μl samples containing approximately 1.5 μg of total protein were denatured with an equal volume of SDS cocktail (4% SDS, 0.02M Tris-HCl, pH 6.8, 40% sucrose, 0.01% Bromophenol blue in the absence (nonreducing) or presence (reducing) of 5% β-mercaptoethanol, and were applied to 8% or 10% SDS polyacrylamide gels. After electrophoresis, the proteins were transferred to Immobilon-P using a BioRad semidry transfer apparatus and the blots were labeled with the anti-peripherin-2 MAb Per2B6 or the anti-rom-1 MAb Rom1C6 (Molday, Hicks & Molday, 1987; Moritz & Molday, 1996) and sheep anti-mouse immunoglobulin–peroxidase for detection by ECL.

2.3 RESULTS

2.3.1 Location of cysteine residues

Previous studies have demonstrated the utility of a heterologous expression system for mutagenesis-based structural studies of peripherin-2 (Goldberg & Molday, 1996a; Goldberg, Moritz & Molday, 1995). This system has now been used to examine the relative importance of the various cysteine residues found in bovine peripherin-2.

Fig 9 depicts the current topological model for peripherin-2 (Connell & Molday, 1990; Molday, 1994) in the outer segment disc membrane and highlights the position and conservation of the 13 cysteine

residues present in the bovine sequence. Residues shaded in black are absolutely conserved in both peripherin-2 and its homologous subunit, rom-1, across all species examined to date (Bascom *et al.*, 1992b; Bascom, Schappert & McInnes, 1993; Begy & Bridges, 1990; Connell & Molday, 1990; Gorin *et al.*, 1993; Kedzierski *et al.*, 1996; Moghrabi, Kedzierski & Travis, 1995; Ray, Acland & Aguirre, 1996; Travis *et al.*, 1989; Travis *et al.*, 1991) (see sections 1.2.2 and 1.2.3). These seven conserved cysteines are confined to the large intradiscal L3-4 loop joining the third and fourth transmembrane segments. Nonconserved residues are present in both the putative transmembrane segments and segments exposed on the cytoplasmic side of the membrane.

2.3.2 Expression and disulfide dimerization

In order to assess the effect of the various mutations on the properties of peripherin-2, each of the 13 cysteine residues in bovine peripherin-2 was individually substituted with serine. As shown in **Fig 10A**, all of the variants could be expressed in COS-1 cells and migrated as monomers (apparent M_r 35K) on SDS-polyacrylamide gels under reducing conditions. Although relative levels of protein expression varied among experiments (a common property of transient transfection systems), none of the mutants showed consistently altered levels of expression relative to WT. These observations indicate that none of the

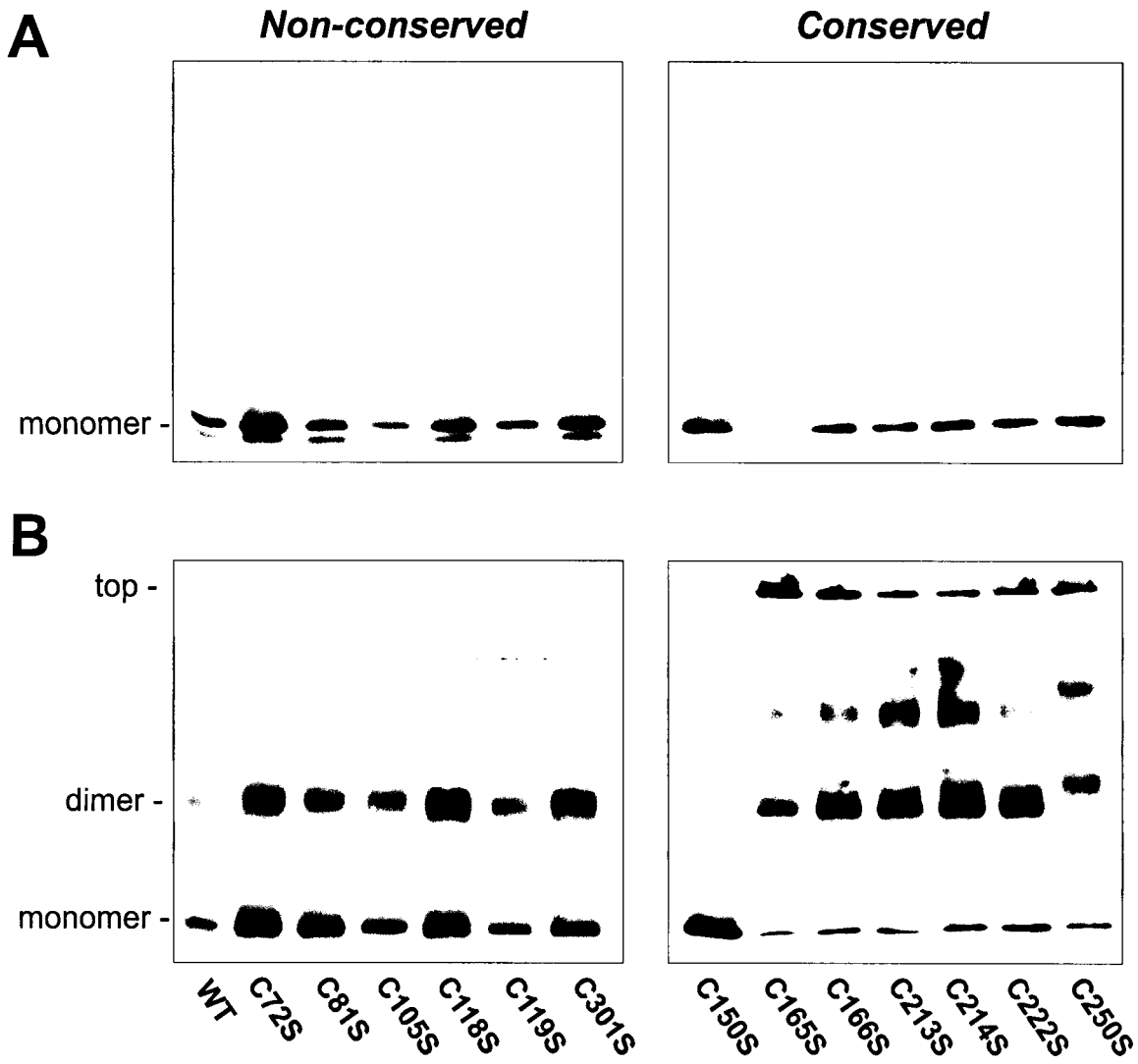

Fig 10. **Expression and dimerization of WT and mutant peripherin-2.** COS-1 cells transfected with plasmids containing the indicated mutants were detergent-solubilized 72 h posttransfection, and approximately 1.5 μg of total protein/lane was subjected to SDS-polyacrylamide gel electrophoresis in the presence (A) or absence (B) of reducing agent (2-mercaptoethanol). Western blots were labeled with anti-peripherin-2 Mab Per2B6 for chemiluminescent detection (see Methods sections 2.2.2 and 2.2.5)

cysteine residues are absolutely required for the biosynthesis of the peripherin-2 polypeptide in COS-1 cells.

The mobilities of the peripherin-2 mutants were also compared under nonreducing conditions to assess the ability of these cysteine variants to form disulfide-linked dimers. As shown in **Fig 10B** (left panel), a substantial portion of the WT and nonconserved cysteine mutants migrated at approximately twice the molecular weight of the monomeric form of peripherin-2, as previously reported for peripherin-2 from rod photoreceptor outer segment membranes (Molday, Hicks & Molday, 1987). The conserved cysteine mutants (**Figure 10B**, right panel), on the other hand, showed distinctly different behaviors. Peripherin-2 with mutations at positions 165, 166, 213, 214, 222, and 250 formed mainly dimers and aggregates found at the top of the gel. In contrast, the conserved C150S mutant migrated solely as a monomer under nonreducing, as well as reducing, conditions.

These results indicate that nonconserved cysteine mutants, like WT peripherin-2, are capable of forming disulfide-linked dimers. Conserved C165S, C166S, C213S, C214S, C222S, and C250S mutants also form dimers under nonreducing conditions but in addition have a strong tendency to form larger aggregates, most likely due to improper folding of these mutants. The inability of the C150S to form disulfide-linked dimers in presence or absence of reducing agents suggests that this

cysteine residue is essential for intermolecular disulfide bond formation. Three nonconserved cysteine mutants (C72S, C118S, and C119S), two conserved cysteine mutants (C165S and C214S), and the intermolecular disulfide dimerization-defective mutant (C150S) were selected for further study.

2.3.3 Interaction with rom-1

Co-immunoprecipitation studies have previously established that peripherin-2 assembles with rom-1 in membranes of both vertebrate photoreceptors and transiently cotransfected COS-1 cells (Bascom *et al.*, 1992b; Goldberg, Moritz & Molday, 1995; Moritz & Molday, 1996). This procedure has now been used to assess the ability of the nonconserved and conserved peripherin-2 cysteine mutants to assemble with WT rom-1.

COS-1 cells were transiently cotransfected with peripherin-2 and rom-1 plasmids and the detergent-solubilized cell extracts were immunoprecipitated with a Per2B6-Sepharose matrix. Western blots of the cell extracts and unbound and bound fractions were subsequently labeled with anti-peripherin-2 and anti-rom-1 antibodies to assess the interaction of WT and mutant peripherin-2 with rom-1. As shown in **Fig 11A**, peripherin-2 immunoreactivity was observed in the bound fraction (lane c) but not in the unbound fraction (lane b) in every case, indicating that the Per2B6-Sepharose matrix quantitatively precipitated WT and the

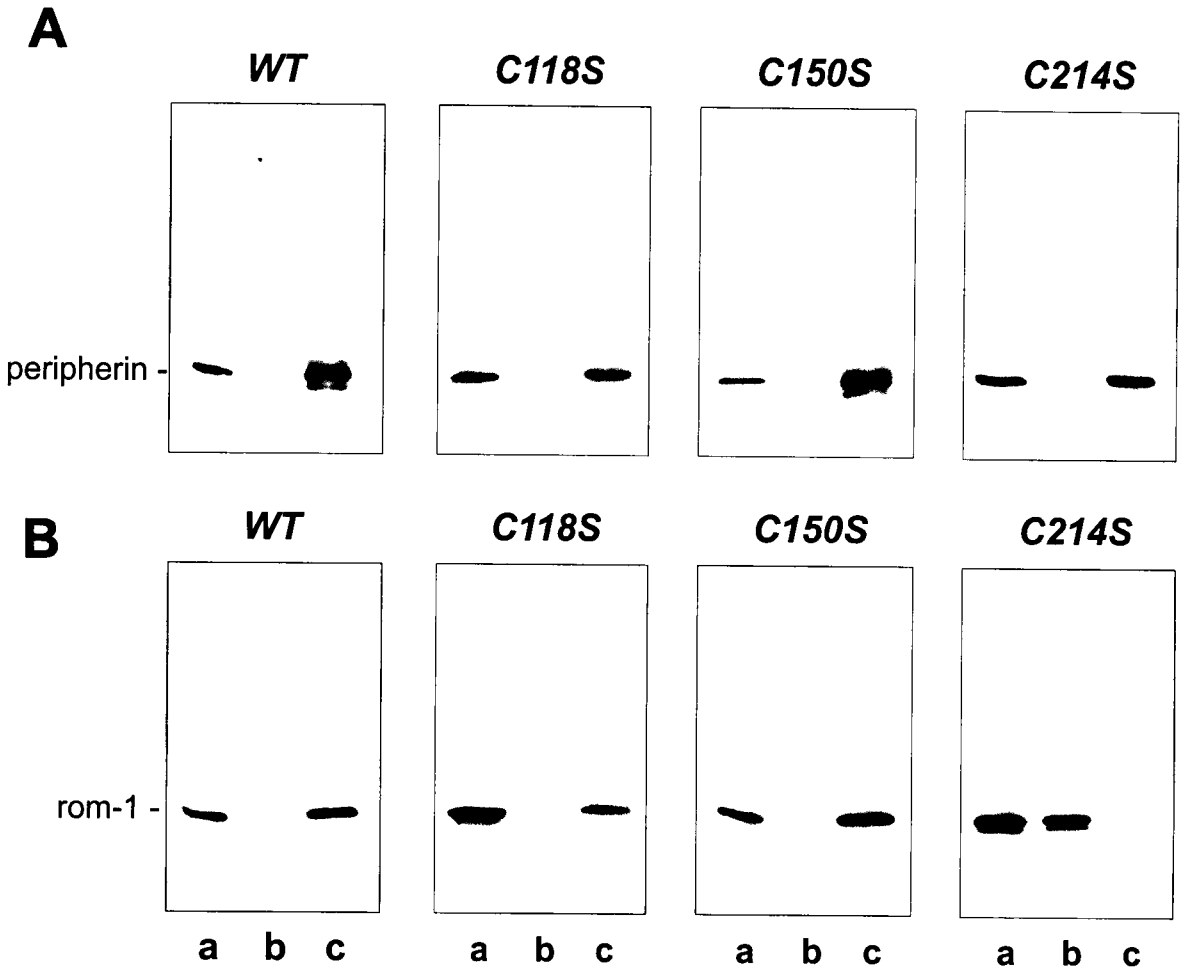

Fig 11. **Coassembly of peripherin-2 cysteine mutants with rom-1.** COS-1 cells were cotransfected with wild-type (WT) or mutant peripherin-2 plasmid and WT rom-1 plasmid. Detergent-solubilized extracts (a) were adsorbed to Per2B6-Sepharose, and after removal of the unbound fractions (b), the bound fractions (c) were eluted with the 2B6 competing peptide. Samples were analyzed on Western blots labeled with either the peripherin-2 Mab per2B6 (A) or the rom-1 Mab Rom1C6 (B) (see Methods sections 2.2.2, 2.2.3 and 2.2.5).

various cysteine peripherin-2 mutants from COS-1 cell extracts. Analogous western blots labeled with an anti-rom-1 antibody Rom 1C6 (**Fig 11B**) further showed that over 90% of the rom-1 coprecipitated with WT peripherin-2 (first panel) and the nonconserved C118S mutant (second panel). Similar results were obtained for the nonconserved C72S and C119S mutants (data not shown). Interestingly, rom-1 also coprecipitated with the C150S disulfide-dimer-defective mutant (**Fig 11B**, third panel, lane c). In contrast, rom-1 did not coprecipitate with the C214S (**Fig 11B**, fourth panel) or C165S mutants (data not shown) but instead was present only in the unbound fraction (**Fig 11B**, fourth panel, lane b).

These studies indicate that the interaction of peripherin-2 with rom-1 requires cysteines at conserved positions 165 and 214 but not at nonconserved postions 72, 118, or 119. Replacement of cysteine with serine at the conserved position 150 prevents disulfide-linked homodimerization but does not prevent peripherin-2 from noncovalently associating with rom-1.

2.3.4 Velocity sedimentation under reducing conditions

Previous studies have shown that the WT peripherin-2:rom-1 complex from rod outer segment and COS-1 cell membranes sediments as a heterotetrameric complex (Goldberg & Molday, 1996b; Goldberg,

Moritz & Molday, 1995). In the absence of rom-1, WT peripherin-2 self-assembles into a homotetrameric protein. This form of the protein is thought to compensate for reduced levels of the heterotetrameric protein in individuals who inherit a null allele of rom-1 (Goldberg & Molday, 1996a).

We have examined the sedimentation behavior of several conserved and nonconserved peripherin-2 cysteine mutants expressed individually or with rom-1. The sedimentation profiles and sedimentation coefficients are given in **Fig 12** and **Table 4**. The nonconserved cysteine mutants exhibited sedimentation profiles and sedimentation coefficients similar to WT peripherin-2 in both the presence and absence of rom-1. Interestingly, the disulfide-dimer-defective C150S mutant also had a sedimentation profile and coefficient similar to WT in the presence and absence of rom-1. In contrast, the conserved C214S and C165S mutants, which failed to assemble with rom-1, sedimented more slowly than WT peripherin-2 when singly expressed in COS-1 cells (**Fig 12** and **Table 4**). In addition, a significant, but variable, fraction of these mutants sedimented near or at the bottom of the centrifuge tube, presumably due to aggregation.

These results indicate that replacement of the nonconserved cysteine residues with serine does not affect peripherin-2 subunit assembly. In contrast, replacement of the conserved cysteines (with the

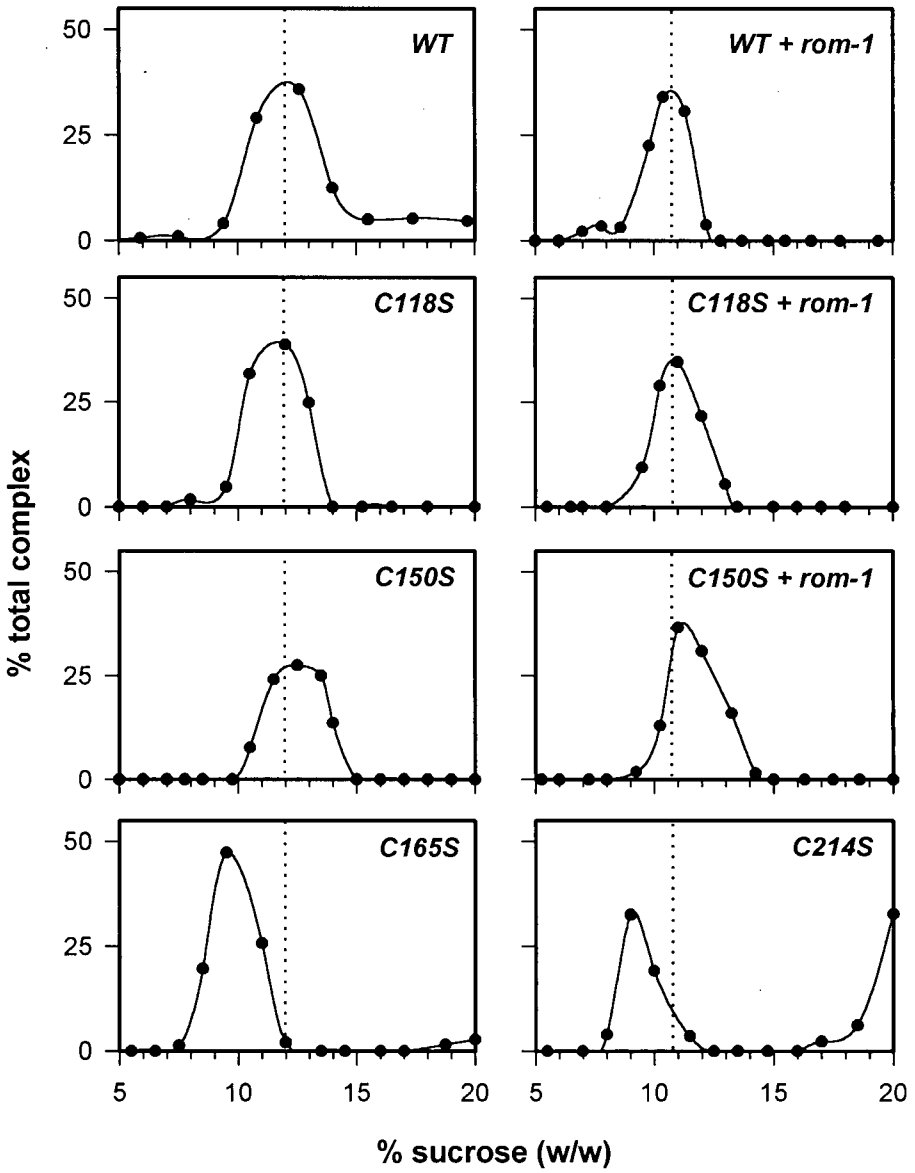

Fig 12. **Velocity sedimentation analysis of peripherin-2 cysteine mutants.** COS-1 cells were transfected with peripherin-2 wild-type (WT) or mutant plasmids alone (C118S, C150S, or C165S) or together with rom-1 (WT + rom-1, C118S + rom-1, or C150S + rom-1). Peripherin-2-containing complexes were purified on a Per2B6-Sepharose matrix and sedimented through a 5-20% sucrose gradient in the presence of 1 mM DTT. Fractions were assayed on western blots for peripherin-2 with Per2B6 antibody for singly transfected cells and with Rom1C6 antibody for co-transfected cells and quantified by laser densitometry (see Methods section 2.2.3). Velocity sedimentation studies of the C165S and C214S mutants co-expressed with rom-1 were not carried out since these mutants do not associate with rom-1. The dashed line indicates the sedimentation position of WT complex.

Table 4
Sedimentation Coefficients for Peripherin-2 and Peripherin-2:rom-1 Complexes[1]

	$s_{20,w}$ (S)		
Variant	– Rom-1	+ Rom-1	Conservation/location[2]
WT[3]	5.4 ± 0.1 (n = 3)	5.0 ± 0.4 (n = 4)	-
C72S	5.1 ± 0.4 (n = 3)	4.8 ± 0.1 (n = 3)	nc/M2
C118S	5.4 ± 0.1 (n = 3)	5.1 ± 0.1 (n = 3)	nc/M3
C119S	5.5 ± 0.2 (n = 3)	5.2 ± 0.1 (n = 3)	nc/M3
C150S	5.2 ± 0.3 (n = 3)	5.0 ± 0.2 (n = 3)	c/L3-4
C165S	3.9 ± 0.1 (n = 3)	not assembled	c/L3-4
C214S	3.9 ± 0.2 (n = 3)	not assembled	c/L3-4

[1]Sedimentation coefficients estimated as described in the Materials and Methods are given for WT and mutant peripherin-2 and peripherin-2-rom-1 complexes ± S.D. (*n* equals the number of independent experiments). Values for WT, C72S, C118S, C119S, and C150S mutants are similar; the WT peripherin-2-rom-1 complex from rod outer segments has been shown to be a tetramer (Goldberg & Molday, 1996b). Values for C165S and C214S expressed in the absence of rom-1 are considerably less than that for the tetrameric form of peripherin-2.

[2]c, conserved; nc, nonconserved; M2, transmembrane segment 2; M3, transmembrane segment 3; L3-4, intradiskal loop joining transmembrane segments 3 and 4 (see Fig 9).

[3]The sedimentation behaviour of WT peripherin-2 and peripherin-2-rom-1 has been characterized previously (Goldberg, Moritz & Molday, 1995). Sedimentation coefficients for these species have been recalculated from the original data using new values for (1) the partial specific volume of the protein-detergent-complex and (2) sucrose gradient geometry, as described in the Methods. We consider that these adjustments more accurately reflect absolute $s_{20,w}$ values as measured.

exception of cysteine at position 150) result in proteins that fail to assemble into tetramers, presumably due to improper folding. The C150S mutant is unique in that replacement of this conserved cysteine affects disulfide-linked dimerization but does not affect its assembly into homo- and heterotetramers.

2.4 DISCUSSION

In this study the contribution of the various cysteine residues to the folding and subunit assembly of peripherin-2 has been determined by individually replacing each cysteine with a serine residue. The 13 cysteine residues in bovine peripherin-2 fall into two groups according to their conservation and effect on protein structure. Group I consists of the six nonconserved cysteine residues present in the putative transmembrane and cytoplasmic segments of peripherin-2 (positions 72, 81, 105, 118, 119, and 301), while group II contains seven highly conserved cysteines found in the intradiscal loop (positions 150, 165, 166, 213, 214, 222, and 250).

Substitution of group I cysteines has no apparent effect on the formation of disulfide-linked homodimers as analyzed by SDS-polyacrylamide gel electrophoresis under nonreducing conditions. Immunoprecipitation studies and velocity sedimentation analyses of three of these mutants (C72S, C118S, and C119S) indicate that, like WT

peripherin-2, they assemble into heterotetramers or homotetramers in the presence or absence of rom-1, respectively. It is likely that the other three nonconserved cysteines behave similarly. On this basis, one can conclude that the nonconserved cysteine residues do not play an important role in the folding or subunit assembly of peripherin-2 and are not likely to be involved in intra- or intermolecular disulfide bonding.

The seven conserved cysteine residues of group II appear to play an important role in the structure of peripherin-2. Six of the seven group II cysteine residues (positions 165, 166, 213, 214, 222, and 250) are required for proper folding and subunit assembly of peripherin-2. Individual replacement of these cysteine residues with serine results in mutant proteins that do not assemble into a native-like tetramer. Both SDS-PAGE and velocity sedimentation studies reveal that these mutants exist as a mixture of large protein aggregates and a distinct species, most likely a dimer. The intradiscal compartment in which these conserved cysteines reside is topologically similar to the extracellular space and is expected to maintain a nonreducing environment. Therefore, it is possible that some or all of these six cysteine residues participate in intramolecular disulfide bonds.

The presence of intramolecular disulfide bonds in peripherin-2 previously has been suggested from the studies of Bascom *et al.* (1992b). Intramolecular disulfide bonds in integral membrane polypeptides are

known to be important for both proper folding and subunit assembly. For example, vertebrate rod and cone opsins have an intramolecular disulfide bond between the third transmembrane helix and second intradiscal loop that is essential for proper protein folding, transport, stability, and light-dependent activation of transducin (Karnik & Khorana, 1990; Kazmi, Sakmar & Ostrer, 1997). Assembly of the GLUT-1 glucose transporter into tetramers also depends strongly on the presence of intramolecular disulfide bonds located in the extracellular domains (Zottola *et al.*, 1995). In the case of peripherin-2, the misfolding and abnormal subunit assembly observed for the six group II cysteine mutants may result from the disruption of intramolecular disulfide bonds. Replacement of the cysteine residues with more polar serine residues, however, may also contribute to the abnormal structural properties observed in these peripherin-2 mutants.

The cysteine at position 150 is unique among the group II conserved cysteine residues in that the C150S mutant is incapable of forming disulfide-linked homodimers but does assemble into a tetramer in the presence or absence of rom-1 as determined by velocity sedimentation analysis. This single cysteine, therefore, is necessary and sufficient for disulfide-linked homodimerization. Interestingly, the folding and subunit association of peripherin-2 does not require this intermolecular disulfide bond; instead subunit assembly appears to be

mediated primarily through noncovalent interactions. This somewhat surprising result is not unprecedented. Recent studies have shown that cleavage of the intersubunit disulfide bridges in bovine dopamine-monooxygenase does not affect that enzyme's tetrameric subunit stoichiometry or activity (Ishida *et al.*, 1996). The same study also concludes that a lack of intersubunit disulfide bonds significantly destabilizes the tetrameric structure, a result that might be predicted from purely thermodynamic considerations. Structural stability of other multisubunit proteins has also been shown to be dependent upon the presence of intersubunit covalent bonds (Reznik *et al.*, 1996). These considerations suggest that the intermolecular disulfide bond at position 150 of peripherin-2 may contribute to the stability of the tetrameric protein complex.

Alternatively, these disulfide bonds may not be directly involved in tetramer formation but instead may link the tetramers into higher order species that are not observed under the conditions used for the velocity sedimentation experiments reported here. Studies addressing this possibility are reported in the following chapter.

The C214S mutation in peripherin-2 has been linked to a monogenic form of autosomal dominant RP characterized by a progressive degeneration of photoreceptors (Saga *et al.*, 1993). A missense mutation in another conserved cysteine residue, C165Y, has

also been reported to cause RP (Souied *et al.*, 1998). Studies presented here indicating that these mutants are misfolded and incapable of forming heterotetramers with rom-1 are consistent with their involvement in photoreceptor degeneration and support the *subunit assembly* model for autosomal dominant RP (Goldberg & Molday, 1996a). In the simplest case, the disease state can result from decreased levels of peripherin-2-containing tetramers in individuals heterozygous for the C214S or C165Y mutations. Reduced levels of peripherin-2 have been shown to result in shortened, highly disorganized outer segments and lead to slow retinal degeneration in heterozygous *rds* mice (Hawkins, Jansen & Sanyal, 1985). Haploinsufficient levels of peripherin-2-containing tetramers have been suggested to account, at least in part, for the digenic form of RP resulting from coinheritance of a L185P peripherin-2 gene and a null allele of rom-1 (Goldberg, Moritz & Molday, 1995). Although reduced levels of peripherin-2-containing tetramers can lead to a disease phenotype, the presence of the misfolded C214S or C165Y mutants may also contribute to the disease phenotype in a dominant negative manner.

Missense mutations in the other conserved cysteine residues are predicted to cause autosomal dominant RP. In contrast, missense mutations in the nonconserved cysteines are expected to have little, if any, effect. Fishman *et al.* (1997) have reported that individuals with a missense mutation in the nonconserved cysteine of codon 72 (C72S

mutation) are normal. These authors have ascribed this mutation as a polymorphism.

Autosomal dominant RP has also been linked to a deletion mutation at the nonconserved 118 or 119 position of peripherin-2 (Farrar *et al.*, 1991b). Studies presented here showing that a serine substitution at either of these nonconserved positions has no obvious effect on peripherin-2 structure or assembly suggests that the deletion of an amino acid, and not the absence of a cysteine residue, is primarily responsible for the disease. Indeed, preliminary heterologous expression studies of the C118del (C119del) peripherin-2 variant indicate that this mutant is highly misfolded (C. Loewen and R. Molday, unpublished results). The shortening of the polypeptide chain, and not loss of cysteine functionality, appears to prevent the proper folding of this mutant.

In conclusion, this mutagenesis study indicates that the conserved cysteine residues within the large intradiscal loop play an important role in the structure of peripherin-2. Six of these cysteine residues are essential for proper protein folding and subunit assembly, possibly through their involvement in intramolecular disulfide bond formation. Abnormal folding and subunit assembly of the C214S and C165S mutants appear to be responsible for the monogenic form of autosomal dominant RP linked to these mutations. The conserved cysteine residue at position 150 is required for disulfide-dependent homodimerization but is not

required for hetero- or homotetramer formation. Since rom-1 is highly homologous to peripherin-2, we expect that conserved cysteine residues in the large intradiscal loop of rom-1 likewise play an essential role in the folding and subunit assembly of this subunit.

CHAPTER 3 – DISULFIDE-MEDIATED OLIGOMERIZATION OF PERIPHERIN-2 AND ROM-1

3.1 INTRODUCTION

Identification of *Cys150* as the cysteine residue responsible for disulfide dimer formation and exclusion of a role for intermolecular disulfide bonding in tetramer formation prompted further investigation into the function of the disulfide dimer. Since previous velocity sedimentation studies were conducted under mildly reducing conditions, the presence of the disulfide dimer in the tetramer was never demonstrated. Therefore, the oligomeric structure of these proteins has been analyzed from reduced and nonreduced ROS and COS-1 cell membranes by a novel two-dimensional separation technique which identifies the contribution of intermolecular disulfide bonds to the structure.

The results of this study suggest that peripherin-2 and rom-1 associate noncovalently to form a mixture of homo- and heterotetrameric core proteins. A significant fraction of peripherin-2-containing core complexes further links together through intermolecular disulfide bonds at Cys150 to form higher order oligomers. These results lead to a new model for the oligomeric structure of peripherin-2 containing proteins in ROS and provide insight into the possible role of these complexes in outer segment morphogenesis and retinal degeneration.

Most of these results have been published elsewhere (Loewen & Molday, 2000). All experiments described in this chapter were performed by the author.

3.2 MATERIALS AND METHODS

3.2.1 ROS preparations and monoclonal antibodies

ROS were isolated from frozen bovine retina by sucrose gradient centrifugation as previously described (Molday, Hicks & Molday, 1987). Monoclonal antibodies to peripherin-2 (Per2B6) and rom-1 (Rom1C6) have been reported (Molday, Hicks & Molday, 1987; Moritz & Molday, 1996).

3.2.2 Dimer reduction kinetics

ROS were washed three times by low speed centrifugation under dim red light with 10 volumes of 10 mM Tris-HCl, pH 7.4, and resuspended at a protein concentration of 2 mg/ml in the same buffer. Reduction in the presence or absence of 1% Triton X-100 was initiated at 25°C by the addition of DTT, cysteine or glutathione to yield a final concentration of 10 mM. Aliquots were removed at 5 min intervals and added to an equal volume of stop buffer (2% Triton X-100, 120mM NEM, 0.2 mg/ml PMSF, 10mM Tris-HCl, pH 7.4). The samples were centrifuged at 90,000 × g for 30 min and the supernatants were subjected to SDS-

PAGE under nonreducing conditions for analysis by Western blotting as described below. For kinetic analysis, the decrease in peripherin-2 or rom-1 dimer as a function of time was quantified by scanning the ECL exposed film with a laser densitometer. Kinetics were fitted to a single exponential decay using Sigma Plot (Jandel Scientific).

3.2.3 DTT and NEM treatment of ROS and immunoaffinity purification

ROS were washed three times in PBS (0.01 M sodium phosphate, 0.15 M NaCl, pH 7.4) and the final pellet was resuspended at a protein concentration of 2 mg/ml in PBS in the presence or absence of 10 mM DTT. After 90 min. at 25°C, ROS samples were solubilized by the drop-wise addition of an equal volume of ice cold solubilization buffer (2% Triton X-100 and 0.2 mg/ml PMSF in PBS) containing 100 mM NEM to obtain a protein concentration of 1 mg/ml. The solution was centrifuged at 90,000xg for 30 min to remove any residual insoluble material and the supernatant (solubilized ROS) was used either directly for velocity sedimentation measurements and crosslinking studies or for purification of peripherin-2 and rom-1.

Peripherin-2:rom-1 complex was typically purified from Triton X-100 solubilized ROS on a Per2B6-Sepharose immunoaffinity matrix as previously described (Goldberg, Moritz & Molday, 1995). Briefly, 200 μl

of solubilized ROS were incubated with 50 μl of matrix for 1 h at 4° C in a Millipore Ultrafree MC 0.45 μm filter unit. The matrix was then washed three times with 0.4 ml of solubilization buffer by low speed centrifugation (10,000 × g, 4 ° C, microfuge) to remove unbound protein, and the bound peripherin-2:rom-1 complex was eluted with 200 μl of solubilization buffer containing 0.1 mg/ml of the 2B6 competing peptide (DAGQAPAAG).

3.2.4 Heterologous COS-1 cell expression

pcPER (wild-type peripherin-2), pcPER-C150S (C150S mutant peripherin-2), and pcROM (wild-type rom1) plasmids used for COS-1 cell transfections have been previously described (Goldberg, Loewen & Molday, 1998; Goldberg, Moritz & Molday, 1995). For heterologous expression, COS-1 cells (~6 × 10^5 cells/100 mm dish) were transfected with 30 μg of plasmid using the calcium phosphate method and harvested 72 h post-transfection as described (Goldberg, Moritz & Molday, 1995). The cells were washed twice with PBS and incubated with 270 μl PBS containing 0.1 mg/ml PMSF and either 10 mM DTT or 40mM NEM. After 90 min at 25°C, the cells were solubilized by the addition of 30 μl of 10% Triton X-100 and incubated for 20 min on ice. The solution was centrifuged at 90,000xg for 10 min and the supernatant was collected and maintained on ice until use.

3.2.5 Velocity sedimentation

Triton X-100 solubilized protein (100 μl) from DTT or NEM treated ROS or COS-1 cell membranes (1 mg/ml total protein) or immunoaffinity-purified peripherin-2:rom-1 (0.01 mg/ml) was applied to 5-20 % (w/w) 2 ml sucrose gradients prepared in PBS and containing 0.1 % Triton X-100. Routinely, 1 mM DTT was included in the gradients for DTT-treated samples. After centrifugation for 12h at 50,000 rpm in a Beckman TLS-55 rotor at 4°C, the bottom of the centrifuge tube was punctured and four-drop fractions were collected by gravity flow. Fractions were incubated with 40 mM NEM for 30 min at 25°C to block free sulfhydryl groups and neutralize any remaining DTT. The samples were then added to an equal volume of SDS cocktail in the absence (or presence) of reducing agent and analyzed by SDS-PAGE and Western blotting.

3.2.6 Glutaraldehyde crosslinking

Reduced or nonreduced, Triton X-100 solubilized ROS (0.1 mg/ml) or purified peripherin-2:rom-1 complex (4 μg/ml) was treated with 50 mM NEM and subsequently incubated with 0.001% or 0.01% glutaraldehyde for 15-30 min at 37°C. Samples were added to an equal volume of SDS cocktail containing β-mercaptoethanol for analysis by SDS-PAGE.

3.2.7 Quantification of peripherin-2 and rom-1 in ROS

Peripherin-2 and rom-1 subunits, used as standards for quantitative analysis, were isolated as follows: 1 ml of DTT-treated ROS membranes (5-10 mg/ml total protein) was solubilized with in an equal volume of 1% SDS in PBS containing 100 mM NEM and PMSF. After centrifugation for 30 min at 100,000 × g, the supernatant was diluted 10-fold in PBS containing 2% Triton X-100 and PMSF. Peripherin-2 was selectively bound to 200 μl Per2B6-Sepharose and rom-1 was bound to 200 μl Rom1C6-Sepharose. After extensive washing in the same buffer, bound protein was eluted with 1 ml of 2% SDS in PBS containing PMSF for 15 min at 37°C. The purity of the proteins was confirmed by SDS-PAGE and the protein concentration was determined by the method of Kaplan and Pedersen (Kaplan & Pedersen, 1985). Under these conditions, the purified preparation of the peripherin-2 subunit lacked rom-1 and purified rom-1 subunit was free of peripherin-2 as determined by Western blotting.

The amount of peripherin-2 and rom-1 in bovine ROS could not be directly determined from Western blots of ROS since rhodopsin is known to block the electro-transfer of peripherin-2 and to a lesser extent rom-1. As a result, the peripherin-2 complex from nonreduced, Triton X-100 solubilized ROS was quantitatively bound to a Per2B6-Sepharose column

as described in section 3.2.3 such that no peripherin-2 was detected in the unbound fraction. After the matrix was thoroughly washed, the bound peripherin-2 complex was quantitatively eluted from the column with 2% SDS. The bound and unbound fractions, along with the peripherin-2 and rom-1 standards, were analyzed by SDS-PAGE and Western blotting under reducing conditions. The amount of peripherin-2 and rom-1 was determined from laser densitometry of the ECL signal from Western blots. Values interpolated from standard curves were reported as an average of 3 or more experiments and correlated with the protein content in ROS (Kaplan & Pedersen, 1985).

3.2.8 Subunit composition of disulfide-linked and glutaraldehyde crosslinked dimers

To determine the composition of disulfide-linked species, 0.1 ml of nonreduced ROS (1 mg/ml total protien) were solubilized in an equal volume of denaturing buffer consisting of 1% SDS, 100 mM NEM and PMSF in PBS. The solution was then diluted 10-fold with PBS containing 2% Triton X-100 and PMSF and the peripherin-2 and rom-1 containing complexes were selectively adsorbed to either Per2B6-Sepharose or Rom1C6-Sepharose as described in section 3.2.3. Bound protein was eluted with 2% SDS in PBS and analyzed under nonreducing conditions by SDS-PAGE and Western blotting.

To examine subunit interactions within the core tetramer, Triton X-100 solubilized and Per2B6-purified peripherin-2:rom-1 complex from DTT-reduced ROS were crosslinked with 0.01% glutaraldehyde as described in section 3.2.6. The immunoaffinity-purified complexes were then treated with SDS denaturing buffer and isolated on Per2B6-Sepharose as described in section 3.2.3.

3.2.9 SDS-PAGE and Western blotting

Samples were denatured with an equal volume of SDS cocktail (4% SDS, 0.02M Tris-HCl, pH 6.8, 40% sucrose, 0.01% Bromophenol blue in the absence (nonreducing) or presence (reducing) of 5% β-mercaptoethanol, and 20 μl were applied to an 8% or 10% SDS polyacrylamide gel. After electrophoresis, the proteins were transferred to Immobilon-P using a BioRad semidry transfer apparatus and the blots were labeled with the Per2B6 or Rom1C6 monoclonal antibodies (Molday, Hicks & Molday, 1987; Moritz & Molday, 1996) and sheep anti-mouse immunoglobulin–peroxidase for detection by ECL (see section 2.2.5).

3.3 RESULTS

3.3.1 Reduction of peripherin-2 in ROS membranes

Previous studies have shown that a substantial portion of peripherin-2 and rom-1 from ROS migrates as disulfide-linked dimers on

nonreducing SDS polyacrylamide gels (Bascom *et al.*, 1992b; Connell & Molday, 1990; Molday, Hicks & Molday, 1987; Travis, Sutcliffe & Bok, 1991). To determine if the intermolecular disulfide bond responsible for these dimers can be reduced within the membrane environment, ROS were treated with 10 mM DTT for various times and the disappearance of peripherin-2 dimer was monitored on Western blots of nonreducing SDS gels. As shown in **Fig 13A & B**, peripherin-2-containing dimer was exponentially reduced to monomer by DTT with a half-time of 9.8 ± 0.7 min. A similar rate of reduction was observed for Triton X-100 solubilized peripherin-2 and for membrane bound and solubilized rom-1 (data not shown). In contrast, glutathione was ineffective as a reducing agent even in the presence of Triton X-100, presumably due to either lower reactivity or inaccessibility of this reagent to the intermolecular disulfide bond (**Fig 13B**). Cysteine, on the other hand, was able to reduce detergent solubilized peripherin-2, but at a slower rate than that observed for DTT (data not shown).

3.3.2 Velocity sedimentation of ROS peripherin-2 and rom-1 under non-reducing conditions

A two dimensional separation technique was devised to assess the contribution of intermolecular disulfide bonds to the oligomeric structure of the peripherin-rom-1 complex from ROS membranes. In the first

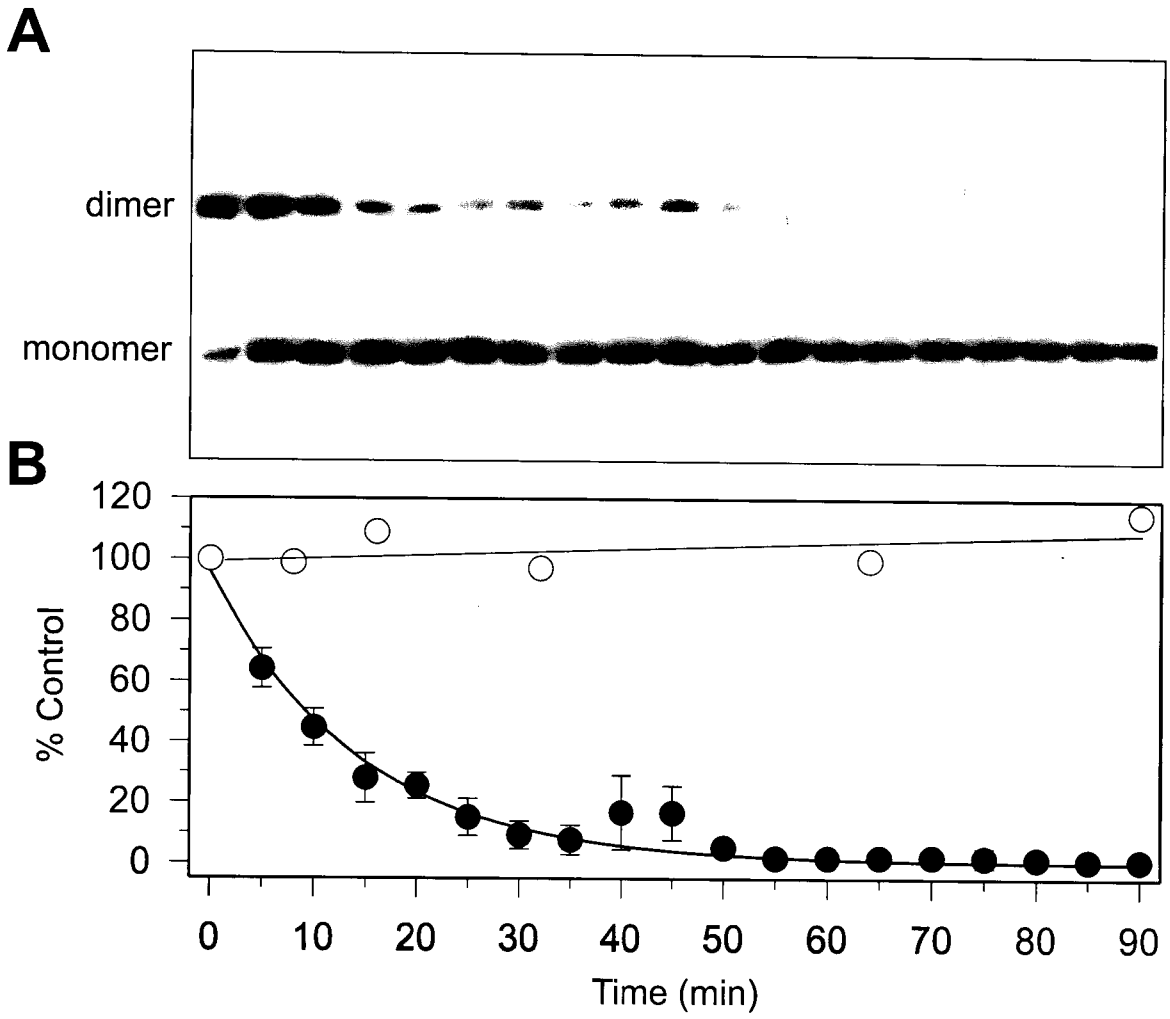

Fig 13. **Rate of reduction of disulfide-linked peripherin-2 dimers in ROS membranes.** Bovine ROS membranes were incubated with 10 mM DTT or 10 mM glutathione in the presence or absence of Triton X-100. After various times, the reaction was stopped by the addition of NEM and peripherin-2 dimer reduction was analyzed on a 10% SDS-polyacrylamide gel under nonreducing conditions. (A) Western blot labeled with the Per2B6 antibody showing the time-dependent reduction of peripherin-2 dimer by DTT. (B) Time course for the reduction of peripherin-2 dimer by 10 mM DTT (●) and 10 mM glutathione in the presence of Triton X-100 (o). Rate of reduction was quantified by laser densitometry of Western blots. DTT induced decrease in dimer was fitted as a single exponential decay with a half-time of 9.8 ± 0.7 min (n = 3) (see Methods section 3.2.2).

dimension, velocity sedimentation was used to resolve oligomeric forms of Triton X-100 solubilized peripherin-2-rom1 complexes from nonreduced (-DTT) and reduced (+DTT) membranes. In the second dimension, fractions from the velocity sedimentation were treated with NEM to block free sulfhydryl groups and subjected to SDS-PAGE under nonreducing conditions for detection of disulfide-linked dimers by Western blotting.

Fig 14A & B show the two dimensional analysis of immunoaffinity purified peripherin-2-rom1 complex from reduced (+DTT) ROS membranes. Both peripherin-2 and rom-1 co-sedimented as a single species (fractions 9-12) with a sedimentation coefficient $s_{20,w}$ of ~ 5.1 S, a value that has been previously reported to correspond to a peripherin-2:rom-1 tetramer (Goldberg, Loewen & Molday, 1998; Goldberg & Molday, 1996b). Further analysis by SDS-PAGE under nonreducing conditions indicated that this species lacked disulfide-linked dimers.

Peripherin-2 containing proteins from nonreduced ROS, treated with NEM to prevent secondary sulfhydryl oxidation, showed a more complex behavior (**Fig 14C & D**). Three peripherin-2 containing components and two rom-1 containing components were resolved by velocity sedimentation. Component *a* (fractions 9-12) sedimented at the same rate as the DTT reduced complex and like this complex consisted solely of peripherin-2 and rom-1 monomers when analyzed on

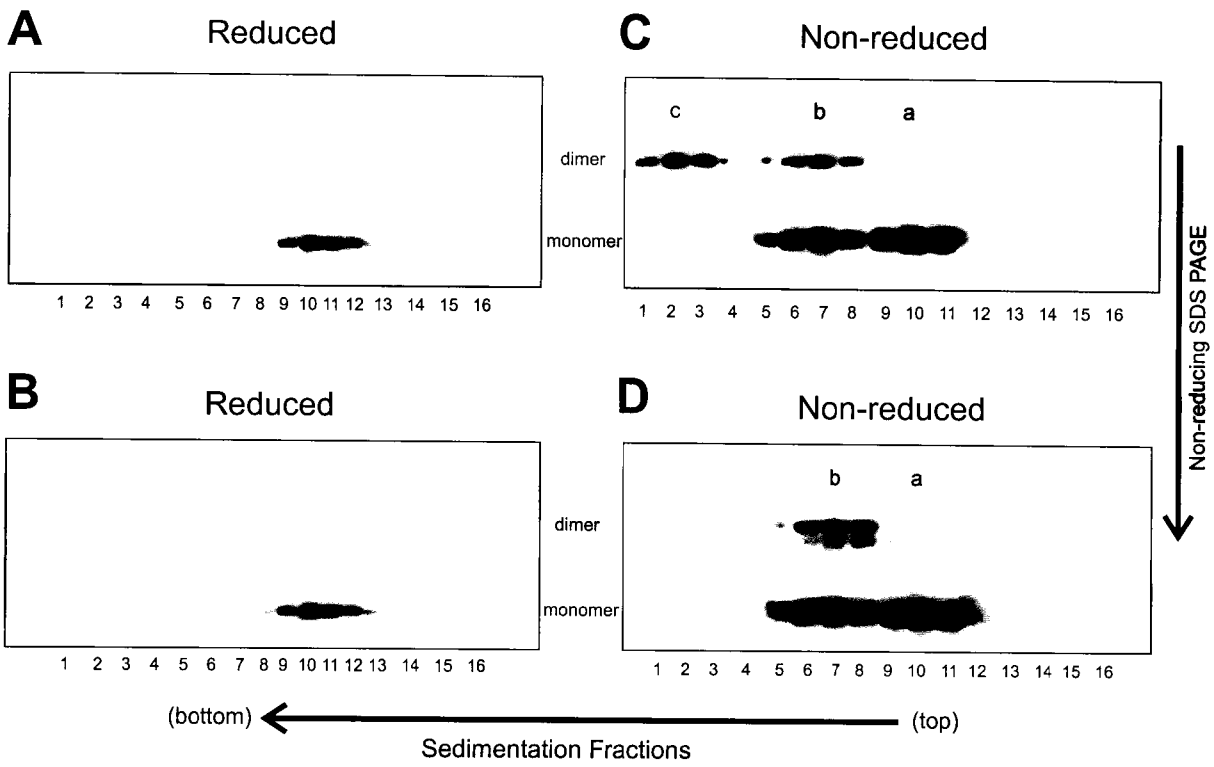

Fig 14. **Velocity sedimentation and Western blot analysis of peripherin-2 and rom-1 from reduced and nonreduced ROS membranes.** DTT-reduced (A&B) or nonreduced (C&D) ROS membranes were solubilized in Triton X-100 containing NEM. Peripherin-2 containing complexes were isolated on a Per2B6-Sepharose affinity matrix and subjected to velocity sedimentation on a sucrose gradient. Fractions were treated with NEM and subjected to SDS-gel electrophoresis under nonreducing conditions. Western blots were labeled for Peripherin-2 with the Per2B6 antibody (A&C) and Rom-1 with the Rom1C6 antibody (B&D). Three peripherin-2 containing components (*a*, *b*, and *c*) and two Rom-1 containing components (*a* and *b*) were resolved from nonreduced ROS membranes (see Methods sections 3.2.3 and 3.2.5).

nonreducing SDS gels. Component *b* (fractions 5-8) sedimented at a faster rate ($s_{20,w}$ = 7.2 S) characteristic of a larger oligomer. This component contained both monomers and disulfide-linked dimers of peripherin-2 and rom-1 proteins when analyzed on nonreducing SDS gels. Peripherin-2 containing dimers appeared as a single band, whereas rom-1 containing dimers were resolved into a doublet. The upper band of the rom-1 doublet co-migrated with the peripherin-2 band and likely corresponds to disulfide-linked peripherin-2:rom-1 heterodimer. The less intense lower band of the rom-1 doublet lacked peripherin-2, and therefore, most likely corresponds to disulfide-linked rom-1 homodimers. Component *c* (fractions 1-3) sedimented with an $s_{20,w}$ of >11 S characteristic of a higher-order oligomer. Interestingly, this component lacked rom-1 and consisted exclusively of disulfide-linked peripherin-2 homodimers. Similar results were obtained when detergent solubilized ROS were subjected to velocity sedimentation without prior isolation of the peripherin-2 complexes except that component *c* was spread more evenly throughout the lower fractions of the gradient indicative of oligomers of various sizes (data not shown).

The relative amounts of peripherin-2 and rom-1 in the three components resolved by velocity sedimentation were determined by Western blotting and laser densitometry. Analysis was performed on the fractions subjected to SDS-PAGE under reducing conditions in which

peripherin-2 and rom-1 migrated as monomers. Approximately, 35% of peripherin-2 was present in the core complex (component a), 25% in the intermediate oligomer (component b) and 40% in the higher order oligomer (component c). In the case of rom-1, 56% of rom-1 was present in component *a* and 44% in component *b*.

These results indicate that peripherin-2 and rom-1 interact through noncovalent bonds to form core homomeric and heteromeric complexes, presumably tetramers. A significant portion of these complexes interacts through intermolecular disulfide bonds to form larger oligomers, a large fraction of which is devoid of rom-1.

3.3.3 Velocity sedimentation of peripherin-2, rom-1, and C150S-peripherin-2 expressed in COS-1 cells under non-reducing conditions

Previously, peripherin-2 and rom-1 separately expressed in COS-1 cells were shown to self-assemble into a multisubunit complex that sedimented as a tetramer under mildly reducing conditions (Goldberg, Loewen & Molday, 1998; Goldberg & Molday, 1996b; Goldberg, Moritz & Molday, 1995). We have now used the two-dimensional separation technique to analyze for the disulfide-linked oligomerization of individually expressed peripherin-2 and rom-1. As shown in **Fig 15A & B**, both peripherin-2 and rom-1 from DTT-treated membranes sedimented as a

single species as previously shown (Goldberg, Moritz & Molday, 1995). Further analysis by SDS-PAGE under nonreducing conditions indicated that these complexes lacked disulfide-linked dimers.

The velocity sedimentation profile of peripherin-2 from nonreduced (-DTT) COS-1 cell membranes showed larger peripherin-2 oligomers in addition to the core complex (**Fig 15D**). The oligomers consisted exclusively of disulfide-linked peripherin-2 dimers when analyzed by SDS-PAGE under nonreducing conditions. In contrast, rom-1 from nonreduced COS-1 cell membranes showed little tendency to form disulfide-linked oligomers, but instead sedimented primarily as the core complex lacking intermolecular disulfide bonds (**Fig 15E**).

Cysteine at position 150 in the large intradiscal loop of peripherin-2 has been reported to be responsible for disulfide-linked dimerization of peripherin-2 (Goldberg, Loewen & Molday, 1998) (see section 2.3.2). To further examine the role of this cysteine in oligomerization, the sedimentation behavior and disulfide linked dimerization of the C150S peripherin-2 mutant was examined. As shown in **Fig 15C & F**, the C150S mutant from reduced (+DTT) and nonreduced (-DTT) COS-1 cell membranes sedimented as a single core complex devoid of intermolecular disulfide bonds. These studies indicate that C150 mediates disulfide-linked oligomerization of peripherin-2 core complexes.

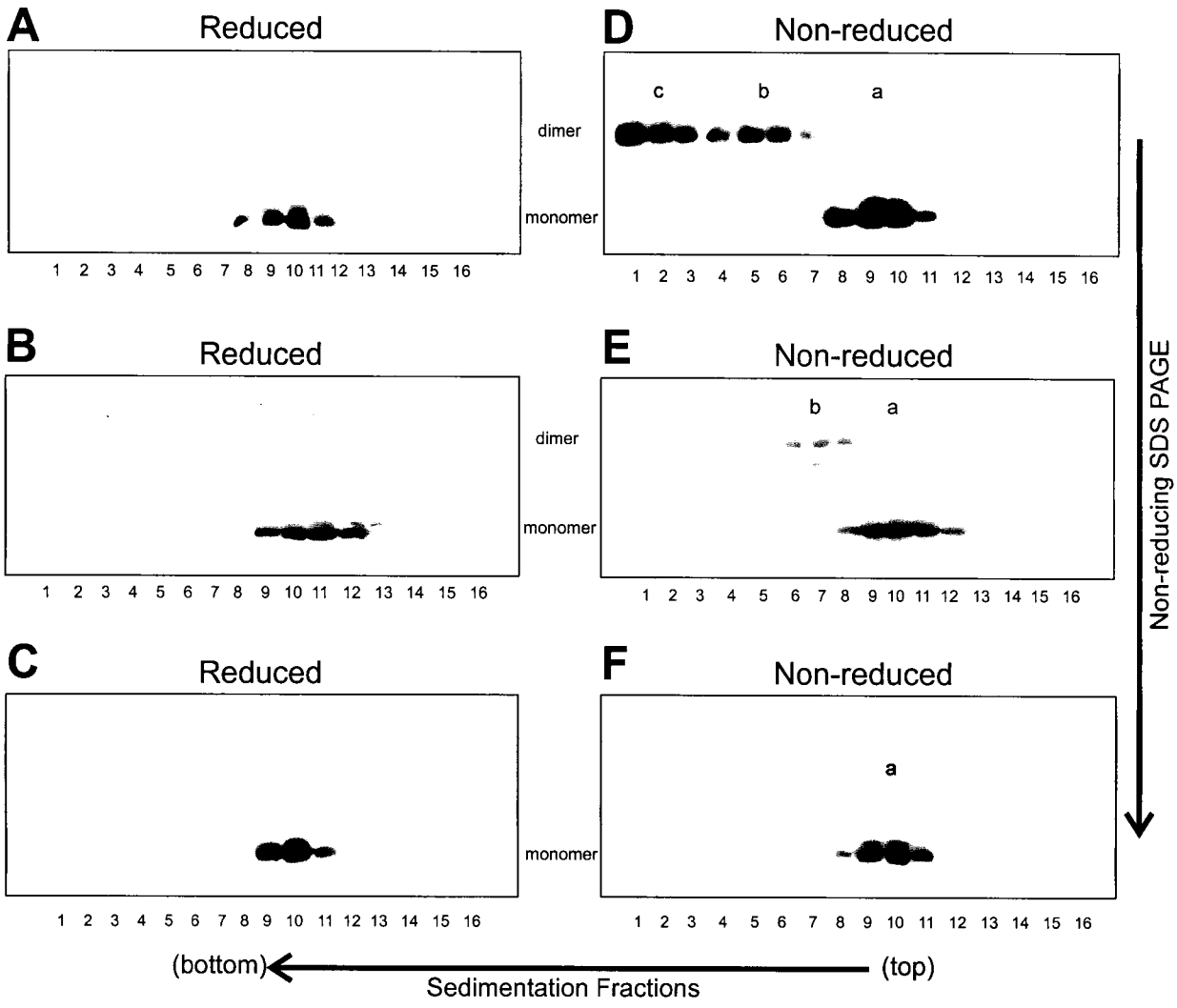

Fig 15. **Velocity sedimentation and Western blot analysis of heterologously expressed peripherin-2 and rom-1 from reduced and nonreduced COS-1 cell membranes**. Peripherin-2 (A&D), Rom-1 (B&E), and C150S (C&F) peripherin-2 were individually expressed in COS-1 cells. Cells pretreated with DTT (A,B&C) or without DTT (D,E&F) were solubilized with Triton X-100 containing NEM and subjected to velocity sedimentation. Fractions were analyzed on nonreducing SDS gels for detection of peripherin-2 with Per2B6 antibody (A,C,D&F) and Rom-1 with Rom1C6 antibody (B&E) (see Methods sections 3.2.4 and 3.2.5).

3.3.4 Crosslinking of ROS peripherin-2 under nonreducing conditions

Covalent crosslinking was used to further analyze subunit associations and disulfide-linked oligomerization of peripherin-2 and-rom-1. In these studies, DTT-reduced and nonreduced ROS membranes were solubilized in Triton X-100, purified on a Per2B6-Sepharose matrix and crosslinked with glutaraldehyde for analysis by SDS-PAGE under reducing conditions. Western blots in **Fig 16A** show that a substantial portion of peripherin-2 and rom-1 from reduced membranes was crosslinked to dimers. Only a faint band corresponding to a tetramer was detected when a relatively high glutaraldehyde concentration (0.01%) was used. In contrast, crosslinking of peripherin-2 and rom-1 from nonreduced, NEM-treated membranes produced a series of high molecular weight crosslinked multimers in addition to monomers and dimers (**Fig 16B**). These results indicate that peripherin-2 and rom-1 from DTT reduced ROS membranes preferentially crosslink into dimers, whereas the protein from nonreduced membranes crosslink into larger multimeric species, a result that is consistent with the presence of large oligomers observed in velocity sedimentation experiments.

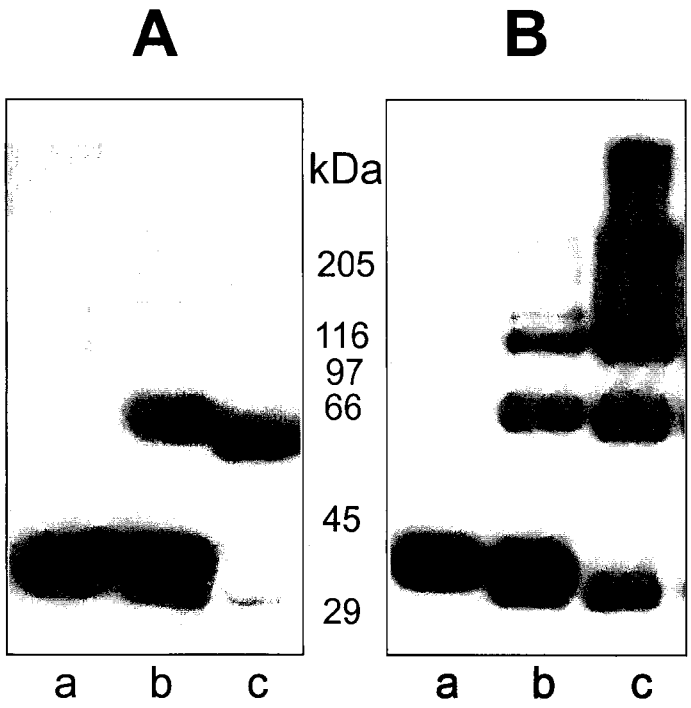

Fig 16. **Cross-linking of peripherin-2 and rom-1 from reduced and nonreduced ROS membranes.** ROS membranes were incubated in the presence (A) or absence (B) of 10 mM DTT and solubilized in Triton X-100 containing NEM. Peripherin-2 containing complexes were purified on Per2B6-Sepharose and cross-linked with 0% (lane a), 0.001% (lane b), and 0.01% glutaraldehyde (lane c). Western blots were labeled for peripherin-2 with the Per2B6 antibody.

3.3.5 Denaturation, isolation, and quantitation of peripherin-2 and rom-1 subunits from ROS

To determine the ratio of peripherin-2 and rom-1 in ROS, an immunoaffinity based method was developed to separate both covalently and noncovalently-linked subunits. After reduction by DTT to disrupt disulfide dimers, ROS samples were denatured in SDS to disrupt noncovalent associations, diluted with Triton X-100 to decrease the SDS concentration, and subjected to affinity chromatography with Per2B6-Sepharose or Rom1C6-Sepharose matrix to isolate peripherin-2 and rom-1 respectively. Purity was assessed by SDS-PAGE and Western blotting (**Fig 17**). Peripherin-2 was present only in the bound fraction and rom-1 was found in the unbound fraction of Per2B6-Sepharose matrix (**Fig 17A**). Similarly, rom-1 was present only in the bound fraction of Rom1C6-Sepharose matrix (**Fig 17B**) and peripherin-2 was detected in the unbound fraction. Therefore, the purified fractions of these immunoaffinity matrices contained only peripherin-2 or rom-1 and were used as standards for quantitation.

The amount of peripherin-2 and rom-1 in ROS was determined by quantifying the amount of each protein present in the bound and unbound fraction of a Per2B6-Sepharose matrix purification performed under non-denaturing conditions (data not shown; see Methods section 3.2.7). Peripherin-2 was only present in the bound fraction and

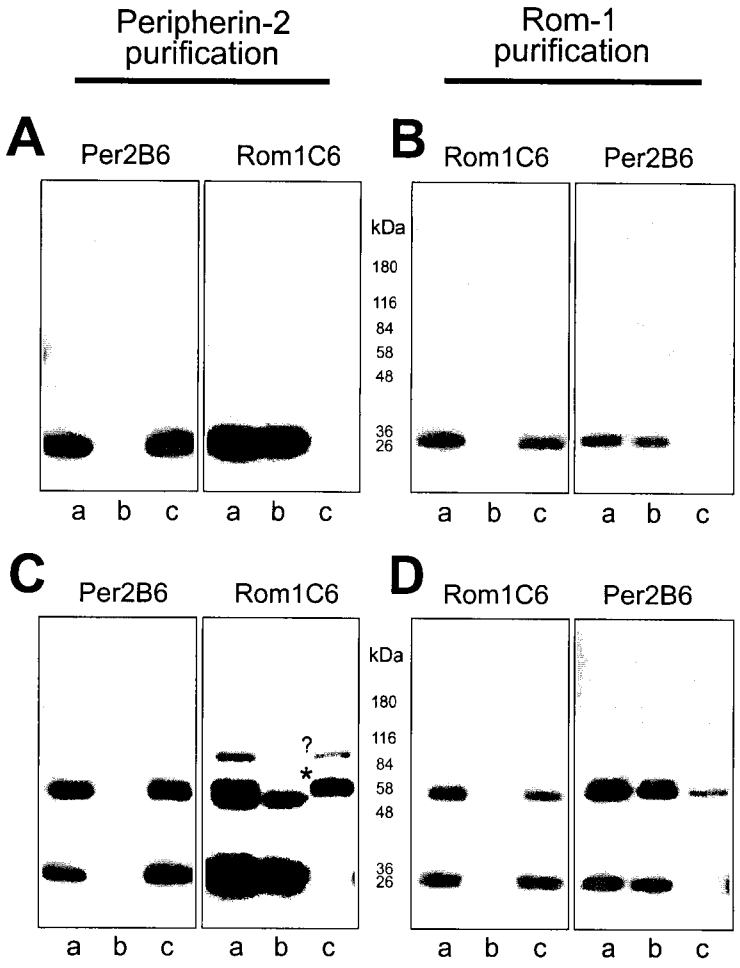

Fig 17. **Analysis of subunits involved in disulfide-linked dimers.** DTT reduced (A&B) or nonreduced (C&D) ROS membranes were denatured in 0.5% SDS to disrupt noncovalent interactions. After dilution with Trition X-100, peripherin-2 containing complexes were isolated on a Per2B6-Sepharose matrix (A&C) and rom-1 containing complexes were isolated on a Rom1C6-Sepharose matrix (B&D). Equivalent volumes of the initial extract (lane a), the unbound fraction (lane b), and the SDS eluted fraction (lane c) were analyzed on Western blots labeled with Per2B6 or Rom1C6 antibody (see Methods section 3.2.8).

constituted 2.1%±0.3 (n=6) of the ROS protein by weight. Rom-1 was present in both the bound and unbound fractions and together comprised 1.1%±0.2 (n=6) of the total ROS protein. Approximately 14% of total rom-1 was detected in the unbound fraction. This rom-1 component lacking peripherin-2 migrated solely as monomers by SDS-PAGE under nonreducing conditions (data not shown). The inability of rom-1 to form disulfide-linked homodimers in the absence of peripherin-2 is consistent with the behavior of rom-1 expressed in COS-1 cells.

3.3.6 Disulfide dimer formation between peripherin-2 and rom-1

The subunit composition of disulfide-linked dimers from non-reduced ROS membranes was determined using the SDS-denaturation-purification method described in section 3.3.5, but reduction by DTT was omitted. **Fig 17C** shows Western blots of the unbound and bound fractions from Per2B6-Sepharose and **Fig 17D** from Rom1C6-Sepharose. The unbound fraction of Per2B6-Sepharose contained rom-1 monomer and a smaller amount of disulfide-linked rom-1 homodimer, but was devoid of peripherin-2. The bound fraction contained both peripherin-2 monomer and disulfide-linked dimer (* in Fig 17C). This dimer migrated more slowly than the rom-1 disulfide-linked homodimer in the unbound fraction. It most likely represents a mixture of disulfide-linked peripherin-2 homodimer and peripherin-2:rom-1 heterodimer that are not

resolved in this gel system. An additional rom-1 containing band was routinely observed above the dimer in the bound fraction (? in Fig 17C). The nature of this species is not known at the present time. The unbound fraction from the Rom1C6-Sepharose matrix contained peripherin-2 monomer and disulfide-linked homodimer, but no rom-1. The bound fraction exhibited bands corresponding to rom-1 monomer and a disulfide-linked dimer. Since peripherin-2 was also present in the latter, this dimer band appears to contain peripherin-2:rom-1 heterodimer. These results indicate that oligomers are generated through disulfide bridges between peripherin-2-peripherin-2 subunits, peripherin-2:rom-1 subunits and rom1-rom-1 subunits of the core complexes.

3.3.7 Crosslinking of peripherin-2 and rom-1 under reducing conditions

The subunit composition of glutaraldehyde-crosslinked dimers of peripherin-2 and rom-1 from DTT treated ROS was also investigated using the SDS-denaturation-purification technique. Per2B6-purified peripherin-2:rom-1 complex from reduced ROS was crosslinked with glutaraldehyde prior to denaturation with SDS and subsequent purification with Per2B6-Sepharose. As shown in **Fig 18B**, the unbound fraction of the Per2B6-Sepharose matrix contained primarily rom-1

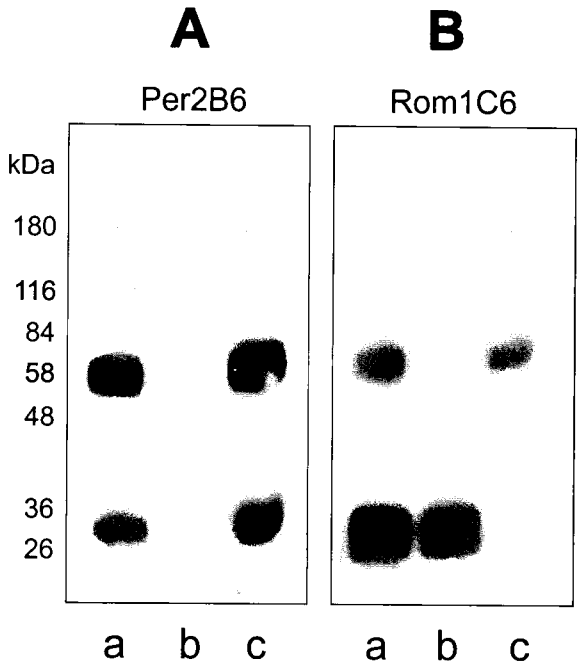

Fig 18. **Glutaraldehyde crosslinking of subunits within the core complex.** Immunoaffinity purified peripherin-2 containing complex from DTT-reduced ROS membranes was cross-linked with 0.01% glutaraldehyde. The complex was treated with SDS to disrupt noncovalent interactions and purified on a Per2B6-Sepharose matrix. The extract (lane a), unbound (lane b) and SDS-eluted fraction (lane c) were analyzed on Western blots labeled with Per2B6 (A) or Rom1C6 (B) antibody under reducing conditions (see Methods sections 3.2.6 and 3.2.8).

monomer. This fraction of rom-1 was not associated with peripherin-2 (compare to Fig 18A, lane b). The bound fraction contained both peripherin-2 monomer and crosslinked dimer (**Fig 18A**, lane c). Rom-1 was also detected in the dimer band indicating that at least a fraction of this dimer is composed of peripherin-2:rom-1 heterodimer. Thus, within the core complexes, peripherin-2 can be covalently crosslinked to itself or to rom-1 to generate dimers. Glutaraldehyde, however, is ineffective in crosslinking two rom-1 subunits.

3.4 DISCUSSION

The peripherin-2:rom-1 complex of ROS disc membranes was previously thought to consist of disulfide-linked homodimers of peripherin-2 and rom-1 that interact noncovalently to form a heterotetrameric protein (Bascom *et al.*, 1992b; Goldberg & Molday, 1996b). This model was based on the findings that **1)** a substantial fraction of peripherin-2 and rom-1 migrates as disulfide-linked homodimers on nonreducing SDS gels; **2)** rom-1 co-purifies with peripherin-2 by immunoaffinity chromatography; and **3)** detergent solubilized peripherin-2:rom-1 complex possesses hydrodynamic properties consistent with a tetrameric complex. However, the hydrodynamic experiments were carried out in the presence of DTT and

the existence of disulfide-linked dimers under these conditions was not determined.

Velocity sedimentation measurements reported here indicate that this simple model is not correct. Instead, our results suggest a novel disulfide-mediated oligomerization model as depicted in **Fig 19**. Peripherin-2 and rom-1 in ROS membranes interact noncovalently to form multisubunit core complexes. A major portion of the peripherin-2-containing complexes links together via intermolecular disulfide bonds to form intermediate and higher order oligomers.

The core complex is a mixture of homomeric and heteromeric multisubunit proteins. Peripherin-2-peripherin-2 homomeric and peripherin-2:rom-1 heteromeric core proteins are the most abundant species and readily form disulfide-linked oligomers. Rom-1 homomeric core protein constitutes only about 10% of these complexes and shows little capacity to form disulfide-linked oligomers. The size of the core complex has been previously estimated to be a tetramer by hydrodynamic measurements (Goldberg & Molday, 1996b). Subunits of the complex, however, preferentially crosslink into dimers by glutaraldehyde and other crosslinking agents. Previous studies indicate that the large intradiscal loop is involved in noncovalent subunit interactions (Goldberg, Loewen & Molday, 1998; Goldberg & Molday, 1996a). It is possible that reactive groups in this segment are not

Fig 19. **Disulfide-mediated oligomerization model for peripherin-2 and rom-1.** Peripherin-2 (dark fill) and rom-1 (white fill) interact noncovalently via their large intradiscal loops to produce homotetrameric and heterotetrameric core complexes. The Cys-150 of peripherin-2 and corresponding Cys-153 of rom-1 located within the large intradiscal loop of these proteins are in their reduced form (SH). A large portion of the peripherin-2 homotetramers link together through Cys-150 mediated intermolecular disulfide bonds to form intermediate size homo-octamers. These oligomers can further associate to form higher order disulfide-linked homo-oligomers. All subunits in the peripherin-2 homo-oligomers contain intermolecular disulfide bonds since only disulfide-linked dimers are observed on nonreducing SDS gels. A significant portion of the peripherin-2-rom-1 heterotetramers are linked together via intermolecular disulfide bonds to form hetero-octamers. Only some of the subunits within these hetero-octamers are disulfide bonded since both monomer and disulfide-linked dimers are observed on nonreducing SDS-gels. Intermolecular disulfide bonds can form between two peripherin-2 subunits, two rom-1 subunits or a peripherin-2 and rom-1 subunit. The hetero-octamers do not form higher order oligomers. Rom-1 homotetramers present in relatively low amounts do not readily form disulfide-linked oligomers.

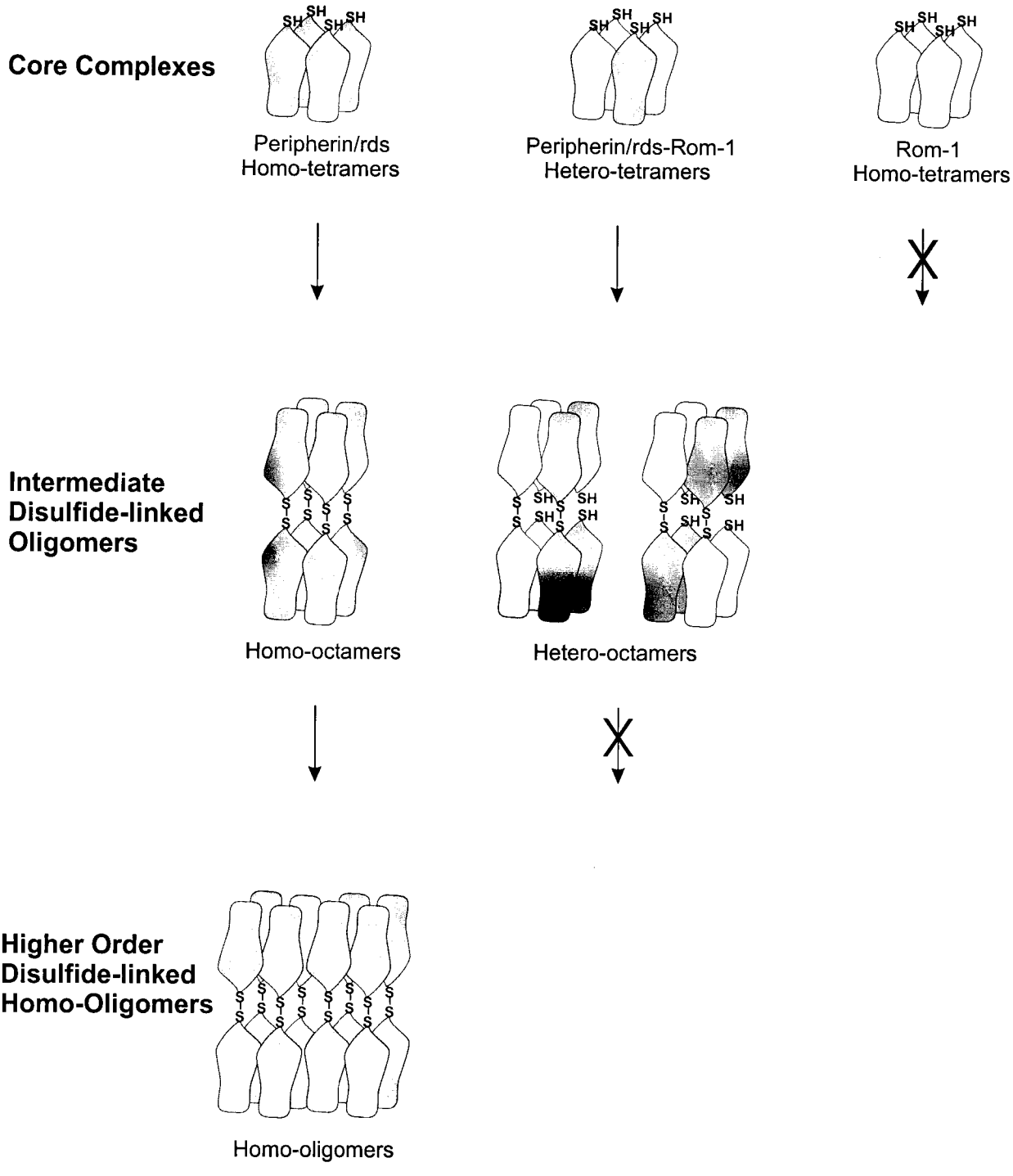
Core Complexes
Peripherin/rds
Homo-tetramers
Peripherin/rds-Rom-1
Hetero-tetramers
Rom-1
Homo-tetramers
Intermediate
Disulfide-linked
Oligomers
Homo-octamers
Hetero-octamers
Higher Order
Disulfide-linked
Homo-Oligomers
Homo-oligomers

accessible for efficient crosslinking of the subunits into tetramers by glutaraldehyde.

Two classes of peripherin-2-containing oligomers are observed by velocity sedimentation under nonreducing conditions. One class designated as component *b* (**Fig 14**) is intermediate in size and contains both peripherin-2 and rom-1 subunits. Only some of the subunits in the hetero-oligomers participate in intermolecular disulfide bonds since both monomers and dimers are observed by SDS-PAGE under nonreducing conditions. The size of this oligomer is estimated to be twice the size of the core complex based on the relationship of the sedimentation coefficients to molecular weights (Martin & Ames, 1961) and the assumption that both species bind similar amounts of detergent per core complex. The intermolecular disulfide bonds that link the peripherin-2 containing core complexes together are formed between two peripherin-2 subunits, a peripherin-2 and a rom-1 subunit, or two rom-1 subunits. The second, large class of oligomers is composed exclusively of peripherin-2 subunits, all of which participate in intermolecular disulfide bonds.

Treatment of ROS membranes with DTT results in the complete breakdown of the oligomers into core complexes indicating that the intermolecular disulfide bonds are readily accessible to this reducing agent and essential for oligomerization. Quantitative analysis indicates

that peripherin-2 is present at almost twice the concentration of rom-1 in ROS, a finding that is consistent with the presence of a significant amount of peripherin-2 homo-oligomers detected by velocity sedimentation analysis. Earlier studies failed to detect the presence of peripherin-2 and rom-1 homotetrameric core complexes in ROS (Bascom *et al.*, 1992b; Moritz & Molday, 1996). This may be due to the inability to detect smaller amounts of peripherin-2 and rom-1 in the presence of large amounts of rhodopsin by Western blotting and/or the use of less sensitive antibodies in these studies.

Peripherin-2 and rom-1 expressed in COS-1 cells show a related pattern of disulfide-mediated oligomerization. A major fraction of the peripherin-2 core complex interacts through intermolecular disulfide bonds to form intermediate and higher order oligomers of various sizes. As in the case of ROS, all the subunits in these oligomers participate in intermolecular disulfide bond formation. Rom-1 expressed in COS-1 cells also self-assembles into a core complex, but this protein shows little tendency to form disulfide-linked oligomers, as observed in ROS. Mutagenesis studies have confirmed that disulfide-linked oligomerization of peripherin-2 is mediated by C150, present within the large intradiscal loop of the protein. The corresponding C153 residue in rom-1 is also likely to participate in intermolecular disulfide bond formation between heterotetrameric core complexes. However, in the absence of peripherin-

2, two C153 residues of rom-1 show little tendency to form intermolecular disulfide bonds, possibly due to limited accessibility or unfavorable alignment of these groups.

These studies taken together indicate that peripherin-2 exhibits a strong tendency to form disulfide-linked oligomers of various sizes. The association of peripherin-2 with rom-1 in the core complex limits the size of the oligomers and the number of subunits that participate in intermolecular disulfide bond formation. Thus, rom-1 can be considered as a negative modulator of peripherin-2 oligomerization.

Intermolecular disulfide bonds are known to be important in the assembly of multisubunit proteins and higher order oligomeric complexes. The light and heavy chains of immunoglobulins and the α and β subunits of the insulin receptor are joined by disulfide bonds. Intermolecular disulfide bonding is important in capsid assembly and disassembly of papillomavirus (Beard *et al.*, 1998), stabilization of vaccinia virus (Locker & Griffiths, 1999) and oligomerization of tenascin-C, an extracellular matrix protein involved in embryogenesis and tumorgensis (Luczak, Redick & Schwarzbauer, 1998).

We speculate that the disulfide-mediated oligomerization of peripherin-2 plays an important role in outer segment disc morphogenesis and stabilization. This is based on the following. The cysteine residues responsible for intermolecular disulfide bonds (C150 in

peripherin-2 and C153 in rom-1) are conserved in all vertebrate peripherin-2 and rom-1 proteins analyzed to date (Goldberg, Loewen & Molday, 1998). Disulfide dimerization of peripherin-2 is a general property of these proteins (Bascom *et al.*, 1992b; Connell *et al.*, 1991; Kedzierski *et al.*, 1996; Molday, Hicks & Molday, 1987; Travis, Sutcliffe & Bok, 1991). Sulfhydryl agents have been reported to disrupt new disc formation (Wetzel, Parsons & Besharse, 1994), and protein disulfide isomerase, a protein that functions in the making and breaking of disulfide bonds, is present in ROS discs (C. Loewen and R. Molday, unpublished). In one model, peripherin-2 and rom-1 containing homomeric and heteromeric core complexes are envisioned to assemble in the endoplasmic reticulum membrane of photoreceptors and translocate in vesicles to the base of outer segments. Specific chaperone proteins may prevent disulfide-linked oligomerization from occurring during this trafficking process. At the base of the outer segment, protein disulfide isomerase would catalyze disulfide-mediated oligomerization of peripherin-2 containing homomeric and heteromeric core complexes across juxtaposed newly forming disc membranes to effectively zipper together the rim region as part of outer segment morphogenesis. The idea that membrane proteins can mediate membrane adhesion is not new. The major structural protein, Po, of peripheral nerve myelin is a tetrameric complex. The extracellular domains of these complexes from

opposing membranes interact with each other to mediate myelin membrane adhesion (Shapiro *et al.*, 1996). In this case, however, protein-protein associations occur through noncovalent interactions.

An alternative mechanism would involve disulfide-linked oligomerization of peripherin-2 containing core complexes laterally within a membrane. These oligomers could be envisioned to initiate the disc rim curvature or promote interactions with other outer segment proteins that participate in outer segment formation. Efforts are now underway to examine more directly the role of disulfide-mediated oligomerization of peripherin-2 in disc morphogenesis.

Peripherin-2 and rom-1 differ significantly with respect to their role in outer segment morphogenesis. Peripherin-2 is essential for outer segment morphogenesis since homozygous rds mice lacking this protein fail to form outer segments (Sanyal & Jansen, 1981). Rom-1, on the other hand, appears to regulate the fine structure of the outer segment discs since homozygous rom-1 knockout mice produce outer segments with slightly enlarged discs (Clarke *et al.*, 2000). Disulfide-mediated oligomerization supports the dominant role of peripherin-2 in outer segment disc morphogenesis. In addition to being more abundant than rom-1 in ROS, peripherin-2 is required for the formation of intermediate and higher order disulfide-linked oligomers, a process that may be crucial for disc morphogenesis as discussed above. Rom-1, on the other hand,

does not form higher order oligomers, and therefore would not be considered to be essential for disc morphogenesis. Rom-1 may simply serve to limit the formation of higher order peripherin-2 oligomer formation through interactions with peripherin-2 and thereby regulate the size of the discs during outer segment morphogenesis.

A relatively large number of missense mutations in the large intradiscal loop of peripherin-2 have been linked to a variety of human retinal degenerative diseases. Previous studies have indicated that some of these mutations affect protein folding and subunit assembly (Goldberg, Loewen & Molday, 1998; Goldberg & Molday, 1996a). A consequence of the misfolding of this large loop may be the inability of the peripherin-2 mutants to form intermolecular disulfide bonds or other interactions required for oligomerization. Such mutations in rom-1 would have less impact since disulfide-linked oligomerization of rom-1 is not crucial to outer segment morphogenesis and structure.

In summary, we have shown here that peripherin-2 and rom-1 associate noncovalently to form homomeric and heteromeric core complexes. Peripherin-2 containing complexes interact via Cys150 mediated intermolecular disulfide bonds to form oligomers that may play an important role in rod and cone outer segment morphogenesis.

CHAPTER 4 – MOLECULAR ANALYSIS OF DIGENIC RP

4.1 INTRODUCTION

Individuals who co-inherit a L185P peripherin-2 mutation and a null or G113E rom-1 mutation are afflicted with retinitis pigmentosa, whereas individuals who inherit only one defective gene are normal (Dryja *et al.*, 1997; Kajiwara, Berson & Dryja, 1994). Biochemical studies have shown that the L185P peripherin-2 mutant assembles with rom-1 to form core heterotetrameric complexes, but unlike WT peripherin-2, it is unable to self-assemble into core homotetramers (Goldberg & Molday, 1996a) (see section 1.4.2). These findings have been incorporated into a disease model in which decreased levels of tetrameric complexes result in RP. **Fig 20** shows the location of these mutations and conserved structural elements in peripherin-2 and rom-1.

This chapter focuses on the molecular interactions involved in digenic RP and the importance of disulfide-mediated oligomerization in maintaining normal photoreceptor function. Analysis of L185P peripherin-2 and several related mutants has lead to greater understanding of the structure of the core complex and of the requirements for disulfide-mediated oligomerization.

Most of the methods used in these studies have been published elsewhere (Loewen, Moritz & Molday, 2001). All experiments described in this chapter were performed by the author except (1) hydrodynamic

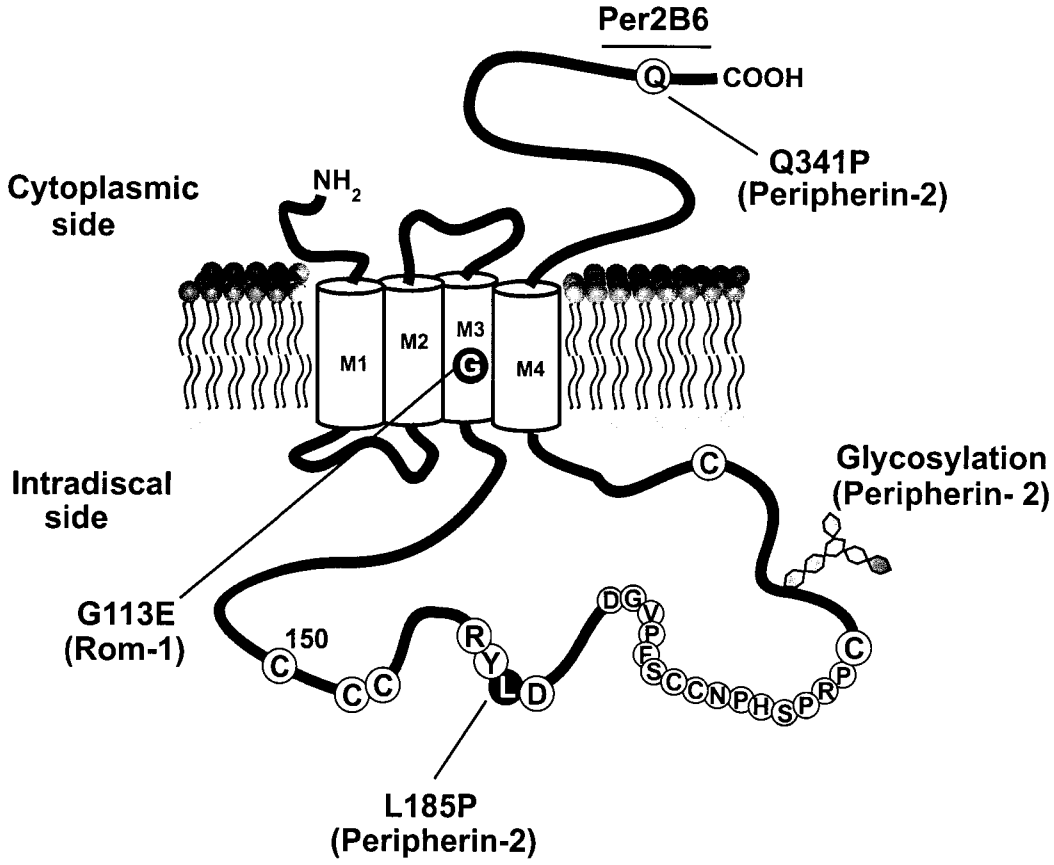

Fig 20. **Topological model of peripherin-2 and rom-1 subunits.** Conserved amino acid segments between peripherin-2 and rom-1 and conserved cysteine residues within the large intradiskal L3-4 loop are shown. The locations of the L185P peripherin-2 and G113E rom-1 missense mutations linked to digenic retinitis pigmentosa are indicated with a black circle. The binding site for the peripherin-2 monoclonal antibody Per2B6 and the Q341P substitution that abolishes binding are also indicated. M1-M4 indicate transmembrane segments 1-4.

analysis of L185P (Fig 21); (2) velocity sedimentation of L188P rom-1 (Fig 23B).

4.2 MATERIALS AND METHODS

4.2.1 Plasmids and heterologous COS-1 cell expression

pcPer (WT peripherin-2), pcPer-L185P (L185P peripherin-2), and pcROM (WT rom-1) have been described (Goldberg, Loewen & Molday, 1998; Goldberg, Moritz & Molday, 1995; Moritz & Molday, 1996). pcPer-L185A (L185A peripherin-2), and pcROM-L188P (L188P rom-1) were constructed by PCR-based mutagenesis (Nelson & Long, 1989). pcPer1D4, containing a Rho1D4 monoclonal antibody epitope tag TETSQVAPA at the C-terminus was created by ligating an oligonucleotide corresponding to the 1D4 epitope onto the 3′ end of the peripherin-2 cDNA. A Q341P change that abolishes the binding of monoclonal antibody Per2B6 was also introduced into this construct by site-directed mutagenesis. pcL185P-1D4 (pcPer1D4 with the L185P mutation) was created by cloning the BamHI-SacII restriction fragment from pcPer-L185P into BamHI-SacII digested pcPer1D4.

COS-1 cells (ca. 6×10^5 cells/100-mm dish) were transfected with a total of 30 μg of plasmid DNA and harvested 72 h post-transfection as described in section 3.2.4.

4.2.2 Hydrodynamic characterization of L185P peripherin-2

Hydrodynamic analysis of the L185P mutant under reducing conditions was carried out as described previously for wild-type peripherin-2 (Goldberg & Molday, 1996b). Briefly, pcPer-L185P transfected cells from one 100 mm dish were solubilized in 300 - 500 μl PBS containing 1% Triton X-100, 2mM DTT, and PMSF, and centrifuged at 90,000 × g for 30 min at 4°C. The supernatant was used to determine the hydrodynamic properties of the detergent-solubilized complex. The Stokes radius was determined by gel exclusion chromatography on a calibrated Sephacryl S-300 column. Velocity sedimentation analysis was performed by centrifugation at 4°C in a Beckman SW 50.1 rotor at 49,000 rpm for 13 h on sucrose gradients in H_2O and 28 h for gradients in D_2O. Fractions were collected and analyzed on Western blots. Calibration standards (Stokes radius, sedimentation coefficient (Svedbergs), partial specific volume) were cytochrome c (1.7 nm, 1.9 S, 0.728 ml/g), malate dehydrogenase (3.5 nm, 4.32 S, 0.734 ml/g), aldolase (4.6 nm, 7.70 S, 0.742 ml/g) and apoferritin (6.7 nm, 17.7 S, 0.73 ml/g) (Cascio *et al.*, 1995; Clarke & Smigel, 1989; Fasman & Chemical Rubber Company, 1975; Siegel & Monty, 1966; Worthington, 1993).

The molecular mass of the detergent-protein complex and the molecular mass of the protein portion were calculated according to the method of Clarke (Clarke & Smigel, 1989). Briefly, the sedimentation

coefficients (s), and viscosities (η) and densities (ρ) at the average sedimentation positions (determined from calibration standards and indicated by the subscript *avg*) were determined in H_2O and D_2O (denoted by the corresponding subscripts *H* and *D*) and used to calculate the partial specific volume ($\bar{\nu}$) of the complex using Equation 1.

$$\bar{\nu} = (s_D \eta_{D_{avg}} / s_H \eta_{H_{avg}} - 1) / (\rho_{H_{avg}} (s_D \eta_{D_{avg}} / s_H \eta_{H_{avg}}) - \rho_{D_{avg}}) \qquad \text{(Eq. 1)}$$

The sedimentation coefficient ($s_{20,w}$) for the complex under standard conditions (20 °C, water) was determined using Equation 2. The values used for $s_{T,m}, \eta_{T,m}$, and $\rho_{T,m}$ are experimentally determined values at the run temperature (subscript *T*) and in sucrose gradients in H_2O or D_2O (subscript *m*). The densities ($\rho_{20,w}$) and viscosities ($\eta_{20,w}$) of water under standard conditions of 20 °C are 0.998 g cm^{-3} and 0.01002 g cm^{-1} s^{-1}.

$$s_{20,w} = s_{T,m} (\eta_{T,m} / \eta_{20,w}) ((1 - \bar{\nu}\rho_{20,w}) / (1 - \bar{\nu}\rho_{T,m})) \qquad \text{(Eq. 2)}$$

The molecular mass of the detergent-protein complex (M_c) was calculated using the sedimentation coefficient ($s_{20,w}$), the partial specific volume ($\bar{\nu}$), and the Stokes radius (a) using Equation 3 (Siegel & Monty, 1966) where *N* is Avogadro's number.

$$M_c = (6\pi\eta_{20,w} Nas_{20,w}) / (1 - \bar{\nu}\rho_{20,w}) \quad \text{(Eq. 3)}$$

Finally, the molecular mass of the protein portion of the L185P peripherin-2 complex (M_p) was calculated using Equation 4. An average value for the partial specific volume for protein (0.74 ml/g) and for the detergent Triton X-100 (0.94 ml/g) were used in the calculation (Goldberg & Molday, 1996b).

$$M_p = M_c / (1 + (\bar{\nu} - 0.74)/(0.94 - \bar{\nu})) \quad \text{(Eq. 4)}$$

4.2.3 Solubilization, immunoprecipitation, and velocity sedimentation analysis of COS-1 cell expressed proteins

Transfected COS-1 cells from 100 mm dishes were scraped from plates, washed with PBS, and incubated with PBS in the presence or absence of 20 mM DTT for 90 min at 25°C. The cells were solubilized with an equal volume (150 µl) of PBS containing 2% Triton X-100, 80mM NEM, and PMSF (pH 7.4) for 10 min on ice. In some experiments, NEM was replaced with 1 mM DTT in the solubilization buffer. The cell extract was centrifuged at 90,000 × g for 30 min at 4°C and supernatant (solubilized fraction) was retained on ice for analysis. Peripherin-2 was purified from the solubilized fraction on a Per2B6-Sepharose immunoaffinity matrix as previously described in section 3.2.3.

Purified peripherin-2 (approximately 1-2 μg protein) was applied to 5-20% (w/w) sucrose gradients prepared in PBS and containing 0.1% Triton X-100 (Goldberg & Molday, 1996a). Routinely, 1mM DTT was included in the gradients for DTT-treated samples analyzed under reducing conditions. After centrifugation for 16 h at 50,000 rpm in a Beckman TLS-55 rotor at 4°C, the bottom of the centrifuge tube was punctured and four-drop fractions were collected for analysis by Western blotting. This procedure was used to determine apparent sedimentation coefficients for comparative purposes.

4.2.4 SDS-PAGE and Western blotting

Samples (25 μl containing 0.1-0.5 μg peripherin-2) were denatured with an equal volume of SDS cocktail (4% SDS, 0.02M Tris-HCl, pH 6.8, 20% glycerol, 0.01% bromophenol blue) in the absence (nonreducing) or presence (reducing) of 5% β-mercaptoethanol, and applied to 8 or 10% SDS-polyacrylamide gels as described (Loewen & Molday, 2000). After electrophoresis, the proteins were transferred to Immobilon-P using a Bio-Rad semidry transfer apparatus. Blots were probed with monoclonal antibodies to peripherin-2 (Per2B6) (Molday, Hicks & Molday, 1987), rom-1 (Rom1C6), or rhodopsin (Rho1D4) (MacKenzie *et al.*, 1984) and sheep anti-mouse immunoglobulin-peroxidase for detection by ECL. The Rom1C6 monoclonal antibody was generated to a GST-fusion protein

containing the intradiscal loop region of rom-1 (Moritz & Molday, 1996). Crosslinking was performed on Triton X-100 solubilized samples with 0.001% glutaraldehyde for 15min at 37°C.

4.3 RESULTS

4.3.1 Molecular mass of L185P peripherin-2 under disulfide-reducing conditions

Previous studies have shown that under reducing conditions (+DTT), the sedimentation coefficient of the L185P peripherin-2 mutant is significantly smaller than that of the tetrameric WT peripherin-2 core complex (Goldberg & Molday, 1996a). To determine how the sedimentation behaviour of this mutant relates to its molecular mass, we carried out a hydrodynamic study of the COS-1 cell expressed L185P protein under reducing conditions. As shown in **Fig 21A**, the L185P mutant eluted from a calibrated gel exclusion column as a single species with a Stokes radius of 4.83 ± .29 nm (n=5), a value that is significantly lower than the value of 6.20 ± .14 nm previously measured for the WT peripherin-2 complex (Goldberg & Molday, 1996b). The sedimentation coefficient and partial specific volume of the L185P mutant were determined by velocity sedimentation in sucrose gradients containing H_2O and D_2O (**Fig 21B**). A single detergent-protein species was observed in each case resulting in a $s_{20,w}$ value of 2.78 ± 0.06 S (n=8) and a partial

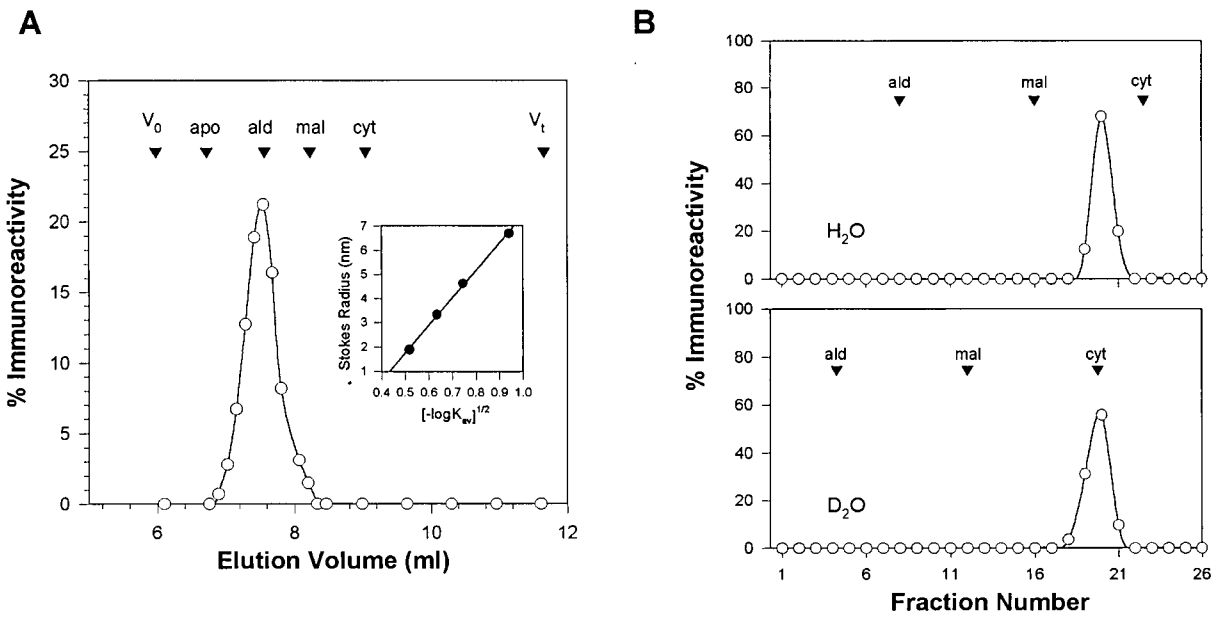

Fig 21. **Hydrodynamic analysis of COS-1 cell expressed L185P peripherin-2 mutant under reducing conditions.** COS-1 cells expressing the L185P peripherin-2 mutant were solubilized in Triton X-100 in the presence of DTT. (A) Gel exclusion chromatography of L185P peripherin-2. Inset shows calibration curve generated from standards: cytochrome c (cyt), malate dehydrogenase (mal), aldolase (ald), and apoferritin (apo) and the void (V o) and included (V t) volumes. (B) Velocity sedimentation of L185P peripherin-2 through 5-20% sucrose gradients made up with H_2O or D_2O. Peripherin-2 was detected on Western blots labeled with the Per2B6 antibody and quantified by densitometry (see Methods section 4.2.2 and 4.2.4).

specific volume of 0.82 ml/g.

There was no difference between the sedimentation profiles of unpurified and immunoaffinity purified complex (data not shown). Furthermore, since the partial specific volume of L185P peripherin-2 was similar to the native complex from rod outer segments (0.83 ml/g for native complex (Goldberg & Molday, 1996b)), the L185P mutant bound similar amounts of detergent as the native complex indicating that it was not grossly misfolded. Using the values determined for Stokes radius, sedimentation coefficient, and partial specific volume, a molecular mass of 91 kDa was calculated for the L185P detergent-protein complex according to the method of Clarke (Clarke & Smigel, 1989). Using an average value for the partial specific volume for protein (0.74 ml/g) and the value for the detergent Triton X-100 (0.94 ml/g) and assuming additivity of partial specific volumes for protein and detergent, the molecular mass was estimated to be 54 kDa for the detergent-free L185P protein complex. This value is intermediate between a L185P monomer (39 kDa) and dimer (78 kDa), but considerably less than the experimental value of 135 kDa previously measured for the native peripherin-2 tetramer (calculated Mr =152,000) from rod outer segments (Goldberg & Molday, 1996b).

To determine if the L185P mutant exists as a monomer or a dimer, a series of co-immunoprecipitation studies with the L185P mutant and a

related L185P-1D4 mutant were carried out. The L185P mutant is recognized by monoclonal antibody Per2B6; the L185P-1D4 mutant contains a 9 amino acid C-terminal epitope tag recognized by monoclonal antibody Rho1D4 and a Q341P mutation (P at position 341 is found in mouse peripherin-2) that abolishes Per2B6 immunoreactivity.

The ability of L185P and L185P-1D4 proteins to interact post-translationally was determined. As shown in **Figure 22A**, when detergent-solubilized L185P and L185P-1D4 were mixed together and immunoprecipitated with Per2B6-Sepharose under disulfide reducing conditions, L185P-1D4 mutant was eluted in the unbound fraction, whereas the L185P mutant was only present in the bound faction. This result indicates that individually expressed L185P and L185P-1D4 proteins do not associate to form a complex. This experiment also demonstrates that the Per2B6-Sepharose matrix selectively binds the L185P mutant, but not the L185P-1D4 mutant.

To determine if L185P and L185P-1D4 mutants can co-assemble into a multi-subunit complex, COS-1 cells were co-transfected with the L185P and L185P-1D4 plasmids. The cells were treated with DTT to reduce intermolecular disulfide bonds and subsequently solubilized in Triton X-100 in the presence of NEM to block free sulfhydryl groups (Loewen & Molday, 2000). The detergent-solubilized extract was applied to a Per2B6-Sepharose column and the unbound and bound (peptide-

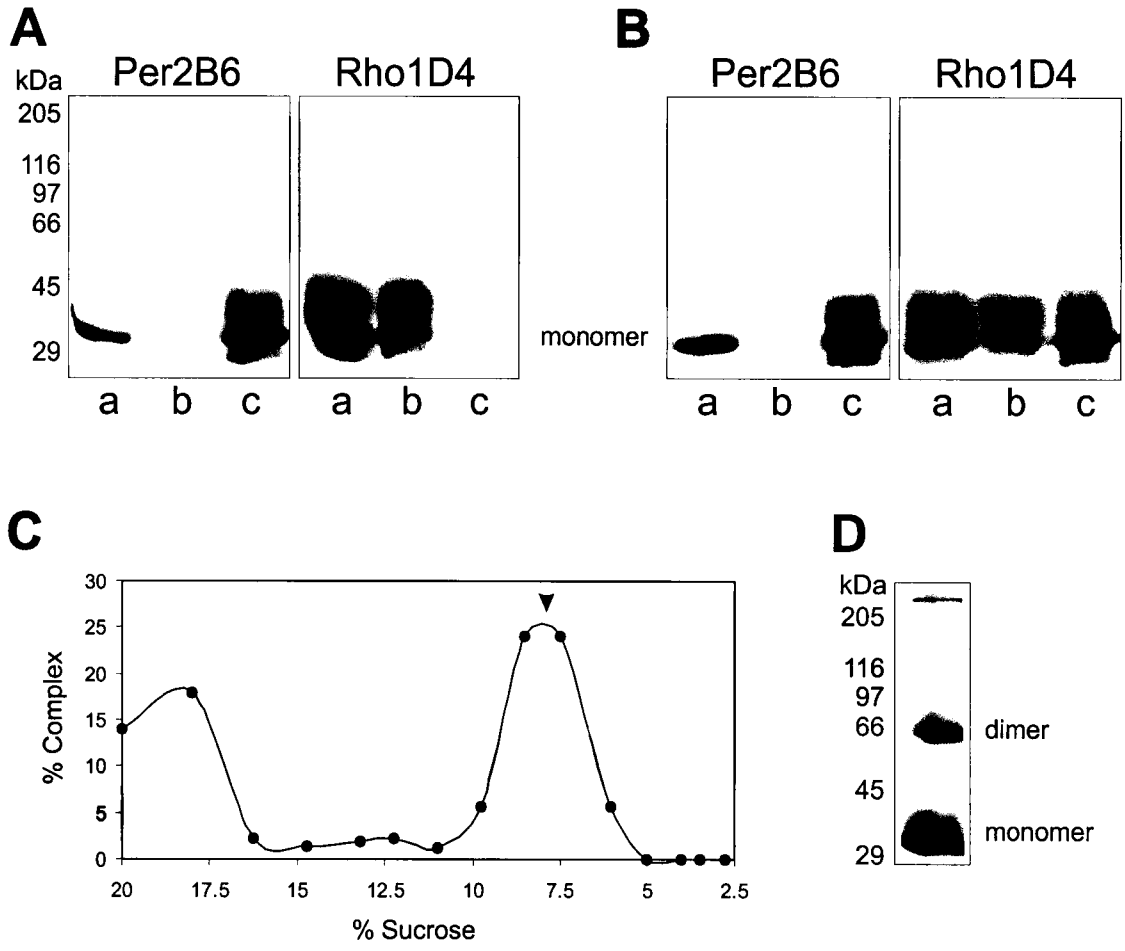

Fig 22. **Immunoprecipitation, velocity sedimentation and crosslinking of the L185P peripherin-2 complex under reducing conditions.** (A) COS-1 cells individually expressing the L185P and L185P-1D4 mutant were reduced with DTT and solubilized in Triton X-100. The extracts were mixed together and immunoprecipitated with Per2B6-Sepharose. The COS-1 cell extract (lane a), unbound fraction (lane b) and bound, peptide-eluted fraction (lane c) were analyzed on Western blots labeled with Per2B6 and Rho1D4 antibodies. (B) COS-1 cells coexpressing L185P and L185P-1D4 peripherin-2 were solubilized in Triton X-100 under reducing conditions, and immunoprecipitated with Per2B6-Sepharose. The COS-1 cell extract (lane a), unbound fraction (lane b), and bound, peptide-eluted fraction (lane c) were analyzed on Western blots labeled with Per2B6 or Rho1D4 antibody. (C) The coprecipitated (bound, peptide-eluted) fraction from (B) was subjected to velocity sedimentation and fractions were analyzed on Western blots labeled with Rho1D4 antibody. The sedimentation position of L185P peripherin-2 (arrowhead) is shown for comparison. (D) Western blot of reduced, immunoaffinity purified L185P peripherin-2 crosslinked with glutaraldehyde and labeled with the Per2B6 antibody (molecular mass standards are given in kDa) (see Methods sections 4.2.3 and 4.2.4).

eluted) fractions were analyzed for L185P and L185P-1D4 by Western blotting. **Fig 22B** shows that all the L185P protein bound to the Per2B6-Sepharose matrix. Approximately 50% of the L185P-1D4 protein coprecipitated with the L185P peripherin-2.

The isolated L185P:L185P-1D4 complex was further analyzed by velocity sedimentation (**Fig 22C**). The major complex had an apparent sedimentation coefficient that was similar to the individually expressed L185P (**Table 5**). An additional complex was apparent near the bottom of the tube. This most likely represents L185P:L185P-1D4 aggregates that form during the immunoaffinity purification procedure. Finally, it was determined if the individually expressed and purified L185P mutant could be crosslinked into dimer. As shown in **Fig 22D**, a significant fraction of detergent-solubilized L185P peripherin-2 migrated as a dimer on a SDS gel after glutaraldehyde crosslinking.

Taken together, the hydrodynamic analysis, coimmunoprecipitation, and crosslinking studies provide strong evidence that the L185P peripherin-2 mutant exists as a dimer under disulfide reducing conditions.

4.3.2 Velocity sedimentation of L185A-peripherin-2 and L188P-rom-1, and interaction of L185P-peripherin-2 with L188P-rom-1

To further evaluate the role of leucine at position 185 on the subunit assembly of peripherin-2, the sedimentation behaviour of a

L185A mutant under disulfide-reducing conditions was analyzed. The L185A mutant, like L185P, sedimented as a single species with an apparent sedimentation coefficient characteristic of a dimer (**Fig 23A**; **Table 5**). This mutant also co-assembled with rom-1 into a tetrameric core complex (data not shown).

Rom-1 contains a leucine residue at an equivalent position (Leu188). The L188P rom-1 mutant sedimented as a single species with an apparent sedimentation coefficient of 3.09 S, a value that is considerably less than that of WT rom-1 tetramer and consistent with a dimer (**Fig 23B**; **Table 5**).

To determine if L185P peripherin-2 can assemble with L188P rom-1, COS-1 cells co-expressing the L185P peripherin-2 and L188P rom-1 were treated with DTT and the detergent-solubilized extract was immunoprecipitated with Per2B6-Sepharose. **Fig 23C** shows that a significant fraction of L188P rom-1 coprecipitated with L185P peripherin-2. This isolated complex sedimented with an apparent sedimentation coefficient of 3.24 S (**Table 5**), a value intermediate between a L185P homodimer ($s_{20,w}$ = 3.64 S) and a L188P homodimer ($s_{20,w}$ = 3.09 S), and consistent with heterodimer formation.

Table 5

Velocity Sedimentation of Peripherin-2 and Rom-1 Core Complexes[1]

Species	$s_{20,w}$ (S)		Core complex
WT peripherin-2[2]	5.4 ± 0.1	(n=3)[3]	homotetramer
WT rom-1	4.6 ± 0.3	(n=6)	homotetramer
WT peripherin-2-1D4	5.2	(n=1)	homotetramer
L185P peripherin-2[4]	3.6 ± 0.2	(n=3)	homodimer
L185A peripherin-2	3.7 ± 0.3	(n=3)	homodimer
L185P:L185P-1D4 peripherin-2	3.7 ± 0.2	(n=3)	heterodimer
L185P peripherin-2:L188P rom-1	3.2	(n=2)	heterodimer
L188P rom-1	3.1 ± 0.2	(n=5)	homodimer

[1] Proteins expressed in COS-1 cells were solubilized in Triton X-100, applied to 5-20% sucrose gradients, and sedimented for 16 h at 50,000 rpm and 4°C in a Beckman TLS-55 rotor under reducing conditions. Fractions were analyzed on Western blots. $s_{20,w}$ values are given in Svedbergs (S) ± S.D.

[2] value previously reported (Goldberg, Loewen & Molday, 1998)

[3] *n* is the number of independent experiments

[4] value previously reported (Goldberg & Molday, 1996a) was recalculated using corrected parameters as described in Goldberg, Loewen & Molday (1998)

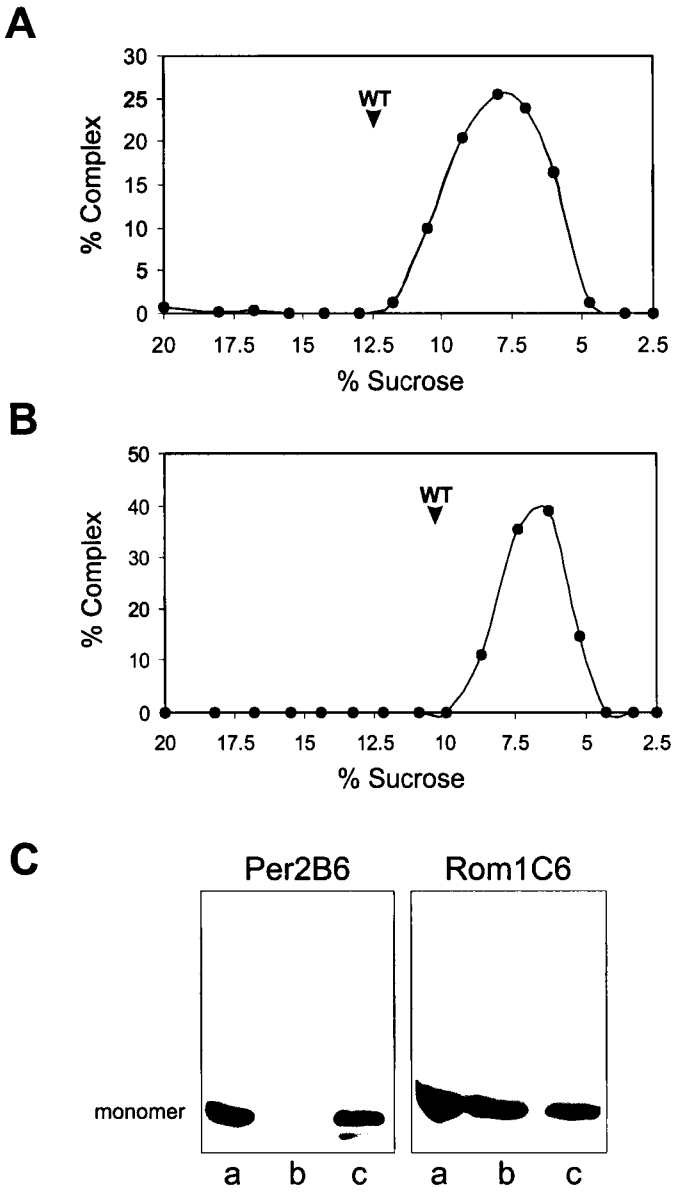

Fig 23. **Velocity sedimentation of L185A peripherin-2 and L188P rom-1 and coprecipitation of L185P peripherin-2 and L188P rom-1 under reducing conditions.** Velocity sedimentation profiles of (A) L185A peripherin-2 and (B) L188P rom-1 mutant individually expressed in COS-1 cells. Positions of WT peripherin-2 and WT rom-1 are shown for comparison in the respective profiles. (C) Detergent-solubilized extracts of COS-1 cells coexpressing L185P peripherin-2 and L188P rom-1 were immunoprecipitated with Per2B6 Sepharose. The extract (a), unbound (b), and bound, peptide-eluted fraction (c) were analyzed on Western blots labeled with Per2B6 and Rom1C6 antibodies (see Methods section 4.2.3).

4.3.3 Velocity sedimentation of L185P peripherin-2 under nonreducing conditions

The WT peripherin-2 core tetramer forms higher order, disulfide-linked oligomers under nonreducing conditions (Loewen & Molday, 2000). To determine if the L185P peripherin-2 dimer also forms disulfide-linked oligomers, COS-1 cells expressing the L185P mutant were treated with NEM and solubilized in Triton X-100 in the absence of DTT. The soluble extract was subjected to velocity sedimentation and fractions were analyzed on nonreducing SDS-polyacrylamide gels (**Fig 24A**). The velocity sedimentation profile showed two distinct species. One species, *a*, had an apparent sedimentation coefficient of 3.62 S, a value similar to the value for reduced L185P (**Table 5**); this species was composed solely of monomers when analyzed on nonreducing SDS gels. A second species, *b*, had an apparent sedimentation coefficient of 5.22 S, a value that is similar to that observed for WT tetrameric peripherin-2 core species (**Table 5**); this species contained disulfide-linked dimers. These results indicate that two L185P peripherin-2 core dimers can link together through intermolecular disulfide bonds to form a tetrameric complex. However, this complex does not form the higher order oligomers observed for WT peripherin-2 (**Fig 24C & D**).

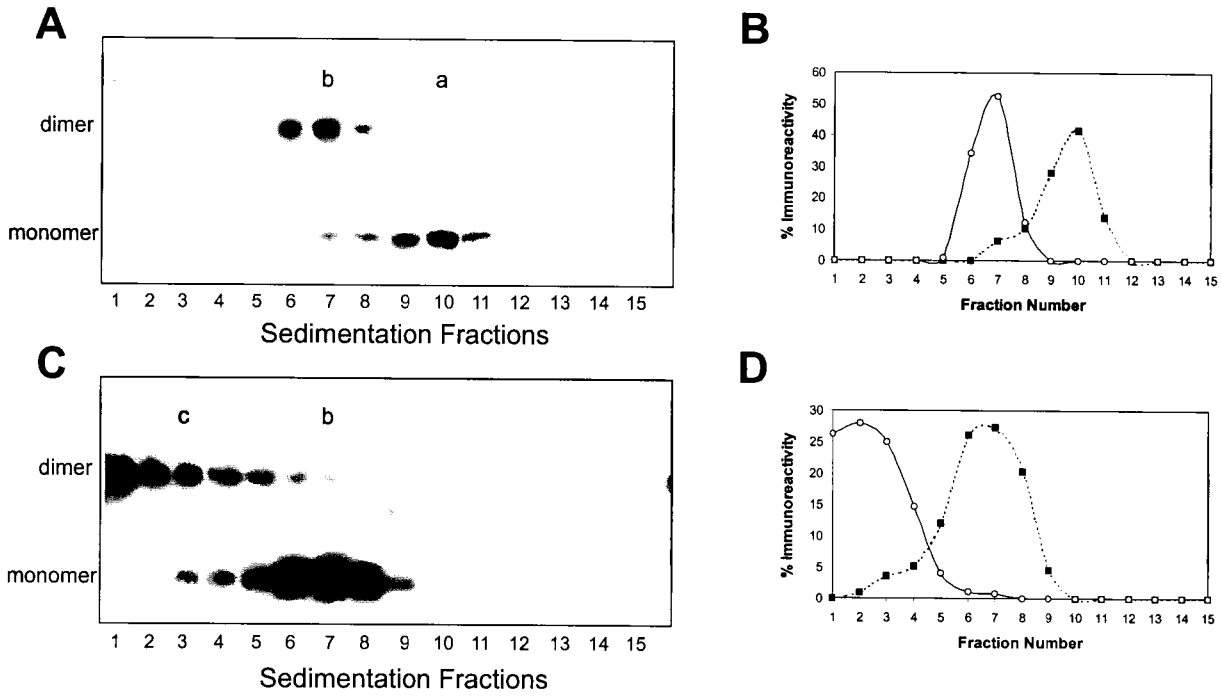

Fig 24. **Velocity sedimentation of L185P and WT peripherin-2 under nonreducing conditions.** COS-1 cells expressing either L185P or WT peripherin-2 were solubilized in Triton X-100 containing NEM and subjected to velocity sedimentation. Western blots of fractions separated on nonreducing SDS gels were labeled with the Per2B6 monoclonal antibody and quantified by densitometry. (A) Western blot of L185P peripherin-2 with sedimentation positions of dimer (a) and tetramer (b) shown, and (B) corresponding densitometric profiles of the monomer (closed squares) and dimer (open circles) bands. (C) Western blot of WT peripherin-2 with sedimentation positions of tetramer (b) and oligomer (c) shown, and (D) corresponding profiles of the monomer and dimer bands (see Methods section 4.2.3).

4.3.4 Oligomerization of WT- and L185P-peripherin-2:rom-1 complexes by velocity sedimentation

Previous studies have shown that both WT and L185P peripherin-2 assemble with WT rom-1 to form heterotetrameric complexes under reducing conditions (Goldberg & Molday, 1996a). To determine if these complexes can form higher order disulfide-linked oligomers, we examined the sedimentation behaviour of immunoaffinity purified WT peripherin-2:rom-1 and the L185P peripherin-2:rom-1 complex under nonreducing conditions. As shown in **Fig 25A**, the WT peripherin-2:rom-1 complex sedimented as two distinct species. Approximately 25% of the total complex sedimented as a heterotetramer (b in **Fig 25A**) devoid of intermolecular disulfide bonds and 75% sedimented as an intermediate oligomer (c in **Fig 25A**), presumably an octamer, containing a high proportion of intermolecular disulfide bonds.

The sedimentation profile of L185P peripherin-2:rom-1 complex is shown in **Fig 25B**. Three distinct species were observed: a heterodimer (a) accounting for approximately 17% of the complex and consisting of monomers; a heterotetramer (b) accounting for 23% of the total complex and containing both monomer and disulfide-dimers; and an intermediate oligomer (octamer) (c) accounting for 60% of total complex and containing disulfide-linked dimers. These results show that most of the L185P peripherin-2 mutant assembles with rom-1 into octameric

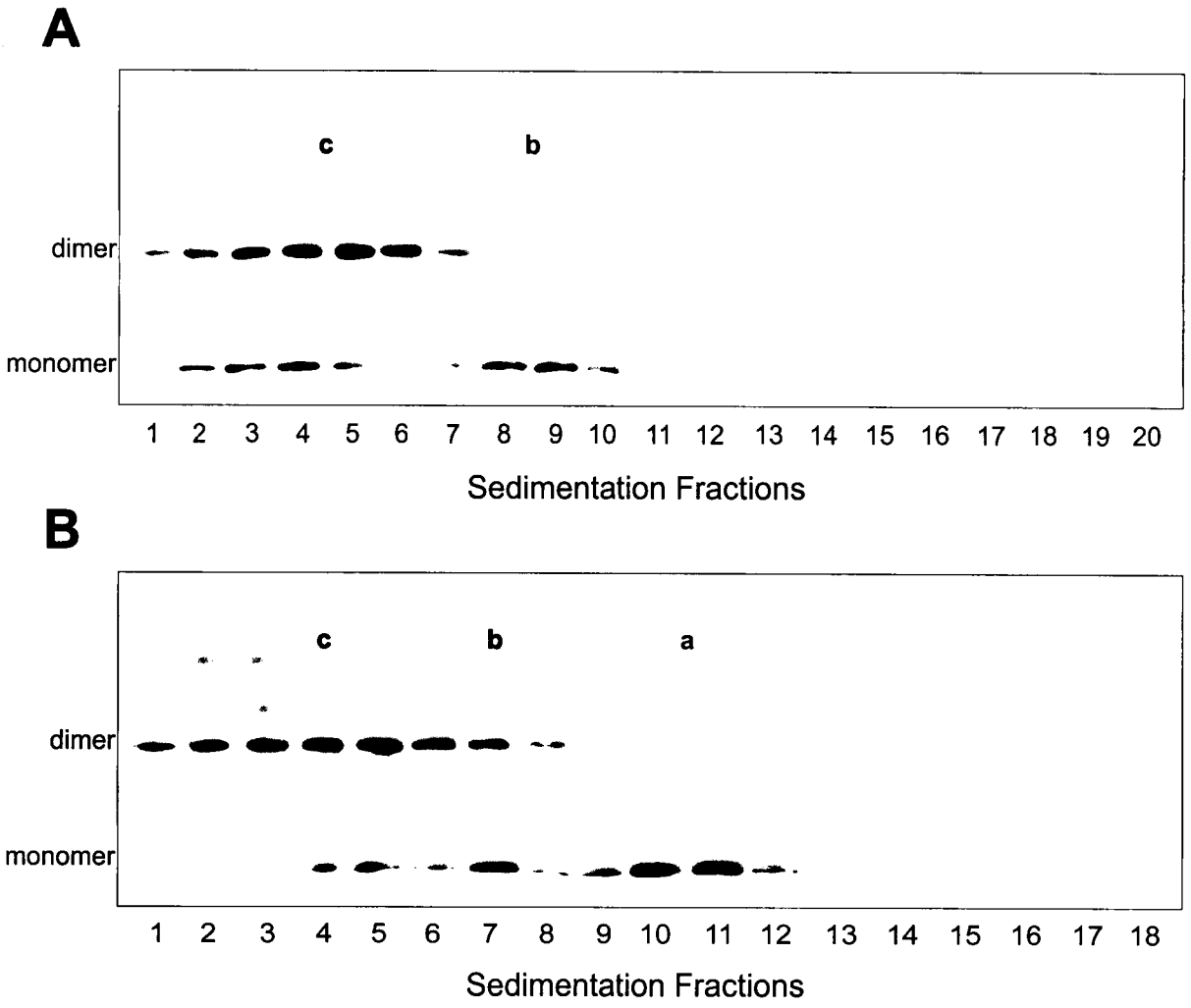

Fig 25. **Velocity sedimentation of WT peripherin-2:rom-1 and L185P:rom-1 complexes under nonreducing conditions.** COS-1 cells coexpressing either WT peripherin-2 and WT rom-1 (A) or L185P and WT rom-1 (B) were solubilized in Triton X-100 containing NEM , purified with Per2B6 Sepharose, and subjected to velocity sedimentation. Fractions were analyzed on nonreducing SDS gels and Western blots were labeled with the Rom1C6 monoclonal antibody. Sedimentation positions of dimer (a), tetramer (b), and octamer (c) are shown (see Methods section 4.2.3).

disulfide-linked complexes similar to that observed for WT peripherin-2:rom-1 complex.

4.3.5 Interaction of L185P-peripherin-2 with peripherin-2-1D4

Individuals with autosomal dominant RP express both WT and mutant peripherin-2 alleles. To determine if L185P peripherin-2 mutant assembles with WT peripherin-2, the L185P mutant was co-expressed with peripherin-2-1D4 containing the C-terminal 1D4 epitope and the Q341P mutation that abolishes Per2B6 immunoreactivity. **Fig 26A** shows that under disulfide reducing conditions over 50% of the peripherin-2-1D4 coprecipitated with the L185P peripherin-2 mutant. Velocity sedimentation analysis of this complex showed a mixed population of heterodimer (*a*) and heterotetramer (*b*) (**Fig 26B**). Under nonreducing conditions, the velocity sedimentation profile of L185P peripherin-2:peripherin-2-1D4 complex (**Fig 26C**) revealed the presence of higher order disulfide-linked oligomers (*c*) as well as heterotetramers (*b*) and heterodimers (*a*). In control experiments, the individually expressed WT-peripherin-2-1D4 exhibited the same sedimentation behavior as WT peripherin-2 (**Table 5**), indicating that addition of the 1D4 epitope had no effect on subunit assembly.

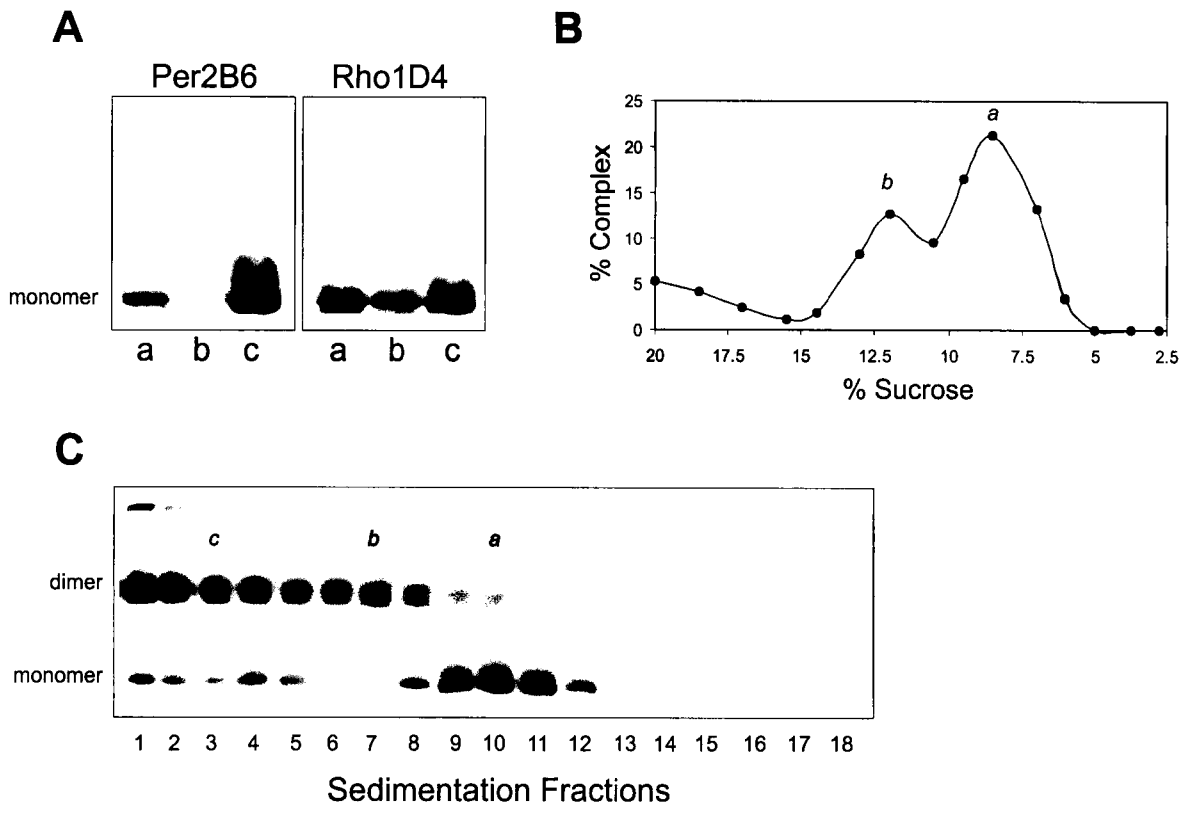

Fig 26. **Immunoprecipitation and velocity sedimentation of L185P peripherin-2:WT peripherin-2-1D4 complexes under reducing and nonreducing conditions.** (A) COS-1 cells coexpressing L185P peripherin-2 and WT peripherin-2-1D4 were reduced with DTT, solubilized in Triton X-100, and immunoprecipitated with Per2B6-Sepharose. The COS-1 cell extract (lane a), unbound fraction (lane b), and bound, peptide-eluted fraction (lane c) were analyzed on Western blots labeled with Per2B6 or Rho1D4 antibody. (B) The coprecipitated complex from (A) was subjected to velocity sedimentation and fractions were analyzed on Western blots labeled with Rho1D4 antibody. (C) Samples were treated as in (A) except under nonreducing conditions (-DTT), and the purified L185P:WT peripherin-2-1D4 complexes were subjected to velocity sedimentation. Western blots of fractions from a nonreducing SDS gel were labeled with the Rho1D4 antibody. Sedimentation positions of dimer (a), tetramer (b), and oligomer (c) are shown (see Methods section 4.2.3).

4.4 DISCUSSION

Previous studies have shown that the L185P peripherin-2 mutant expressed in COS-1 cells has a sedimentation coefficient that is considerably smaller than that of the WT peripherin-2 core tetramer (Goldberg & Molday, 1996a). We have determined the size of this mutant by hydrodynamic analysis, co-immunoprecipitation and crosslinking. Although hydrodynamic analysis gave a molecular mass that was intermediate between a monomer and dimer, both coprecipitation and crosslinking provided strong evidence that the detergent-solubilized L185P mutant exists as a dimer under disulfide reducing conditions. The low value for the molecular mass of the L185P dimer determined by hydrodynamic measurements is consistent with the underestimation of the molecular mass of the native tetrameric peripherin-2:rom-1 complex reported using this technique (Goldberg & Molday, 1996b). This underestimation in molecular mass can arise in part from the assumption that the protein binds the same amount of detergent in H_2O and D_2O (Clarke & Smigel, 1989). The estimated partial specific volume of the protein can also contribute to an inaccurate value for the molecular mass of the protein. Partial specific volumes in the range of 0.71 – 0.75 ml/g are generally used for proteins. The true value, however, is dependent not only the amino acid composition of the protein, but also on carbohydrate in the case of a glycoprotein as well as the possible

presence of small amounts of bound lipid (Clarke & Smigel, 1989). Since L185P peripherin-2 is glycosylated in COS-1 cells (data not shown) and may also contain a small amount of tightly bound lipid in the detergent solubilized state, the value of 0.74 ml/g used here may represent an underestimation of the actual value for the partial specific volume of the protein.

The role of the conserved leucine residue at position 185 in subunit assembly was determined by analyzing several mutants. The L185A peripherin-2 mutant behaved like the L185P mutant. It formed a core dimer when individually expressed, but assembled into a heterotetramer when co-expressed with rom-1. This indicates that defective homotetramer formation of the L185P mutant is due to the absence of a leucine at position 185 and not the introduction of a proline residue. The ability of these mutants to interact with rom-1 to form a native-like tetramer further indicates that the mutants are not grossly misfolded. Rom-1 has a leucine residue at an equivalent position (L188) within a conserved segment of the large intradiscal loop (**Fig 20**). Replacement of this leucine with proline also prevented rom-1 from assembling into homotetramers. Together these studies indicate that L185 in peripherin-2 and L188 in rom-1 play essential roles in the association of dimers into core tetramers.

The fact that these mutants exist as dimers, and not monomers, provides additional insight into the quaternary structure of the peripherin-2 and rom-1 core complexes. The interactions responsible for dimer formation are distinct from those responsible for tetramer formation since dimerization is not dependent on leucine at position 185 in peripherin-2 (or leucine 188 in rom-1). On this basis we infer that the WT peripherin-2 and rom-1 core tetramer exhibits pseudo two-fold symmetry. This leads to a model in which the core tetramer can be considered as a 'dimer-of-dimers' (**Fig 27**). The domain responsible for dimer formation is not known at the present time. However, the ability of L185P peripherin-2 to associate with L188P rom-1 to form a heterodimer (**Fig 23C**) suggests that the dimerization domain of these subunits, like the tetramerization domain, must be structurally similar.

The contribution of leucine and other bulky hydrophobic residues to the formation and maintenance of protein-protein interactions is well documented for intracellular proteins (transcription factors of the bZIP class like GCN4 (O'Shea *et al.*, 1991); the regulatory subunit of PKAIIb (Li & Rubin, 1995)); extracellular matrix proteins (tenascins, laminins, thrombospondins (Kammerer, 1997)); and integral membrane proteins (glycophorin A (MacKenzie, Prestegard & Engelman, 1997), metabotropic glutamate receptor (Kunishima *et al.*, 2000)). Recently, the crystal structure of the dimeric extracellular ligand binding region of the

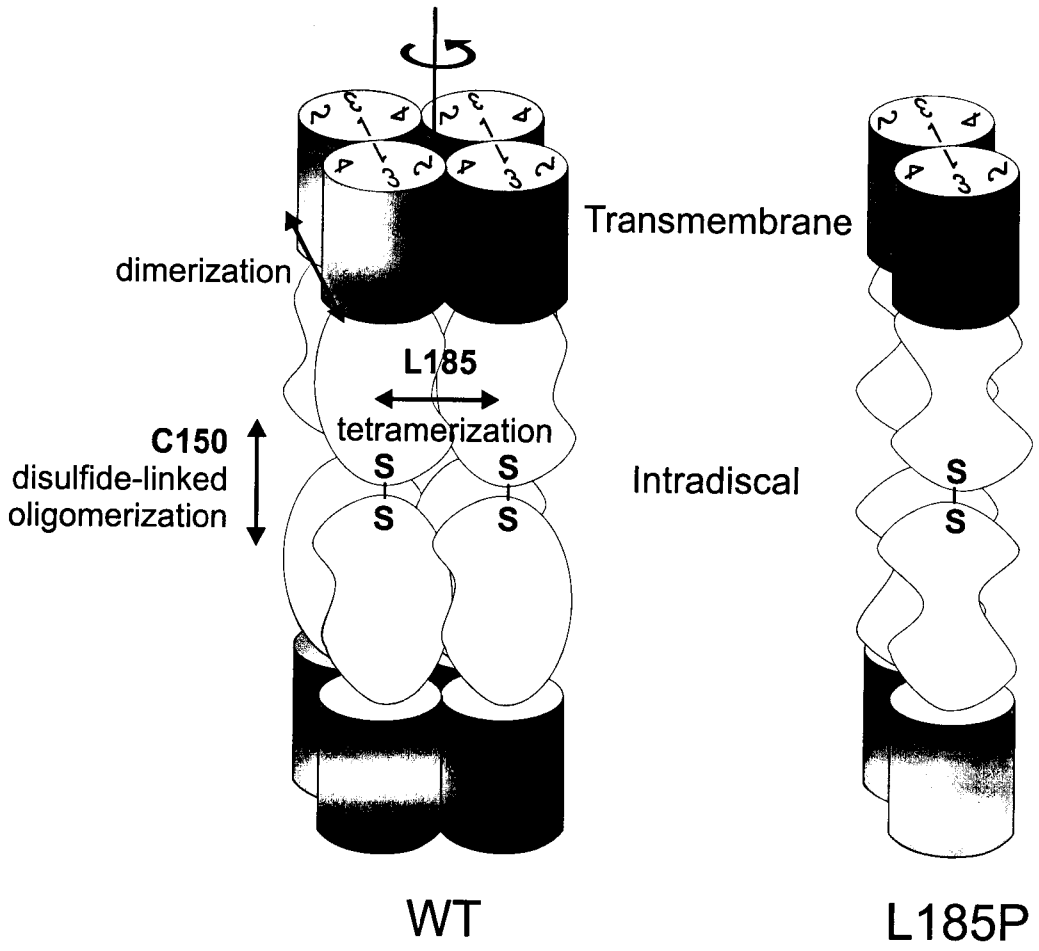

Fig 27. **Model for the oligomeric structure of peripherin-2 and the L185P mutant.** WT peripherin-2 monomers (transmembrane domain shown as a cylinder) interact to form a core noncovalent tetramer with a two-fold axis of symmetry. Leucine at position 185 (L185) of the intradiskal loop is required for tetramer formation (tetramerization). Dimer formation (dimerization) may involve interactions between transmembrane, intradiskal, or cytoplasmic domains (omitted for simplicity). The core tetramers link-up through C150-mediated intermolecular disulfide bonds to form higher order oligomers (only the octamer is shown). The L185P peripherin-2 mutant consists of a core dimer that can link through C150 mediated intermolecular disulfide bonds to form a tetramer, but not a higher order oligomer. Numbers on cylinders illustrate the two-fold symmetry of the core tetramer and the concept that it consists of a dimer of dimers (dimerization has been drawn as head-to-head). Rom-1 also forms homotetramers and heterotetramers with peripherin-2, but limits oligomerization to octamers.

metabotropic glutamate receptor (mGluR), a seven transmembrane G-protein coupled receptor, has been solved (Kunishima *et al.*, 2000). In this case, four conserved leucines and one isoleucine contribute to the dimer interface. In the intradiscal loop region of peripherin-2 and rom-1, there are 9 conserved leucine and several conserved isoleucine residues in addition to L185. It is possible that at least some of these residues also contribute to inter-subunit interactions of peripherin-2 and rom-1. Interestingly, many of these hydrophobic residues are also conserved in other members of the *tetraspanin* family of proteins including CD9, CD37, CD53, CD63, CD81/82, CD151, A15, and SJ23 (see Wright & Tomlinson (1994) for review; alignment performed using BLAST conserved domain database search). This leads to the possibility that these proteins also exist as oligomeric complexes whose subunit interactions are mediated by these hydrophobic residues.

Peripherin-2 containing core tetramers further link together through C150 mediated intermolecular disulfide bonds to form higher order oligomers (Loewen & Molday, 2000). In this study, we have shown that two L185P dimers link together to form a disulfide-linked tetramer (**Fig 27**), but this complex does not further assemble into the higher order oligomers observed for WT-peripherin-2. This indicates that core tetramer formation is not required for intermolecular disulfide bond formation, but it is required for the generation of higher order oligomers.

This finding together with previous studies showing that C150S peripherin-2 mutants form core noncovalent tetramers, but not higher order oligomers (Loewen & Molday, 2000), indicates that higher order oligomerization involves both noncovalent and covalent (disulfide) interactions. The noncovalent interactions involved in higher order oligomerization are likely to be similar to those involved in tetramerization (**Fig 27**). Formation of C150 mediated intermolecular disulfide bonds between adjacent tetramers may initiate a conformational change within the intradiscal loop that facilitates noncovalent interactions responsible for oligomerization.

Disulfide-linked oligomers appear to be important in outer segment disc formation. *In vitro* expression of WT peripherin-2 under nonreducing conditions has been reported to result in flattened microsomal vesicles whereas expression of WT peripherin-2 under reducing conditions or expression of C150S peripherin-2 under nonreducing conditions results in round vesicles (Wrigley *et al.*, 2000). It is not known if the disulfide-linked L185P tetramers cause the flattening of these membranes, or if higher order oligomers are required for this process.

Individuals with autosomal dominant digenic RP express a WT allele along with the mutant allele. To understand in more detail the molecular basis for this disease, we examined the interaction of L185P peripherin-2 mutant with WT peripherin-2 and WT rom-1. Co-expression of L185P and

WT peripherin-2 resulted in a mixture of dimeric and tetrameric core complexes that further interacted through intermolecular disulfide bonds to form oligomers. L185P peripherin-2 also assembled with rom-1 to form predominantly core tetramers as previously shown (Goldberg & Molday, 1996a). Like the WT proteins, the L185P peripherin-2:rom-1 heterotetramers further associated via intermolecular disulfide bonds into disulfide linked intermediate oligomers, most likely octamers. On the basis of these results, we conclude that the L185P mutant can interact with WT proteins to form higher order oligomers that most likely contribute to the formation and stabilization of outer segment discs.

Autosomal dominant digenic RP is a complex disease requiring the coinheritance of a L185P peripherin-2 allele and an effective rom-1 null allele (Dryja *et al.*, 1997; Goldberg & Molday, 1996a; Kajiwara, Berson & Dryja, 1994). Individuals who inherit only one of these mutant alleles are essentially normal. Our data suggests that the level of peripherin-2-containing oligomers is critical in the manifestation of this disease. Since the L185P peripherin-2 mutant is incapable of forming homotetramers and corresponding higher order disulfide-linked oligomers, individuals who inherit this mutation along with a null allele in rom-1, will have a level of peripherin-containing oligomers below the critical threshold level required for the formation of stable outer segments. The presence of disorganized, unstable outer segments will lead to photoreceptor

degeneration as observed for heterozygous *rds* mice (Hawkins, Jansen & Sanyal, 1985). In the case of individuals who inherit only the L185P peripherin-2 mutation, a significant amount of the L185P will assemble with WT rom-1, as well as WT peripherin-2, to form 'functional' oligomers. This would have the effect of raising the level of oligomers above the threshold needed to form stable outer segments. These individuals would experience little if any photoreceptor degeneration and have essentially normal vision. Individuals who inherit only a rom-1 null allele, would be expected to have normal levels of peripherin-2, and half the level of rom-1. Reduced levels of rom-1, however, have no appreciable effect on outer segment structure or photoreceptor viability as shown in recent studies of heterozygous rom-1 knockout mice (Clarke *et al.*, 2000). Hence, individuals who inherit only a null allele or a G113E missense mutation in rom-1 would have a sufficient level of peripherin-2 containing oligomers to support photoreceptor outer segment structure and photoreceptor viability.

The L185P peripherin-2 mutant is distinct from peripherin-2 mutants that cause monogenic autosomal dominant RP. For example, the C214S and C165S peripherin-2 mutants are highly misfolded and do not form core tetramers or higher order oligomers in the presence or absence of rom-1 (Goldberg, Loewen & Molday, 1998; Loewen & Molday, 2000). Furthermore, expression of the C165Y mutant fails to result in the

formation of flattened vesicles (Wrigley *et al.*, 2000). Hence, individuals with these mutations would have a significantly decreased level of functional oligomers in the presence or absence of rom-1 resulting in unstable, disorganized outer segment discs and photoreceptor degeneration. A dominant negative effect of these misfolded mutants, however, may also contribute to photoreceptor degeneration and the autosomal dominant RP phenotype.

CHAPTER 5 – EXPRESSION OF PERIPHERIN-2 VARIANTS IN TRANSGENIC *XENOPUS LAEVIS*

5.1 INTRODUCTION

The unique highly polarized nature of photoreceptor cells makes them an excellent system to study protein and membrane trafficking. However, their intimate association with RPE cells in the eye prevents easy manipulation in cell culture because these contacts are not maintained. Rods in cell culture quickly lose their outer segments and do not divide (Townes-Anderson, MacLeish & Raviola, 1985). Studies on targeting of mutant rhodopsins in MDCK cells have been valuable, but have left many questions unanswered (Chuang & Sung, 1998). In contrast, studies in transgenic mice and rats have proven very useful in understanding more about the requirements for outer segment targeting of rhodopsin and how mutations lead to photoreceptor degeneration and disease (Green *et al.*, 2000; Sung *et al.*, 1994). However, the high cost and lengthy time requirements of these studies preclude extensive molecular manipulation of the transgenes. Recent studies using transgenic *Xenopus laevis* have been successful in defining a C-terminal peptide sequence in rhodopsin that is required for ROS localization (Tam *et al.*, 2000). The low cost and speed of this procedure allows for extensive manipulation of transgenes and generation of large numbers of transgenic lines.

Using the transgenic *Xenopus* technology in a collaboration with David Papermaster's lab at the University of Connecticut, the effects of mutations in peripherin-2 on protein targeting and photoreceptor structure have been examined. This technique involves expression of the protein of interest as a GFP-fusion protein which facilitates easy and rapid screening for transgenic animals and allows direct localization of the protein using microscopy techniques. The transgene is under control of the *Xenopus* opsin promoter and is only expressed in the rod photoreceptors. The technique of restriction endonuclease mediated integration (REMI) is used to incorporate the transgene into *Xenopus* sperm (Amaya & Kroll, 1999). In REMI, both the sperm nuclei and the plasmid containing the transgene are mildly digested with the same restriction endonuclease. When mixed together, the transgene incorporates into a complementary restriction site(s) in the sperm DNA. Microinjection of the mixture into a *Xenopus* oocyte results in ligation of the sperm DNA containing the transgene and fertilization. If the transgene incorporates prior to the first cell division, then every cell in the animal will harbour it.

GFP has been fused to the C-terminus of peripherin-2 to prevent interference with protein translation and membrane insertion. Several disease-causing mutants have been constructed to determine the effects of these mutations *in vivo* (**Fig 28**). The L185P and C214S mutants have

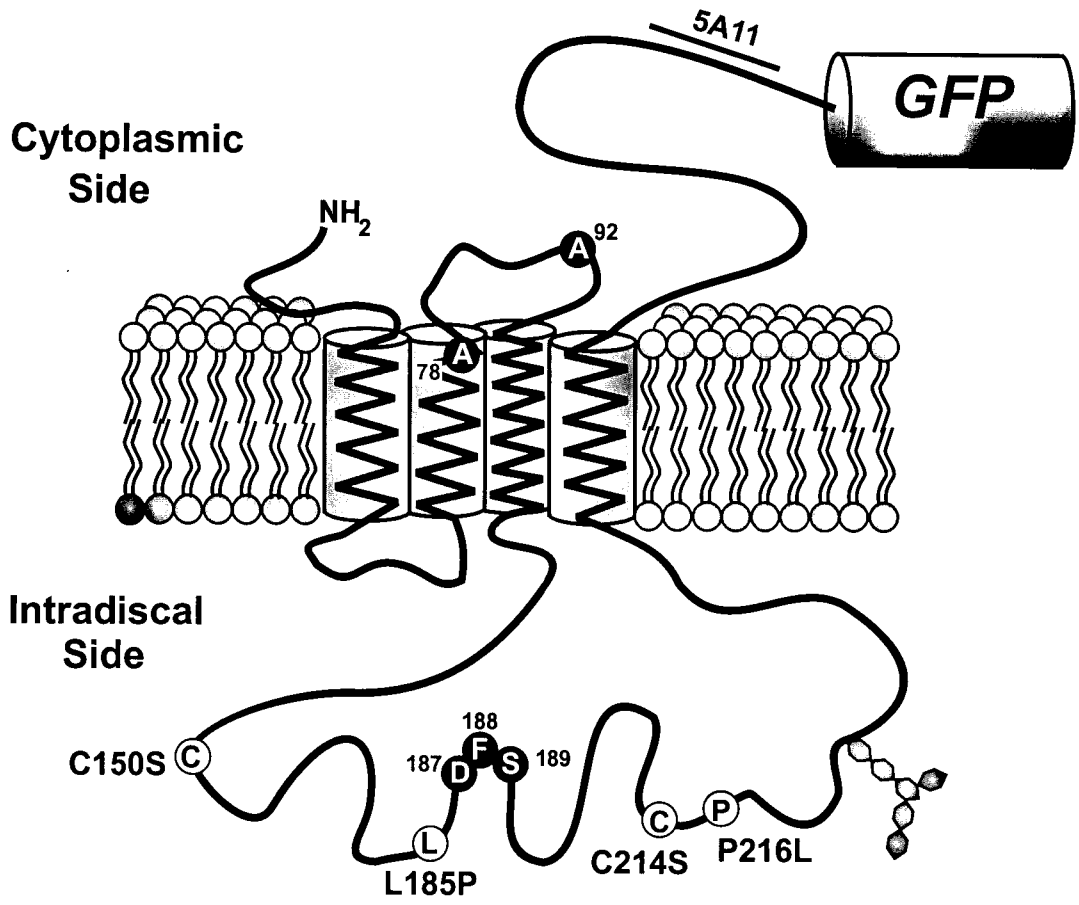

Fig 28. **Topological model for *Xenopus* peripherin-2.** Location of GFP fusion and Per5A11 MAb epitope are shown. Location of C150S and RP-causing mutations are given in open circles. Amino acids differing from the published sequence are given in black circles.

been characterized biochemically in some detail previously (Goldberg, Loewen & Molday, 1998; Loewen, Moritz & Molday, 2001) (see sections 1.4.2, 2.4, and 4.4). Additionally, the effects of expression of C150S peripherin-2-GFP on rod structure and disc morphogenesis have been examined with the hope of understanding more about the role of disulfide-mediated oligomerization in these processes.

All transgenic animals used in this study were produced at the University of Connecticut by the author together with O. Moritz and B. Tam. Confocal microscopy was performed at the University of Connecticut Health Sciences Center Microscopy Unit. All other procedures were performed by the author at U.B.C., with the exception of sectioning for electron microscopy which was performed by Laurie Molday.

5.2 MATERIALS AND METHODS

5.2.1 Molecular biology

Xenopus laevis prph-2 was cloned from total retinal RNA by PCR using sequence-specific primers based on the published sequence for *Xrds-38* (Kedzierski *et al.*, 1996). PCR primers contained unique restriction sites for cloning into pcDNA I/amp (Invitrogen). Cloned PCR products were sequenced entirely on both strands. The *Xenopus* peripherin-2-GFP fusion construct was created by PCR removing the *prph-2* stop codon and cloning in frame into the XhoI and EcoRI sites of peGFP-

N2 (CLONTECH Laboratories, Inc.) ahead of GFP. This construct was used for expression of the peripherin-2-GFP fusion protein in COS-1 cells. For expression in transgenic *X. laevis*, the XhoI-NotI fragment of *Xenopus* peripherin-2-GFP (including GFP) was subcloned into the XhoI and NotI sites of the plasmid XOP1.3GFP-N1 which contains a portion of the *X. laevis* opsin promoter sequence and is based on the plasmid peGFP-N1 obtained from CLONTECH Laboratories, Inc. (Tam *et al.*, 2000). Mutagenesis was performed on this construct to introduce individually the RP-causing mutations L185P, C214S, and P216L using the Quik Change PCR-based protocol (Stratagene). Bovine peripherin-2-GFP and C214S-peripherin-2-GFP fusion constructs were created in a similar manner as *Xenopus* peripherin-2-GFP. Stop codons were removed by PCR and the constructs were cloned in frame into the EcoRI and BamHI sites of peGFP-N3. A subsequent EcoRI-NotI fragment containing the insert plus GFP was subcloned into the BamHI and NotI sites of the plasmid XOP1.3GFP-N1. All constructs created by PCR were sequenced to confirm that no errors were introduced. All transgenic expression constructs were linearized by digestion with restriction enzyme and purified using the GeneClean Kit (Bio101).

5.2.2 Monoclonal antibody production

Oligonucleotides were synthesized to the *Xenopus* peripherin-2 C-terminal amino acid sequence KDTIKSSWELVKSMGKLNKVE and were cloned into the PGEX and PMAL expression vectors for preparation of GST and MBP fusion proteins, respectively. Purified GST fusion protein from *E. coli* was used to immunize Swiss Webster mice. The monoclonal antibody Per2A5 was prepared from a sero-positive mouse as previously described (MacKenzie & Molday, 1982). Screening was performed on Western blots containing MBP fusion protein and by immunofluorescence microscopy of adult *Xenopus* retinal cryosections.

5.2.3 Transgenesis, GFP screening, and tadpole rearing

Transgenic frogs were generated using a modified protocol (Moritz *et al.*, 1999) based on that of Kroll and Amaya (Kroll & Amaya, 1996) and Amaya and Kroll (Amaya & Kroll, 1999). *X. laevis* sperm nuclei were incubated with 0.3× high speed egg extract, 0.05 U restriction enzyme, and 100–200 ng linearized vector DNA. The reaction mixture was then diluted to 0.3 nuclei/nl and 10 nl was injected per egg. The resulting embryos were kept at 18°C in 0.1× Marc's Modified Ringer, 6% Ficoll solution for 48 h and then switched to 0.1× Gerhart's Ringer Solution (Wu & Gerhart, 1991). At 5–6 d postfertilization (dpf) roughly corresponding to stages 40–42 (Nieuwkoop & Faber, 1994), tadpoles were screened for

GFP expression using a Leica MZ8 dissecting microscope equipped with epifluorescence optics and a GFP filter set. Animals were placed into glass Pasteur pipettes to immobilize them. Tadpoles expressing GFP were easily identified by the green fluorescence emitted from their eyes. At 14 dpf, transgenic tadpoles were placed in tanks with 0.1× Gerhart's Ringer Solution and reared at 18ºC on a 12/12 h light/dark cycle. Adult *X. laevis* were obtained from Nasco or Xenopus Express.

5.2.4 Immuno-EM

Transgenic tadpoles were sacrificed at 14 and 28 d.p.f. (stage 48-62) and fixed in 4% paraformaldehyde, 0.1 M sodium phosphate buffer, pH 7.5. After overnight fixation, eyes were excised and embedded in LR White according to the manufacturer's instructions (London Resin Company). Thin sections were labeled overnight with a rabbit anti-GFP polyclonal antibody (CLONTECH Laboratories, Inc.) diluted 1:100 in 1% bovine serum albumin (BSA), 0.1 M Tris, pH 7.4. The reactions were washed three times and labeled for 1 h with anti-rabbit secondary antibody conjugated to 10 nm colloidal gold (British BioCell International) diluted 1:5 in 0.1 M Tris, pH 7.4, 1% BSA. A minimum of two transgenic animals was examined by immuno-EM for each construct.

5.2.5 Immunocytochemistry, confocal and deconvolution microscopy

Transgenic tadpoles were sacrificed between stages 48–62. After immobilizing the tadpoles in 0.02% Tricaine, their eyes were excised and fixed in 4% paraformaldehyde, sodium phosphate buffer, pH 7.5, overnight. Fixed eyes were embedded in OCT tissue embedding medium (Tissue-Tek) and frozen in a dry ice/isopentane bath. Cryostat sections (14 μm) were blocked (10% BSA, 0.1% Triton X-100 in PBS) and labeled overnight with 0.1 mg/ml Texas Red–conjugated wheat germ agglutinin (TR-WGA) (Molecular Probes) and 0.01 mg/ml Hoescht 33342 stain (Sigma-Aldrich) to label photoreceptor membranes and nuclei, respectively. Sections were also labelled with anti-*Xenopus* peripherin-2 monoclonal antibody Per2A5. Labeling was done in the presence of 1 mM $CaCl_2$, 1 mM $MgCl_2$, 1%BSA, and 0.1% Triton X-100 in PBS. Labeled sections were analyzed using a ZEISS confocal laser scanning microscope (models 410 and 510). A minimum of three transgenic animals was examined by confocal microscopy for each construct. The conditions used for deconvolution microscopy involved 3 nearest neighbors for low mag images (10X NA 0.45) and the images in the Z-series were spaced 0.5 μm apart in all cases. Openlab version 2.03 (Improvision) software was used to do the analysis.

5.2.6 Transfections and plasmids

COS-1 cells (ca. 6×10^5 cells/100-mm dish) were transfected with a total of 30 μg of plasmid DNA by the calcium phosphate method and harvested 72 h post-transfection as described in section 3.2.4. Plasmids used were *Xenopus* peripherin-2-GFP (described above), pcPer (bovine WT peripherin-2 cloned into pcDNA I/amp) (Goldberg, Loewen & Molday, 1998), pcPer-C214S (bovine peripherin-2 with the C214S mutation cloned into pcDNA I/amp) (Goldberg, Loewen & Molday, 1998), and pcPer-P216L (bovine peripherin-2 with the P216L mutation cloned into pcDNA I/amp).

5.2.7 Biochemistry

Transfected COS-1 cells were scraped from 100 mm dishes, washed with PBS, and incubated with PBS in the presence or absence of 20 mM DTT for 90 min at 25°C. The cells were solubilized with an equal volume (150 μl) of PBS containing 2% Triton X-100, 80mM NEM, and PMSF (pH 7.4) for 10 min on ice. The cell extract was centrifuged at 90,000 × g for 30 min at 4°C and the supernatant (detergent solubilized fraction) was retained on ice for analysis. Immunopurification of bovine peripherin-2 was performed with Per2B6-Sepharose immunoaffinity matrix as previously described in section 3.2.3.

For velocity sedimentation experiments done under nonreducing conditions, 100 μl of nonreduced solubilized cell extract was applied to 5-

20% (w/w) sucrose gradients prepared in PBS and containing 0.1% Triton X-100 (Loewen & Molday, 2000) (see methods section 3.2.5). After centrifugation for 16 h at 50,000 rpm in a Beckman TLS-55 rotor at 4°C, the bottom of the centrifuge tube was punctured and four-drop fractions were collected for analysis on Western blots.

Protein crosslinking was performed on detergent solubilized cell extracts with 0.005% glutaraldehyde for 15 min at 37°C. For gel electrophoresis, samples were denatured with an equal volume of SDS cocktail (4% SDS, 0.02M Tris-HCl, pH 6.8, 20% glycerol, 0.01% bromophenol blue) in the absence (nonreducing) or presence (reducing) of 5% β-mercaptoethanol, and applied to 6% or 8% SDS-polyacrylamide gels. After electrophoresis, the proteins were transferred to Immobilon-P using a Bio-Rad semidry transfer apparatus. Western Blots were probed with a monoclonal antibody against bovine peripherin-2 (Per2B6) (Molday, Hicks & Molday, 1987) and a polyclonal antibody against GFP (CLONTECH Laboratories Inc.) and sheep anti-mouse or donkey anti-rabbit immunoglobulin-peroxidase (Amersham-Pharmacia) for detection by ECL.

5.3 RESULTS

5.3.1 Cloning X. laevis peripherin-2

Xenopus Prph-2 cDNA from adult *X. laevis* retina has been cloned by PCR using primers generated to the published sequence of Xrds-38 (Kedzierski *et al.*, 1996) and sequenced. The sequence of *Xenopus Prph-2* differed from the published sequence. Five amino acid changes were found at A78, A92, D187, F188, and S189. These amino acids are completely conserved in all mammalian orthologs sequenced to date including mouse, rat, cat, dog, bovine, and human (**Fig 28**), and therefore most likely represent the true sequence of *Xenopus* peripherin-2. The nucleotide and protein sequence have been deposited in the GenBank database.

5.3.2 Molecular characterization of Xenopus peripherin-2-GFP

Xenopus and bovine peripherin-2-GFP fusion proteins were expressed in COS-1 cells in order to determine if GFP fused to their C-terminus affects their biochemical properties. Previous studies have demonstrated that bovine peripherin-2 forms core noncovalent tetramers that associate via disulfide bonds between C150 residues to form intermediate and higher-order disulfide-linked oligomers (Loewen & Molday, 2000). The bovine peripherin-2-GFP fusion protein exhibited the same properties as bovine peripherin-2 when analyzed for disulfide-dimerization, crosslinking in the reduced and nonreduced states, and

association with peripherin-2 and rom-1 (data not shown). Therefore it can be concluded that GFP has little or no effect on its structural properties.

Xenopus peripherin-2-GFP also behaves similarly to bovine peripherin-2. It localized to internal vesicles of COS-1 cells and was not present on the plasma membrane (data not shown). Like bovine peripherin-2, it formed disulfide-dimers (**Fig 29A**, lane b) and crosslinked predominantly into dimers under reducing conditions (**Fig 29A**, lane c). Crosslinking under nonreducing conditions revealed the presence of higher molecular weight bands (**Fig 29A**, lane d) indicative of disulfide-linked oligomer formation (Loewen & Molday, 2000). Disulfide-linked oligomerization of *Xenopus* peripherin-2-GFP is mediated by C150, like bovine (data not shown). *Xenopus* peripherin-2-GFP also interacted with bovine peripherin-2 in co-immunoprecipitation experiments (**Fig 29**, lane e).

5.3.3 Immunolocalization of endogenous peripherin-2

The cellular and subcellular localization of endogenous peripherin-2 in *Xenopus* tadpoles was determined using the monoclonal antibody Per2A5 directed to the C-terminal tail of *Xenopus* peripherin-2. **Fig 30B** shows specific localization to rod and cone outer segment membranes. The vertical striations are observed in ROS. This pattern of labelling is

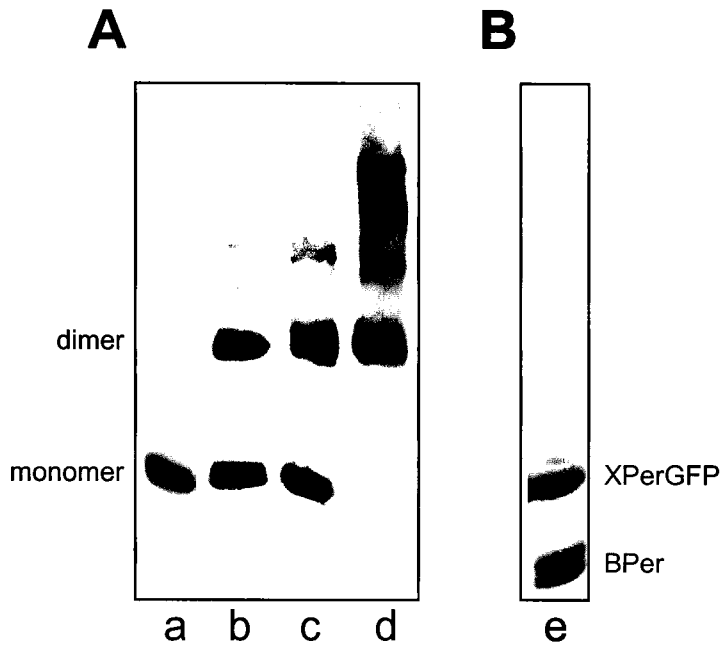

Fig 29. **Molecular characterization of *Xenopus* peripherin-2-GFP fusion protein.** (A) Xenopus peripherin-2-GFP was expressed in COS-1 cells and the cells were treated with (reduced) or without DTT (nonreduced) and solubilized in buffer containing Triton X-100 and NEM. Reduced (lane a) and nonreduced (lane b) extract was subjected to SDS-PAGE under reducing and nonreducing conditions respectively. Reduced (lane c) and nonreduced (lane d) extract was crosslinked with glutaraldehyde and subjected to SDS-PAGE under reducing conditions. Western blot analysis was performed with anti-GFP antibody. (B) *Xenopus* peripherin-2-GFP and bovine peripherin-2 were coexpressed in COS-1 cells, solubilized in buffer containing Triton X-100 and NEM, and immunoprecipitated with anti-peripherin-2 monoclonal antibody Per2B6 coupled to Sepharose. The peptide-eluted bound fraction was subjected to SDS-PAGE under reducing conditions and the Western blot was probed with Per2B6 and anti-GFP antibodies (lane e; bovine peripherin-2 (BPer) and Xenopus peripherin-2-GFP (XPerGFP) are labeled) (see Methods sections 5.2.6 and 5.2.7).

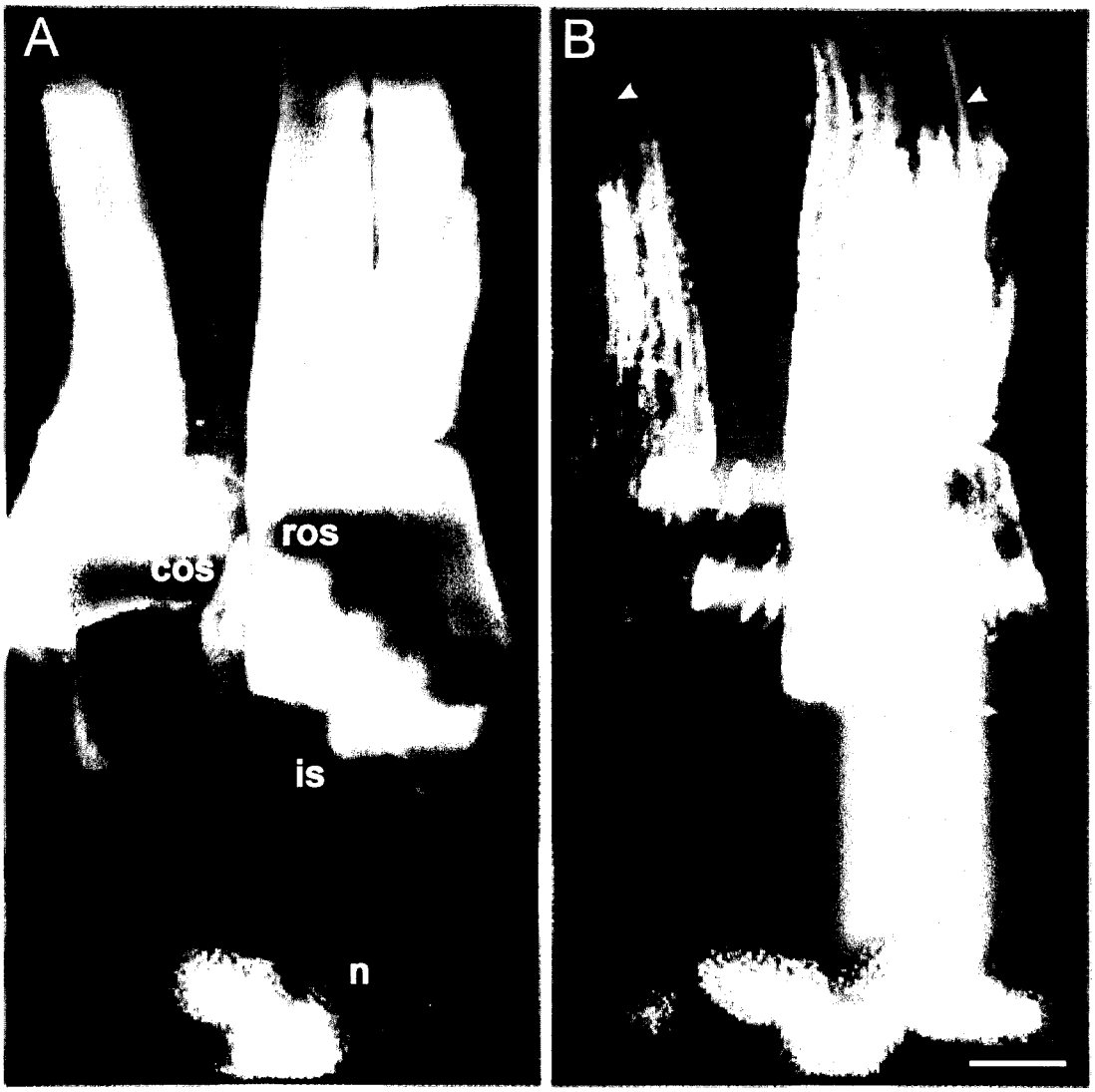

Fig 30. **Endogenous *Xenopus* peripherin-2 localizes to rod and cone outer segments.** Confocal micrographs of a non-transgenic retina labelled with TR-WGA (A) and anti-Xenopus peripherin-2 monoclonal antibody Per2A5 (B). Nuclei were stained with Hoescht33342. In (A), TR-WGA labelling (red) primarily represents opsin localization and is greatest in rod and cone outer segments. (B) Peripherin-2 (green) localizes to incisures (vertical striations marked with arrowheads) of rod outer segment discs and to one edge of cone outer segments (arrow) (see Methods section 5.2.5). ros, rod outer segment; cos, cone outer segment; is, rod inner segment; n, nucleus. Bar, 5 μm.

consistent with the localization of peripherin-2 to disc rims and incisures in ROS of *Xenopus* tadpoles, similar to that observed in mammals (Arikawa *et al.*, 1992) and adult *Xenopus* (Kedzierski *et al.*, 1996). In cones, labelling is restricted to along one side of the cone outer segment, a pattern consistent with localization to the rim region of cone outer segment membranes.

5.3.4 Expression of Xenopus peripherin-2-GFP in transgenic Xenopus rods

The Xenopus peripherin-2-GFP transgene is under control of the *Xenopus* opsin promoter, which directs specific expression to rod cells in the retina. **Fig 31A** shows rod photoreceptor-specific expression of the transgene (in yellow) in the context of a whole *Xenopus* tadpole eye (**Fig 31B**). The contiguous row of photoreceptor nuclei and long uniform appearance of the rod outer segments indicate that retinal degeneration is not occuring. Fusion protein is also observed in phagosomes of RPE cells, indicating that proper disc morphogenesis and shedding has occurred.

Specific targeting of the fusion protein to rod outer segments is observed in **Fig 31C**. Very little fusion protein is located in the inner segments of rods. Non-uniform or mosaic expression of the transgene is observed and varies from eye to eye and rod to rod. This is a property of

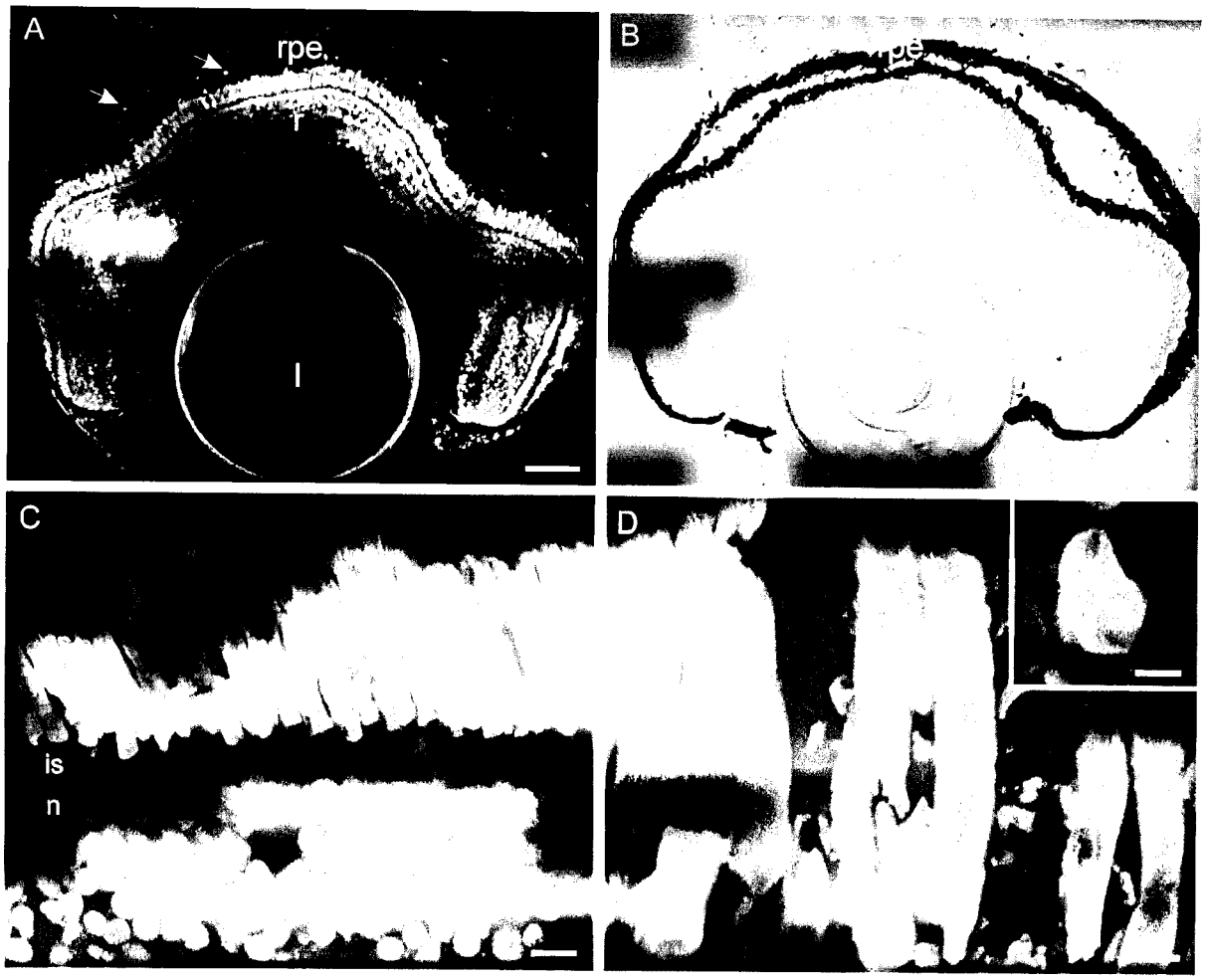

Fig 31. ***Xenopus* peripherin-2-GFP fusion protein targets to rod outer segment membranes.** Cryosections of whole tadpole eyes were labelled with TR-WGA (red) and Hoescht 33342 (blue). (A) Deconvolution epifluorescence microscopy and (B) corresponding DIC image of a retina expressing *Xenopus* peripherin-2-GFP (green and yellow) shows localization of the fusion protein to rod photoreceptors. Fusion protein is also present in phagosomes of RPE cells (arrow). (C&D) Confocal micrographs of retinas expressing *Xenopus* peripherin-2-GFP show outer segment targeting of the fusion protein and localization to disc incisures (arrowheads). Almost no GFP fluorescence is detected in the inner segments. (Inset) Cross-section of a rod outer segment shows disc rim and incisure labelling (see Methods sections 5.2.5). l, lens; r, retina; rpe, retinal pigment epithelium; os, rod outer segment; is, rod inner segment; n, nucleus. Bars: (A&B) 100 μm ; (C) 10 μm; (D) 5 μm; (Inset) 1 μm.

the expression system and is due to differences in sites of integration and number of transgenes incorporated per animal (Moritz *et al.*, 2001). **Fig 31D** shows targeting of the fusion protein to disc incisures (vertical striations) and disc rims (**Fig 31D**, inset), a similar localization as observed for endogenous peripherin-2. At higher expression levels, GFP fluorescence saturates the disc rim and the striated pattern is no longer observed.

Immuno-electron microscopy of transgenic rods confirmed fusion protein localization to disc rims and incisures (**Fig 32**). In regions expressing moderate levels of peripherin-2-GFP (**Fig 32B,C**), it was confined to rims and incisures. In regions expressing high levels (**Fig 32A**), fusion protein was also observed in lamellar regions in addition to rims. High expression levels of fusion protein also correlated with smaller discs and narrower outer segment diameter in many rods (**Fig 32A**).

5.3.5 Expression of bovine peripherin-2-GFP in transgenic Xenopus

To investigate if the requirements for proper outer segment localization of peripherin-2 are conserved across species, bovine peripherin-2-GFP was expressed in transgenic tadpoles and its distribution was examined. **Fig 33A** shows that the bovine fusion protein targeted to rod outer segments and disc incisures. No fusion protein was

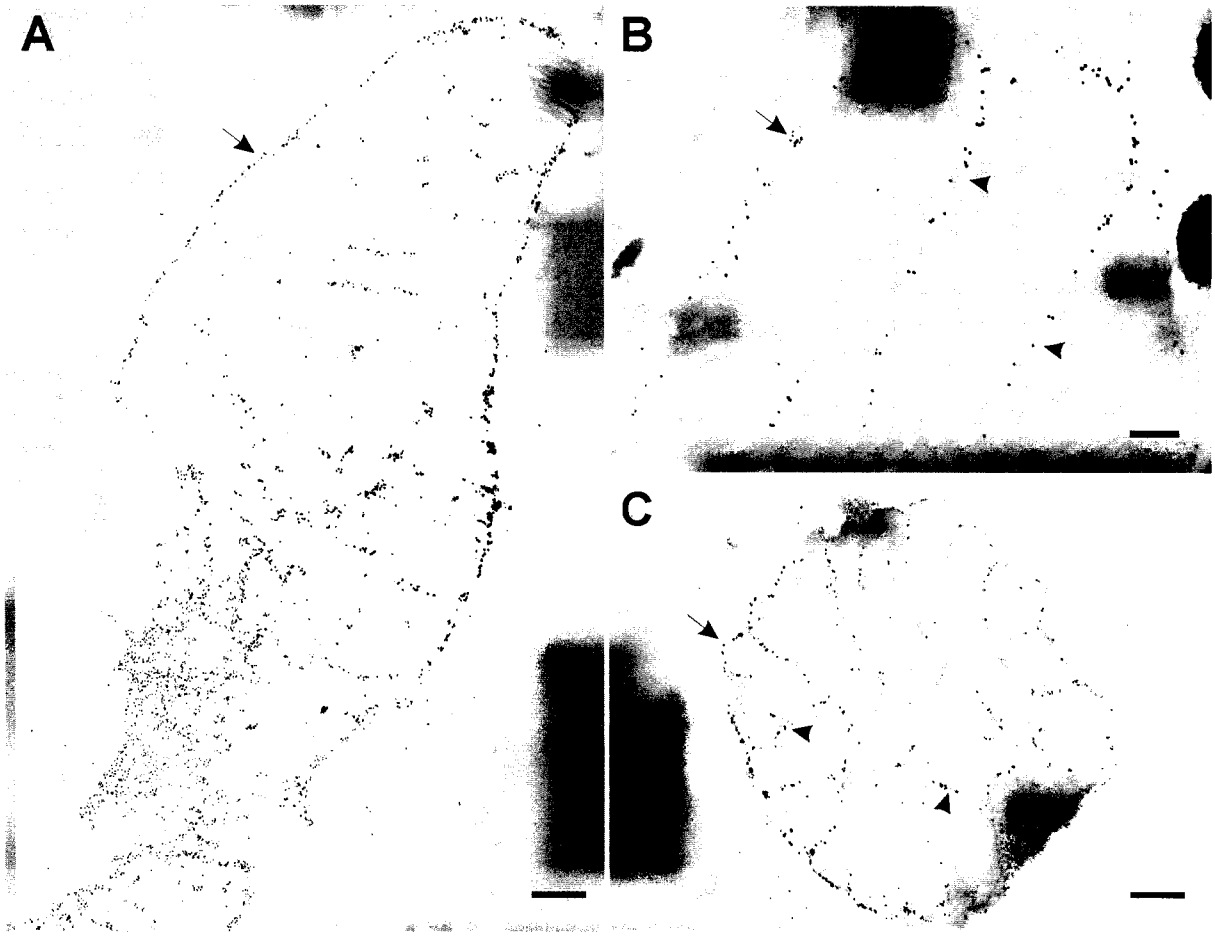

Fig 32. **Immuno-EM reveals targeting of *Xenopus* peripherin-2-GFP fusion protein to disc rims (arrows) and incisures (arrowheads).** Ultrathin sections of transgenic rods were labeled with anti-GFP antibody followed by a gold-conjugated secondary. (A) Composite image of a longitudinal section of a rod expressing high levels of transgene. (B) Longitudinal section of a rod expressing moderate levels of transgene. (C) Cross-section of a rod expressing moderate levels of transgene (see Methods section 5.2.4). Bars: (A) 500 nm;(B) 200 nm;(C) 500 nm.

visible in the inner segments. Because the anti-*Xenopus* peripherin-2 antibody Per2A5 did not cross react with bovine peripherin-2, the effects of transgene expression on endogenous peripherin-2 could be examined (**Fig 33 B-D**). The bovine fusion protein co-localized with endogenous peripherin-2 to incisures of ROS. Comparing the Per2A5 labelling of the rod expressing fusion protein to the rod not expressing fusion protein illustrates the similar localization of endogenous peripherin-2, and suggests that the fusion protein did not cause mistargeting of the endogenous protein. The fusion protein is likely in complex with endogenous peripherin-2.

5.3.6 Transgenic expression of the Retinitis Pigmentosa-causing C214S mutant

The C214S mutation in peripherin-2 is known to cause autosomal dominant retinitis pigmentosa, where rods are primarily affected (Saga *et al.*, 1993). Previous biochemical studies have shown that this mutation prevents core tetramer formation and interaction with rom-1 (Goldberg, Loewen & Molday, 1998). A model describing the molecular basis for disease has been developed that stresses the importance of maintaining above-threshold levels of functional complexes in the outer segments of rods to prevent disease (Goldberg, Loewen & Molday, 1998; Goldberg & Molday, 1996a; Loewen, Moritz & Molday, 2001). The effects of the

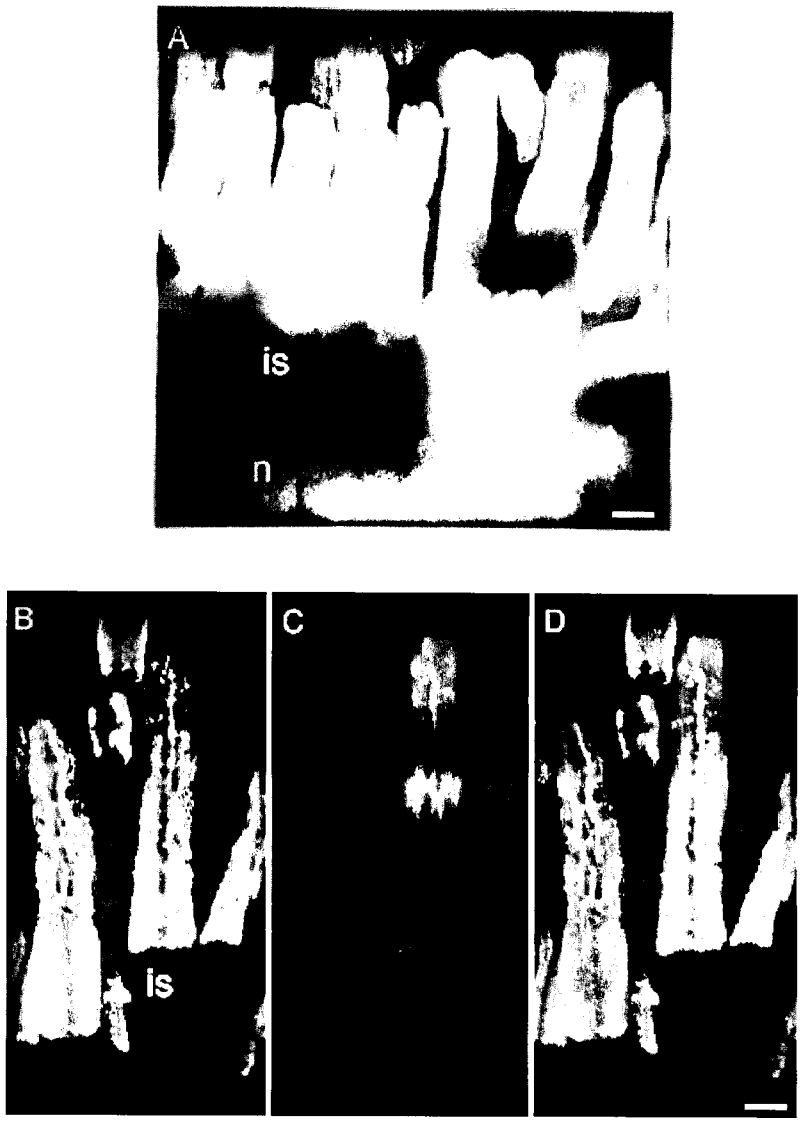

Fig 33. **Bovine peripherin-2-GFP fusion protein targets to rod outer segment membranes and colocalizes with endogenous *Xenopus* peripherin-2.** (A) Confocal micrograph of a retina expressing bovine peripherin-2-GFP (green) labelled with TR-WGA (red) and Hoescht 33342 (blue). (B-D) Confocal micrographs of a retina expressing bovine peripherin-2-GFP labelled with Per2A5 monoclonal antibody showing Per2A5 labelling (B), GFP fluorescence (C), and the combined image (D) (see Methods section 5.2.5). Fusion protein colocalizes with endogenous Xenopus peripherin-2 to the incisures of rod outer segment disc membranes (yellow). os, rod outer segment; is, rod inner segment; n, nucleus. Bars, 5 μm.

C214S peripherin-2 mutation on its expression and subcellular localization in transgenic *Xenopus* rods have been investigated. **Fig 34A & B** show that *Xenopus* C214S-peripherin-2-GFP fusion protein mistargeted to the inner segments and cell bodies of rods. In rods expressing moderate levels of fusion protein, localization was confined to inner segments and cell bodies, whereas in rods expressing higher levels of transgene, fusion protein was observed additionally in outer segments with accumulation near the base. Rod degeneration was not observed.

Fig 34C shows the expression of bovine C214S-peripherin-2-GFP. The same phenotype was observed as with the *Xenopus* fusion protein; mistargeting to the inner segment and cell body. Mistargeting of the fusion protein did not however cause mistargeting of endogenous peripherin-2 (**Fig 34D & E**). Endogenous peripherin-2 did not colocalize with the bovine fusion protein in the inner segment and cell body, but instead was localized to the outer segment similarly to rods not expressing fusion protein. This data suggests that the fusion protein did not interact with endogenous peripherin-2.

Immuno-electron microscopy of rods expressing *Xenopus* peripherin-2-GFP confirmed fusion protein localization to inner segment membranes and shows accumulation at the connecting cilium (**Fig 35A**). Outer segment discs of rods expressing the mutant fusion protein appeared normal (**Fig 35B**). In outer segments, fusion protein localized

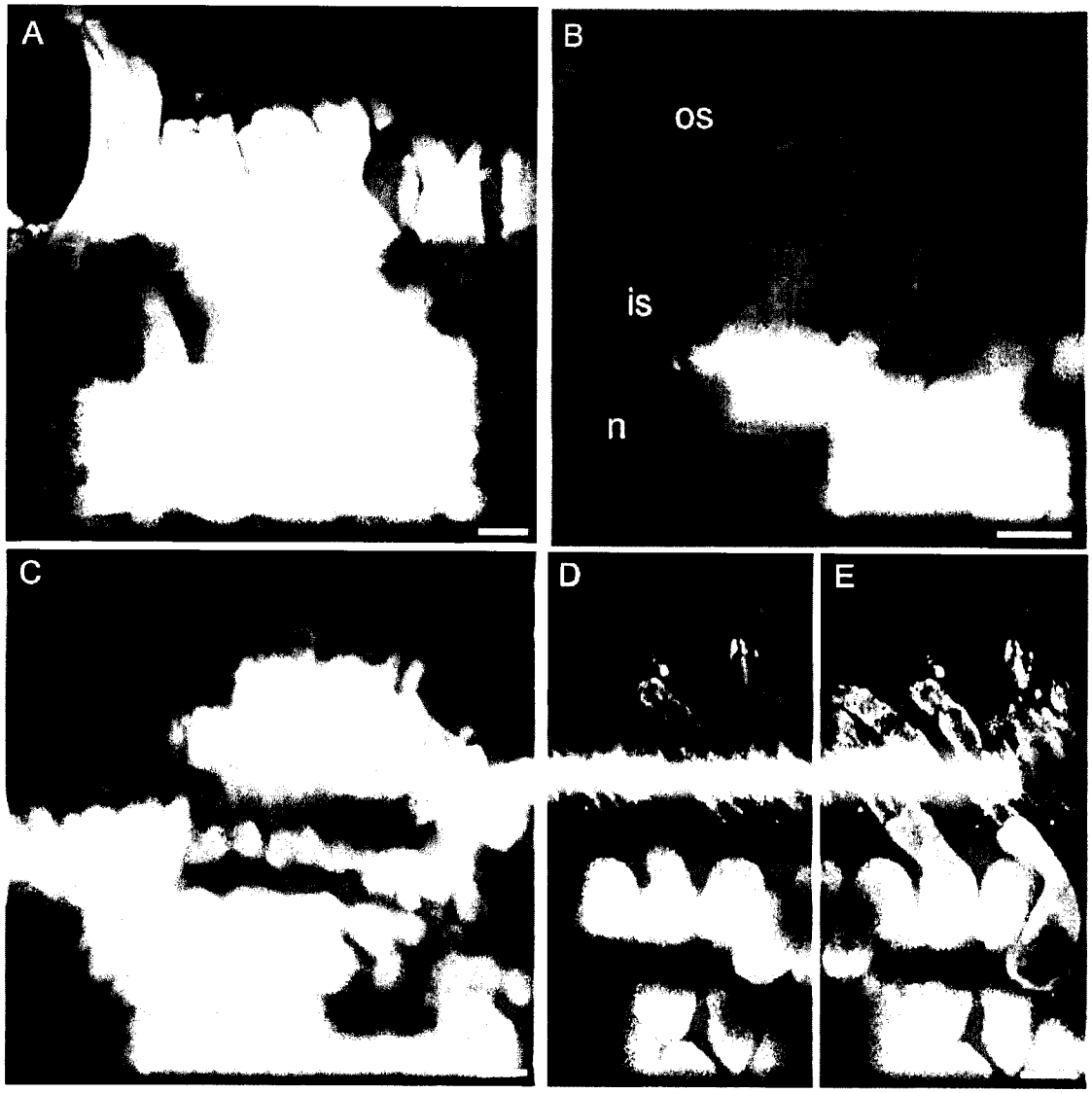

Fig 34. **C214S peripherin-2 mistargets to the rod inner segment and cell body, and does not cause mistargetting of endogenous peripherin-2.** (A&B) Confocal micrographs of retinas expressing *Xenopus* C214S-peripherin-2-GFP (green) labelled with TR-WGA (red) and Hoescht 33342 (blue). (C) Confocal micrograph of a retina expressing bovine C214S-peripherin-2-GFP (green) labelled with TR-WGA (red) and Hoescht 33342 (blue). (D&E) Confocal micrographs of a retina expressing bovine C214S-peripherin-2-GFP (green) labelled with Per2A5 monoclonal antibody (red) and Hoescht 33342 (blue) showing Per2A5 labelling (D) and the overlap with GFP fluorescence (E) (see Methods section 5.2.5). os, rod outer segment; is, rod inner segment; n, nucleus. Bars: (A,B,D&E) 5 μm; (C) 10 μm.

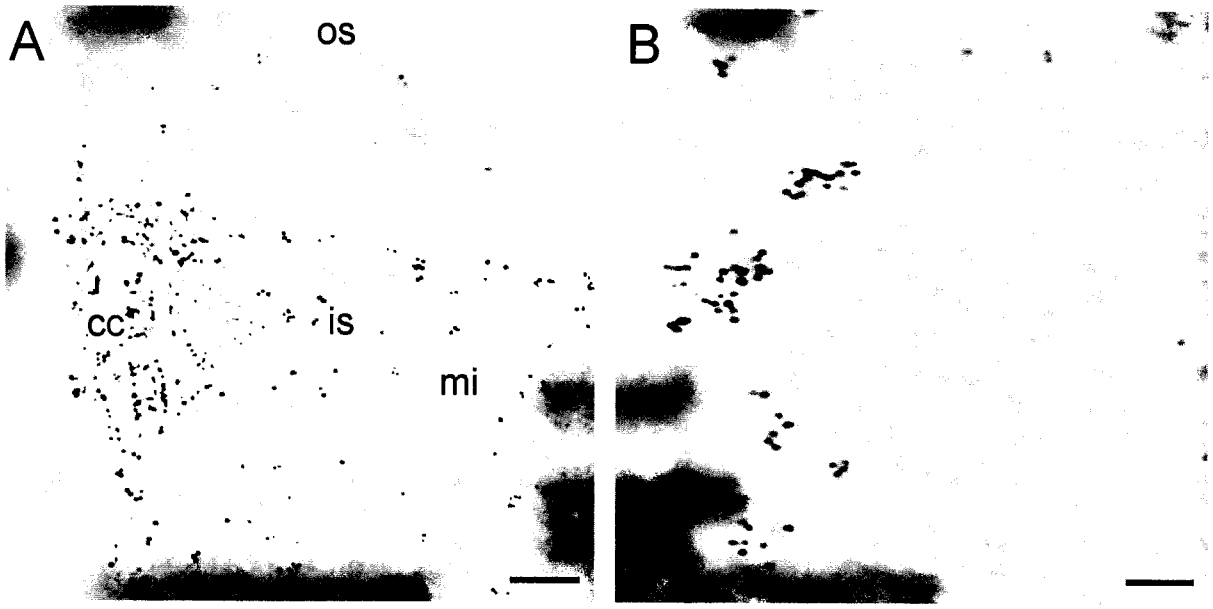

Fig 35. **Immuno-EM reveals accumulation of *Xenopus* C214S peripherin-2-GFP fusion protein at the connecting cilium in the inner segment.** Ultrathin sections of transgenic rods were labeled with anti-GFP antibody followed by gold-conjugated secondary. (A) Longitudinal section through a transgenic rod shows fusion protein accumulation at the connecting cilium (cc) and in the rod inner segment (is). (B) Fusion protein accumulates along the connecting cilium edge of the outer segment but does not disrupt disc structure. os, rod outer segment; is, rod inner segment; mi, mitochondrion (see Methods section 5.2.4). Bars: (A) 200 nm; (B) 100 nm.

in a punctate pattern along the edge of the rod continuous with the connecting cilium (**Fig 35B**). Labelling of disc incisures was not observed.

The molecular properties of bovine C214S peripherin-2 have been examined by velocity sedimentation and SDS-PAGE analysis under nonreducing conditions. This two-dimensional separation technique examines the size of detergent solubilized oligomeric complexes under nondenaturing conditions and the contribution of intermolecular disulfide bonds to complex formation. **Fig 36A** shows that core noncovalent tetramers and higher order disulfide-linked oligomers do not form for the C214S mutant. Instead, the C214S core complex sediments as a noncovalent dimer (a) and as disulfide bonded tetramers (b) (see section 4.3.3) (Loewen, Moritz & Molday, 2001). Considerable aggregation is also present as faster sedimenting species in the sucrose gradient. It consists of high molecular weight disulfide-linked bands on the SDS gel (compare to the WT-like profile in **Fig 36B**). Aggregation of this mutant has been observed on nonreducing SDS gels and by velocity sedimentation under reducing conditions previously (Goldberg, Loewen & Molday, 1998). The inability of this mutant to form core tetramers and well-defined disulfide-linked oligomers provides a molecular rationale for the mistargeting of fusion protein in transgenic rods.

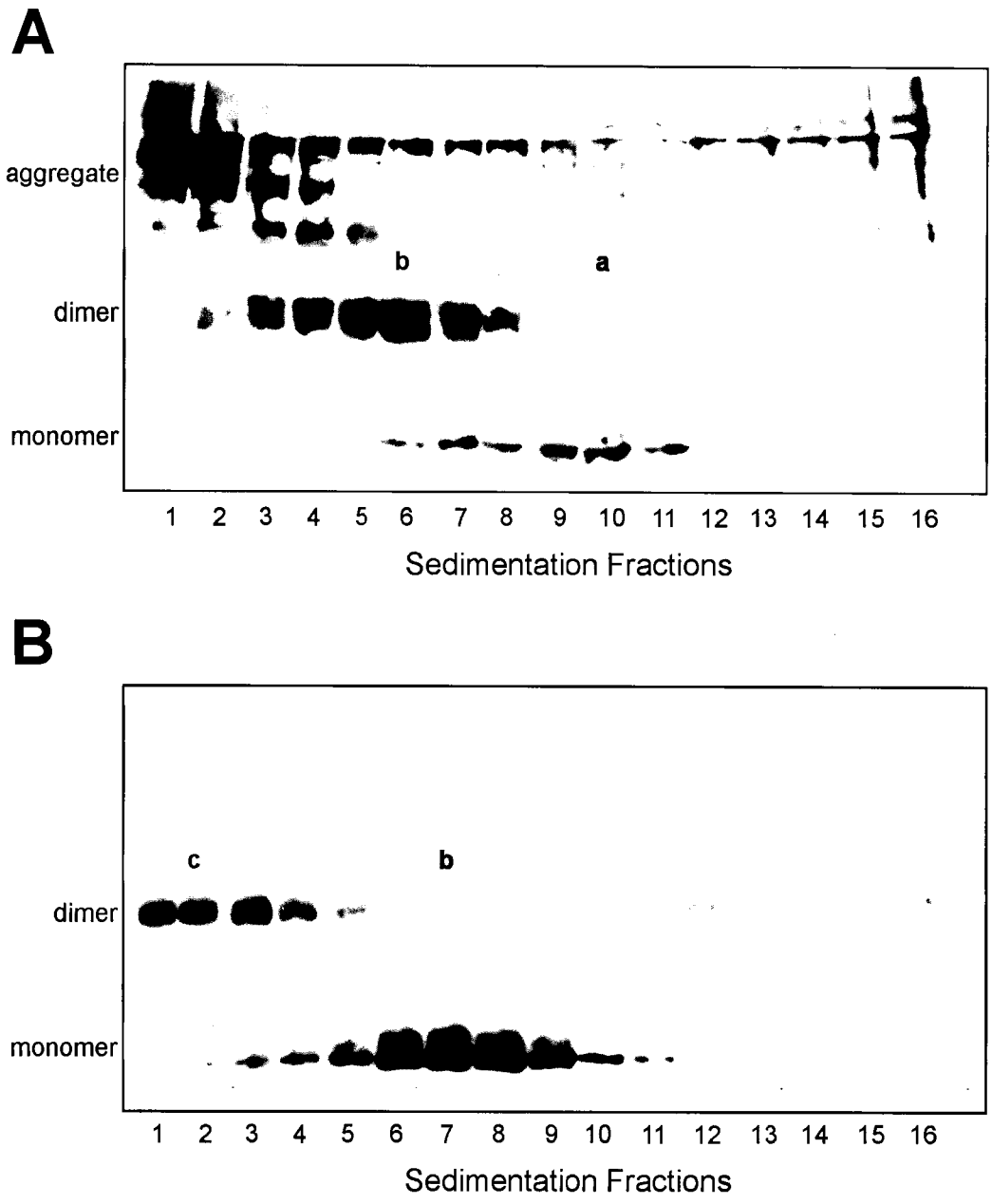

Fig 36. **Velocity sedimentation analysis of C214S and P216L peripherin-2 under nonreducing conditions.** (A) Bovine C214S peripherin-2 was expressed in COS-1 cells, solubilized in buffer containing Triton X-100 and NEM, and subjected to velocity sedimentation on 5-20% sucrose gradients under nonreducing conditions. Fractions were collected from the tube bottom and subjected to SDS-PAGE under nonreducing conditions. Western blots were labelled with Per2B6 antibody. (B) Bovine P216L peripherin-2 was expressed in COS-1 cells and treated as in (A). Sedimentation positions of dimer (a), tetramer (b), and oligomer (c) are indicated (see Methods sections 5.2.6 and 5.2.7).

5.3.7 Transgenic expression of the digenic RP-causing L185P mutant

Digenic retinitis pigmentosa is a complex disease that requires both an L185P mutation in peripherin-2 and a null or G113E mutation in rom-1. Only individuals that inherit both alleles display the disease phenotype. Recently, the effects of the L185P mutation on peripherin-2 core and oligomeric structure have been characterized in detail (Loewen, Moritz & Molday, 2001). L185P peripherin-2 exists as a core heterodimer. A significant fraction further associates through disulfide bonding to form tetramers. However, these tetramers do not form higher order oligomers unless they are associated with WT peripherin-2 or rom-1.

The L185P mutant has been expressed in transgenic rods and its subcellular localization has been examined (**Fig 37**). The *Xenopus* L185P-peripherin-2-GFP fusion protein localized to rod outer segments, inner segments and cell bodies. The degree of mistargeting was much less than observed for the C214S mutant, as significant amounts of fusion protein were observed in the outer segments. Localization to disc incisures was also observed. Rod degeneration was not apparent.

5.3.8 Transgenic expression of the RP-causing P216L mutant

Fig 38A shows the expression of *Xenopus* P216L-peripherin-2-GFP fusion protein in rods of a transgenic retina. A dramatic difference was

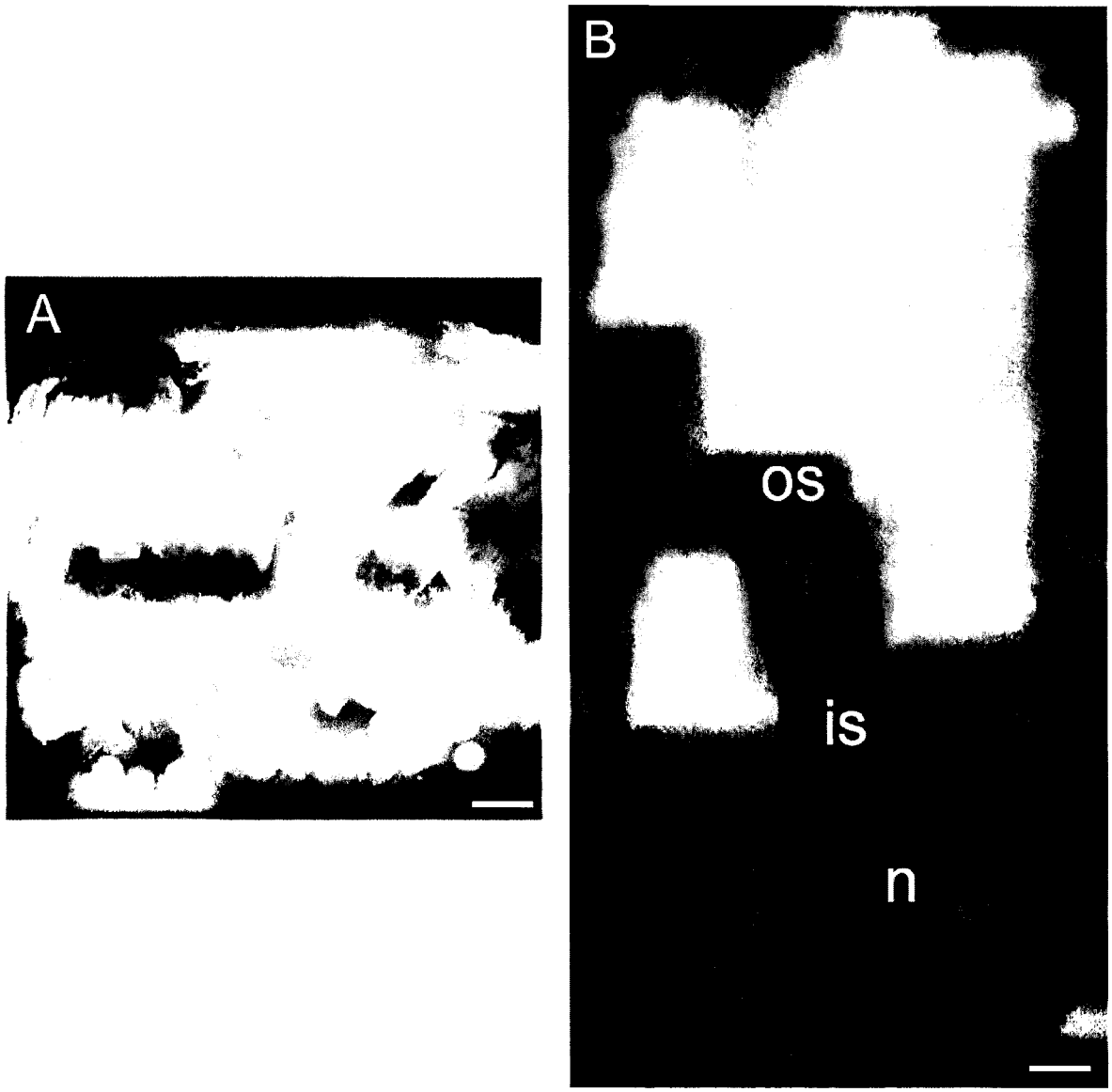

Fig 37. **L185P peripherin-2-GFP targets to the rod outer segment, the rod inner segment,and the cell body.** (A&B) Confocal micrographs of a retina expressing Xenopus L185P-peripherin-2-GFP (green) labelled with TR-WGA (red) and Hoescht 33342 (blue) (see Methods section 5.2.5). os, rod outer segment; is, rod inner segment; n, nucleus. Bars: (A) 10 μm; (B) 2.5 μm.

observed between the cell morphologies of rods in the peripheral retina and rods in the central retina (**Fig 38B**). Peripheral rods were long and uniform in appearance and the fusion protein localized to outer segments and incisures similarly to WT (**Fig 38C**). Rods in the central retina however, appeared shortened and highly disorganized. Fusion protein localized to whorls of membranes in outer segments but was not found in inner segments (**Fig 38D & E**). No incisures were visible. Rod nuclei were also more disorganized in the central retina than in the peripheral retina. The P216L mutation did not cause mistargeting of the fusion protein to the inner segments or cell bodies of rods as observed for the C214S and L185P mutations. The P216L mutation however, affected ROS morphology and resulted in photoreceptor degeneration.

Immuno-electron microscopy revealed that in peripheral rods prior to degeneration, fusion protein localized to disc rims and incisures (**Fig 39A**). Disc structure and organization appeared normal. In central degenerating rods, fusion protein colocalized with whorls of outer segment membranes (**Fig 39B & C**). A breakdown of outer segment organization similar to what is observed in the rds/+ heterozygous mouse and the P216L transgenic mouse was observed (Kedzierski *et al.*, 1997; Sanyal & Jansen, 1981).

Velocity sedimentation and SDS-PAGE analysis of bovine P216L-peripherin-2 under nonreducing conditions (**Fig 36B**) revealed that this

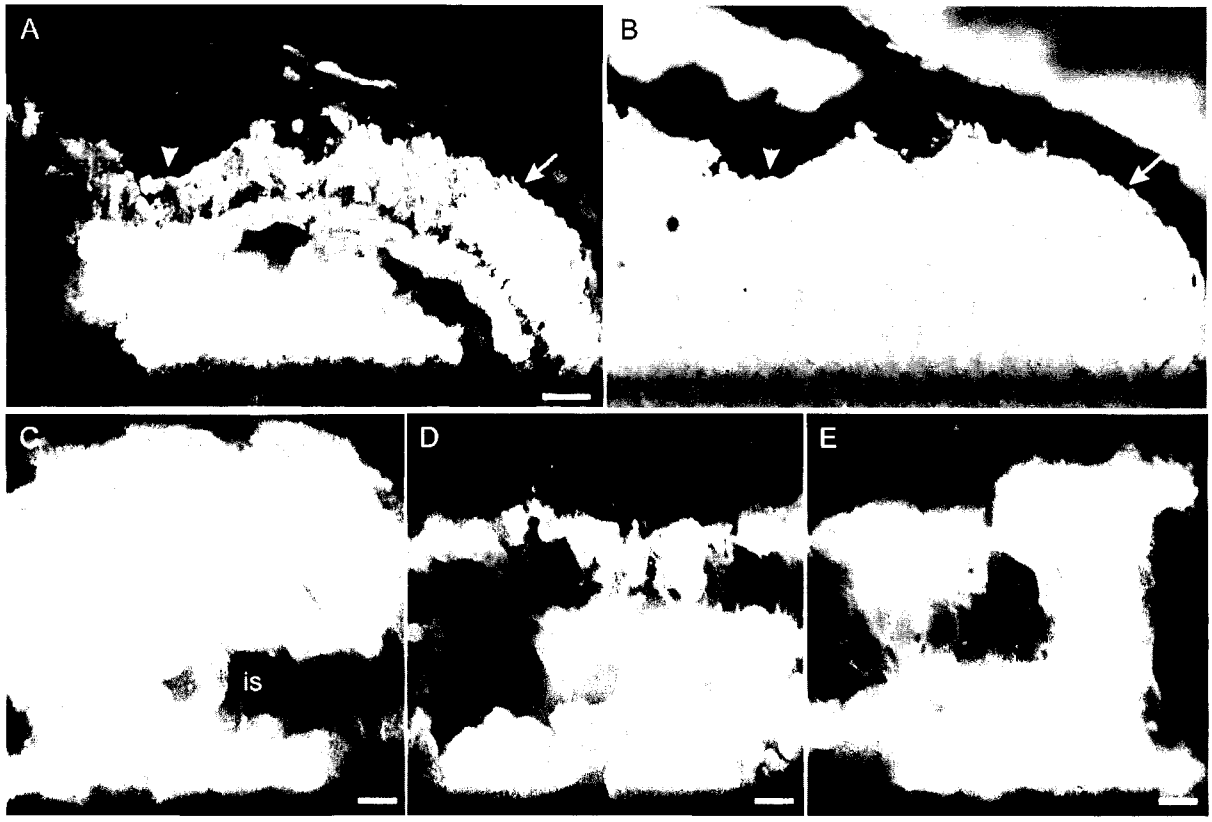

Fig 38. **P216L peripherin-2-GFP targets to the rod outer segment and causes rod degeneration.** (A) Deconvolution epifluorescence microscopy and (B) corresponding DIC image of a retina expressing *Xenopus* P216L-peripherin-2-GFP (green) labelled with TR-WGA (red) and Hoescht 33342 (blue). Rods in the peripheral retina are marked with an arrow and rods in the central retina are marked with an arrowhead. Confocal micrographs of peripheral (C) and central (D&E) regions of the same retina show specific targeting of the fusion protein to the outer segment and degeneration of the central rods. No fusion protein is visible in the inner segment or cell body of either the peripheral or the central rods (see Methods section 5.2.5). os, rod outer segment; is, rod inner segment; n, nucleus. Bars: (A&B) 20 μm; (C) 5 μm; (D) 10 μm; (E) 5 μm.

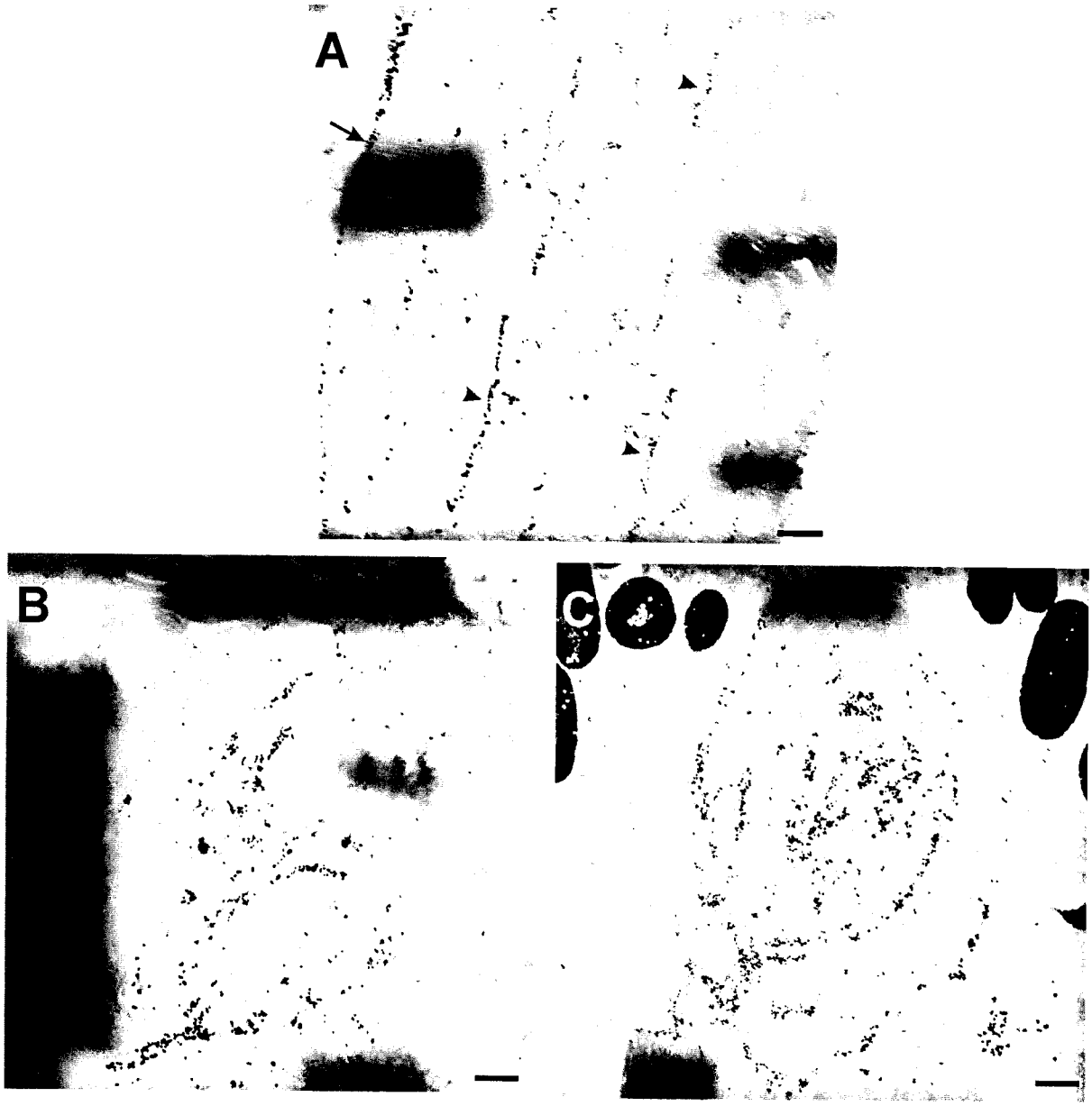

Fig 39. **Immuno-EM of rods expressing *Xenopus* P216L peripherin-2-GFP.** (A) Immuno-EM of a peripheral rod shows transgene localization to disc rims (arrows) and incisures (arrowheads). (B&C) Rods of the central retina show highly disorganized shortened outer segments consisiting of whorls of membranes with transgene labelling throughout (see Methods section 5.2.4). Bars, 250 nm.

mutation did not disrupt core tetramer formation or disulfide-mediated oligomerization. This result explains the observed expression pattern in *Xenopus* rods. Since core formation and disulfide-mediated oligomerization remain intact, the fusion protein did not mistarget to inner segments or cell bodies. Instead, the presence of the mutant protein in rod outer segments resulted in photoreceptor degeneration. This must be due to an additional undefined molecular defect.

5.5.9 Transgenic expression of C150S peripherin-2

To determine the role of disulfide-mediated oligomerization of peripherin-2 in protein targeting and disc morphogenesis, we have expressed *Xenopus* C150S peripherin-2-GFP in transgenic rods and examined the effects by confocal microscopy. C150S peripherin-2 forms core tetramers but is incapable of disulfide-mediated oligomerization (Loewen & Molday, 2000). **Fig 40** shows that C150S peripherin-2-GFP targets specifically to ROS. No fusion protein is visible in inner segments. However, localization to disc incisures is not readily observed as with WT fusion protein or endogenous peripherin-2. In some cases, a single column of labeling near the center of the outer segment is observed (**Fig 40**). This may represent a single, deep incisure.

Rod degeneration was not observed in any C150S animals. Both conventional and immuno-electron microscopy of rods expressing C150S

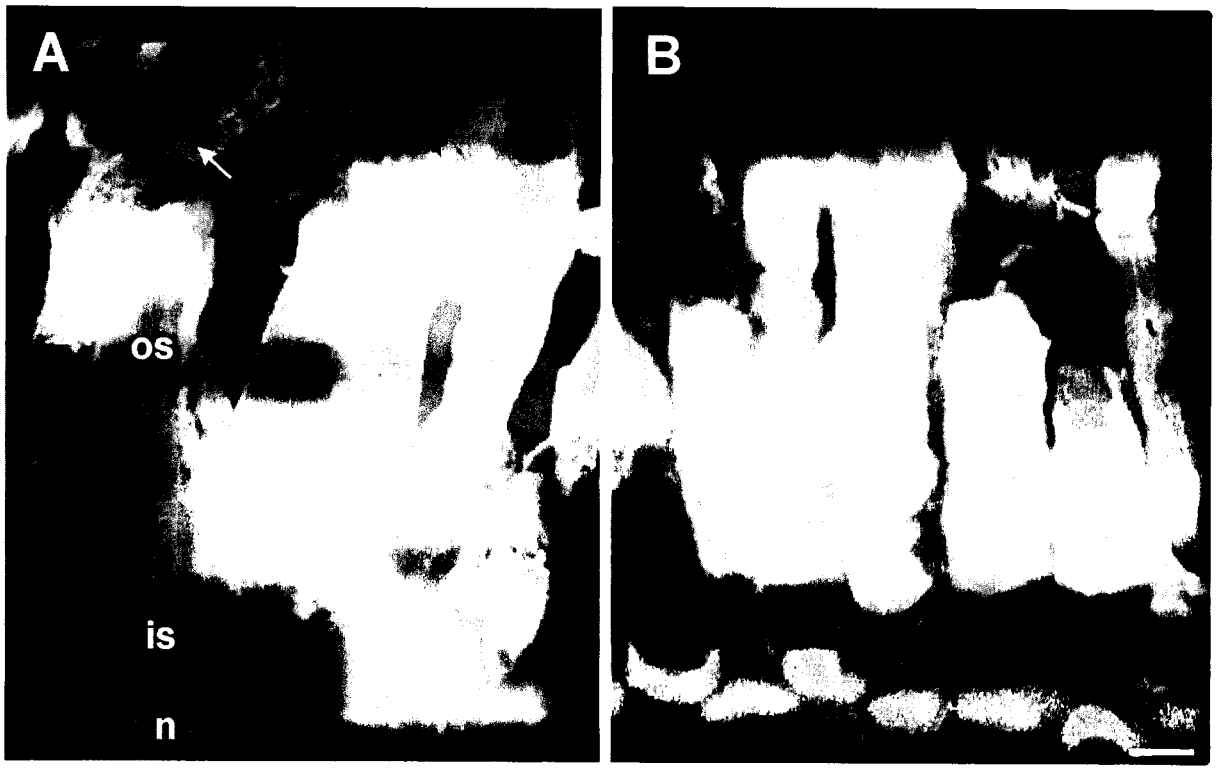

Fig 40. **C150S peripherin-2-GFP targets to ROS, but does not localize to disc incisures.** (A) Confocal micrograph of a retina expressing *Xenopus* C150S-peripherin-2-GFP (green) labeled with TR-WGA (red) and Hoescht 33342 (blue). Fusion protein in outer segments is often observed in a central canal in ROS (arrows; * indicates a cross-section of a ROS). This structure may represent a single incisure. (B) Retina expressing peripherin-2-GFP shown for comparison (see Methods section 5.2.5). os, rod outer segment; is, rod inner segment; n, nucleus. Bar, 5 μm.

peripherin-2-GFP did not reveal any significant structural abnormalities in discs or in organization of the outer segment (data not shown). However, fewer incisures were observed per rod and in some rods, small vesicles were present amongst the discs in the outer segment. These results imply that oligomerization of peripherin-2 is involved in rim and incisure formation and possibly disc stability. The lack of a dominant phenotype is likely the result of having an abundance of endogenous WT peripherin-2 present in these animals.

5.3.10 Expression levels of transgenes

To ensure that the effects observed for the transgenes were not artefacts of high expression levels, we examined retinas expressing WT and mutant peripherin-2-GFP that were processed in parallel by confocal microscopy using the same settings (i.e., laser attenuation, brightness, and contrast). Therefore GFP intensity and thus fusion protein concentration is directly comparable between micrographs. Although GFP intensity is highest in rods expressing peripherin-2-GFP (**Fig 41A**), very little fusion protein was located in rod inner segments. In contrast, micrographs of rods expressing L185P-peripherin-2-GFP (**Fig 41B**) and C214S-peripherin-2-GFP (**Fig 41C**) at lower levels than in *A* showed considerable mislocalization of fusion protein to inner segments and cell bodies. Mislocalization was therefore not a result of high expression of

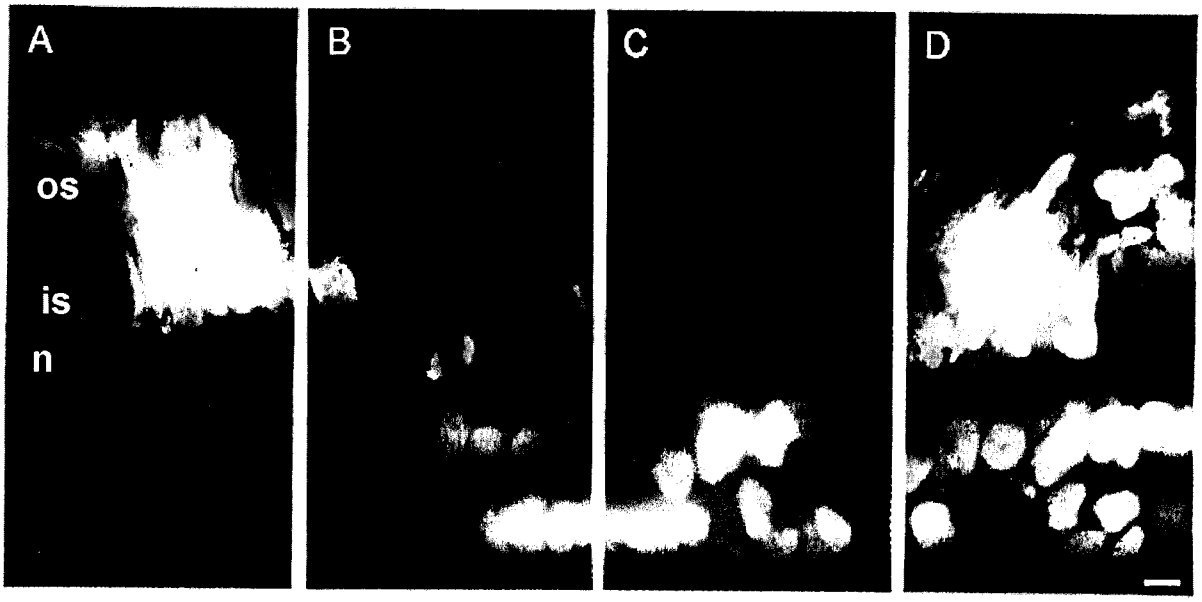

Fig 41. **Overexpression of the Xenopus fusion proteins is not the cause of delocalization to the rod inner segment or rod degeneration.** Transgenic eyes expressing Xenopus peripherin-2-GFP (A), L185P-peripherin-2-GFP (B), C214S-peripherin-2-GFP (C), and P216L peripherin-2-GFP (D) were excised, fixed, and sectioned in parallel. Cryosections from each eye were consecutively imaged by confocal microscopy. All image acquisition settings were identical for all four samples and postmicroscopy processing was done in parallel to the images (see Methods section 5.2.5). GFP (green) and Hoescht 33342 (blue). os, rod outer segment; is, rod inner segment; n, nucleus. Bar, 5 μm.

the mutant fusion proteins. In rods expressing P216L-peripherin-2-GFP (**Fig 41D**), fusion protein was not observed in inner segments or cell bodies. Overall expression of this fusion protein was comparable to peripherin-2-GFP (compare to **Fig 41A**). Therefore the degeneration observed in rods expressing the P216L mutant was not due to high expression levels.

5.4 DISCUSSION

A molecular rationale for how mutations in peripherin-2 cause RP has been developed, but has not been tested in vivo (Goldberg, Loewen & Molday, 1998; Goldberg & Molday, 1996a; Loewen, Moritz & Molday, 2001). This model stresses the importance of having sufficient levels of functional oligomeric complexes in the outer segment. Decreased levels result in photoreceptor degeneration and loss of vision. It is unclear if the mutant proteins are simply mistargeted to the inner segment thereby resulting in an overall reduction of outer segment peripherin-2, or if they are targeted to the outer segment where they exert a dominant negative effect on photoreceptor function. We have developed an *in vivo* system using transgenic *Xenopus* to examine the effects of RP-causing mutations in peripherin-2 on rod photoreceptors. We demonstrate for the first time that transgenic *Xenopus* can be used as a model system to study RP-

linked disease genes and the molecular basis for photoreceptor degeneration.

We show that defects in core tetramer formation result in mistargeting of C214S and L185P peripherin-2 to rod inner segments. Therefore, individuals with mutations that result in defective tetramer formation likely have the disease because of decreased levels of total peripherin-2 in ROS. Core tetramer assembly is necessary for targeting of peripherin-2 to rod outer segments. Additionally, a dominant-negative effect was observed with the P216L mutation in peripherin-2. This mutation did not disrupt core or oligomer formation and did not cause mistargeting in rods, but did result in photoreceptor degeneration. Therefore, RP caused by mutations in peripherin-2 also results from interference with the function of WT protein in outer segments in a dominant-negative manner.

Disc morphogenesis in rod and cone photoreceptors is a highly dynamic process that is essential for photoreceptor viability and vision. New discs are created continuously at a rate of 1 disc every 7-10 minutes (Besharse, Hollyfield & Rayborn, 1977; Young, 1976). Peripherin-2 is critical for disc formation, probably by creating and then stabilizing the disc rim (Arikawa *et al.*, 1992). Therefore, a steady supply of peripherin-2 to the outer segments of photoreceptors is required to maintain proper disc morphogenesis. Disc morphogenesis has been studied in *Xenopus*

laevis using entrapment dyes like Lucifer yellow in conjunction with various pharmacological compounds (Hale, Fisher & Matsumoto, 1996; Matsumoto & Besharse, 1985), but the molecular basis has not been determined. Because photoreceptors are highly polarized cells, they are also an excellent model system to study protein targeting, especially trafficking of membrane proteins. The size of *Xenopus* photoreceptors, which are 5-10 times that of their mammalian counterparts, makes them easy to analyze ultrastructurally by microscopy techniques. We have exploited these advantages in conjunction with the ease and speed of the transgenesis technology to study the effects of disease causing mutations in peripherin-2 on protein targeting and photoreceptor morphology.

We must make certain considerations when analyzing our results. First, transgenesis is a gene "knock-in" procedure where a full complement of endogenous peripherin-2 is present in transgenic rods. We are, therefore, studying the effects of the mutant transgenes over those of the functional endogenous protein. Because mutations in peripherin-2 cause autosomal dominant RP where WT protein is also present (see Table 2 of Introduction), we feel that studying these mutants in *Xenopus* does mimic the disease state. It is more difficult to isolate the effects of the transgene alone on rod function, however. Secondly, mosaic expression of the transgene is an unavoidable consequence of the current transgenesis procedure (Moritz *et al.*, 2001).

Hence, transgene expression levels will vary from rod to rod and retina to retina. An advantage of this variability however, is that a rod expressing the transgene can be compared to a neighbouring rod from the same retina not expressing transgene to determine effects on cell morphology and targeting of endogenous peripherin-2. To compensate for effects due to varying expression levels, relative quantitative confocal microscopy has been performed on all animals so the relative concentrations of fusion proteins can be directly compared. Thirdly, proteins are expressed with GFP fused to their C-terminus to facilitate rapid and easy screening for transgenic animals, and for fusion protein localization by fluorescence microscopy (**Fig 28**).

It is possible that GFP may interfere with the function of peripherin-2. This may occur by (1) interfering with targeting to outer segment discs; (2) disrupting the putative C-terminal fusion domain; (3) disrupting interactions with other proteins; or (4) disrupting core and oligomer formation. Our results indicate that GFP does not interfere with peripherin-2 function since peripherin-2-GFP (1) targets to incisures and rims of rod outer segment discs similarly to endogenous peripherin-2; (2) is found in phagosomes of RPE cells suggesting that proper fusion and shedding occurs; (3) does not cause rod degeneration; and (4) forms core and oligomeric complexes similarly to WT bovine peripherin-2.

We have characterized rods expressing *Xenopus* peripherin-2-GFP by confocal and electron microscopy (**Fig 31 & 32**). Localization of the fusion protein to outer segments confirms that GFP does not interfere with outer segment targeting. Very little fusion protein was observed in inner segments. This is indicative of a very fast rate of trafficking to the outer segment (Moritz *et al.*, 2001). Targeting of fusion protein to disc rims and incisures confirms proper formation of these structures. In regions of outer segments expressing very high levels of fusion protein, localization is not restricted to rims and incisures, but is observed in the lamellar regions of discs or other membrane structures (**Fig 32A**). This is likely due to an overflow effect caused by excess fusion protein into non-rim regions rather than a GFP-related mistargeting. It is not known what effects the fusion protein has on these regions, but in many rods, smaller discs and smaller outer segment diameter are observed in regions of high expression. It is possible that the increased levels of peripherin-2 result in increased rates of rim formation and hence smaller discs, assuming the rate of membrane evagination remains the same. If the fusion protein inhibited disc formation, fusion protein accumulation at the base of the outer segment proximal to the connecting cilium would be expected. Neither this nor a phenotype similar to what is observed in the rds/+ heterozygous mouse was observed. Retinal degeneration did not occur in any *Xenopus* peripherin-2-GFP transgenic animals. Therefore, in

the full range of expression levels, which may be comparable to rhodopsin levels and higher than endogenous peripherin-2, the fusion protein did not cause photoreceptor degeneration. This is an important control for determining the effects of disease-causing mutations on photoreceptor morphology and survival.

Expression of bovine peripherin-2-GFP in transgenic *Xenopus* resulted in a similar localization as the *Xenopus* ortholog (**Fig 33**). These results are significant because it shows that the protein sorting machinery has been conserved through evolution and that it is possible to study mammalian genes in this system. Therefore, experiments can be designed in transgenic *Xenopus* to elucidate the signals and mechanisms of protein targeting using *Xenopus* or mammalian orthologs of genes. By expressing bovine peripherin-2-GFP, it was possible to examine the effects of fusion protein on the localization of endogenous peripherin-2. The bovine fusion protein co-localized with endogenous peripherin-2 to rod outer segments and disc incisures (**Fig 33**). These data in conjunction with our molecular data showing that bovine peripherin-2 assembles with *Xenopus* peripherin-2 (**Fig 29**) strongly suggest that these proteins are in complex in transgenic rods. Further evidence comes from rods expressing extremely high levels of bovine fusion protein. Colocalized mistargeting of both the fusion protein and endogenous peripherin-2 to inner segments was observed (data not shown). We

believe that this mistargeting is due to the abnormally high levels of transgene expression (much higher than observed for Xenopus peripherin-2-GFP) and is not a result of an inherent mistargeting property of the bovine fusion protein. Otherwise mistargeting would be observed at moderate to low fusion protein levels similarly to the C214S mutant. These results do confirm that the fusion protein is in complex with endogenous peripherin-2.

We have examined the effects of the RP-causing C214S mutation in peripherin-2 by expression in transgenic *Xenopus* (**Fig 34**). An obvious targeting defect is present in this protein which prevents most of it from reaching the outer segment. Mutant fusion protein accumulates in membranes of the inner segment and cell body. In rods expressing higher levels, fusion protein accumulates near the base of the outer segment. Electron microscopy (**Fig 35**) revealed that fusion protein accumulated at the connecting cilium in the inner segment and along the edge of the outer segment proximal to the connecting cilium. Fusion protein incorporation into disc incisures was not observed. These results indicate that fusion protein that reaches the outer segment is not incorporated effectively into disc rims. The mutant fusion protein did not disrupt disc structure, which suggests that it is not interfering with the function of endogenous peripherin-2. We did not observe mistargeting of endogenous peripherin-2 to inner segments or cell bodies in these

animals (**Fig 34**). This is further evidence that the mutant fusion protein does not interact with WT *in vivo*. This finding is supported by our previous studies that show that the C214S mutant does not interact with rom-1 (Goldberg, Loewen & Molday, 1998). It is likely that photoreceptor degeneration did not occur in these animals because the mutant protein did not interfere with the targeting or function of endogenous peripherin-2. In humans, the C214S mutation likely prevents targeting to the outer segment and interaction with endogenous WT peripherin-2. This leads to decreased total levels of peripherin-2 in rod outer segments and a disease phenotype. Retinal degeneration is observed in the heterozygous rds/+ mouse which results from a 50% reduction in total peripherin-2 (Cheng *et al.*, 1997; Sanyal & Jansen, 1981).

To understand the molecular basis for mistargeting of the C214S mutant in transgenic *Xenopus*, we have determined if the mutant protein is capable of core tetramer formation and disulfide-mediated oligomerization (**Fig 36**). WT peripherin-2 forms core noncovalent tetramers that assemble into large disulfide-linked oligomers of various sizes (Loewen & Molday, 2000). These oligomers are thought to be important for disc morphogenesis possibly by binding opposing disc membranes and creating disc rims (Loewen & Molday, 2000; Loewen, Moritz & Molday, 2001; Wrigley *et al.*, 2000). We find that the C214S mutation prevents core tetramer formation and disulfide-mediated

oligomerization and results in non-specific aggregation of the protein. The inability of C214S peripherin-2 to form these native complexes must be the cause of the mistargeting observed in transgenic *Xenopus*. Mistargeting could result from retention in the ER and Golgi membranes by molecular chaperones because of the misfolded nature of the protein, or because a functional outer segment sorting signal is no longer present. Accumulation of fusion protein at the connecting cilium in post-Golgi membranes (**Fig 35**) and low levels of fusion protein in the ER (data not shown) argue for the latter in which mistargeting likely results from the disruption of an outer segment sorting signal. Core tetramer formation is likely required for signalling to the outer segment and will be discussed in greater detail below.

Recently, the molecular interactions and defects that result in digenic RP have been examined in detail (Loewen, Moritz & Molday, 2001). The L185P core complex is a noncovalent dimer that can disulfide bond to form a covalent tetramer. It cannot oligomerize into larger disulfide-linked complexes unless WT peripherin-2 or rom-1 is present. Therefore, the core tetramer is required for disulfide-mediated oligomerization. The molecular rescue of L185P by WT peripherin-2 is not 100% efficient, however, and a fraction of noncovalent heterodimer remains. It has been proposed that decreased levels of oligomers in the outer segment results in photoreceptor degeneration (Loewen, Moritz &

Molday, 2001). We have expressed the L185P mutation in transgenic *Xenopus* and found that a fraction of the fusion protein mistargets to the inner segment while the majority is located in the outer segment. It is likely that the mutant fusion protein assembles with endogenous WT peripherin-2 to form a mixture of disulfide-linked oligomers and noncovalent dimers similar to what is observed in COS-1 cell experiments. The oligomers probably target to the outer segment where they may function normally, and the non-tetrameric core complexes likely mistarget to the inner segment in a fashion similar to that observed for the C214S mutant.

Rod degeneration was not observed in these animals. This is probably because the ratio of mutant fusion protein to endogenous WT peripherin-2 did not reach a degenerative threshold level. In human RP, where the ratio of mutant to WT is predicted to be 1:1, mistargeting of dimeric complex to the inner segment would result in a significant decrease in total outer segment peripherin-2. Therefore, like the C214S mutation, we predict that the L185P mutation causes disease by decreasing the total level of peripherin-2 in the outer segment - a result of mistargeting of mutant dimers to the inner segment.

Only one RP-causing mutation, P216L, has been examined *in vivo* in transgenic mice (Kedzierski *et al.*, 1996). In the rds/+ heterozygous background, which mimics the human disease state, the P216L mutation

caused photoreceptor degeneration and cell death. Because the transgene was indistinguishable from endogenous peripherin-2, it was not possible to determine its subcellular localization and hence any targeting defects due to the mutation. We have shown in transgenic *Xenopus* that the P216L mutant targets to outer segment disc rims and incisures, but causes photoreceptor degeneration. It does not mistarget to rod inner segments or cell bodies. Degeneration was confined to the rods of the central retina. The outer segments of these cells were shortened and highly disorganized consisting of whorls of membranes. Cones were unaffected at this stage. Because photoreceptors of the central retina are considerably older than peripheral rods (Hollyfield, 1971) we reason that a time-dependent degeneration results from the presence of mutant protein in the outer segments. This type of central to periphery directed degeneration has been observed in transgenic *Xenopus* rods expressing rab8 mutants (O. Moritz, personal communication). Further analysis of transgenic animals at various later stages will be required to rigorously define the time course of degeneration and to see if peripheral rods eventually degenerate.

The molecular defect leading to this degeneration is currently not known. Biochemical analysis of bovine P216L peripherin-2 has not revealed any defects in core tetramer formation or disulfide-mediated oligomerization (**Fig 36**). However, these results are consistent with the

localization observed in rods prior to degeneration. Since the mutant is not defective structurally, it targets properly to disc incisures and rims in the outer segment. A defective molecular event downstream of assembly of the mutant into discs must result in destabilization and rod degeneration. Close examination of the degenerating outer segments reveals that organized disc structure is no longer present and mutant protein is located throughout whorls of membranes, similarly to the rds/+ heterozygous mouse. It is possible that over time the presence of the mutant protein in discs destabilizes their structure or disrupts critical interactions with other factors that regulate disc stability and organization. We have not yet examined the stability of peripherin-2 mutants, and interaction of peripherin-2 with other outer segment proteins is currently under investigation. There is no evidence for a role for peripherin-2 in visual transduction. However, ABCR localizes to disc rims and incisures (Molday, 1998). Its activity might be affected by malformed disc rims.

Rod photoreceptors must possess multiple protein sorting/trafficking pathways to accomplish the task of targeting proteins specifically to the various compartments of the outer segment. The Na/Ca-K exchanger and the cGMP-gated channel for example are only located in the plasma membrane whereas peripherin-2, rom-1 and ABCR are only found in the rim region of discs (Molday, 1998). Rhodopsin on

the other hand is excluded from the rims, but is located in the lamellar region of discs and in the plasma membrane (Molday, 1998). Sorting signatures must therefore exist in these proteins to target them to their correct locations. Proteins targeted to the same location likely possess similar signals. Recently, the C-terminal eight amino acids of rhodopsin have been shown to comprise an outer segment sorting/retention signal using transgenic *Xenopus* (Tam *et al.*, 2000).

We have identified a component of this signal in peripherin-2 (**Fig 42**). Both the C214S and the L185P mutations in peripherin-2 cause mistargeting of fusion protein to rod inner segments in transgenic *Xenopus*. Both of these mutations result in defective core tetramer formation. The P216L mutation does not disrupt core or oligomer formation and does not cause mistargeting in transgenic rods. Analysis of transgenic rods expressing *Xenopus* C150S-peripherin-2-GFP did not result in any mistargeting of fusion protein to the inner segment. This mutation prevents disulfide-mediated oligomerization, but not core tetramer formation (Loewen & Molday, 2000). These results indicate that the core tetramer, not the disulfide-linked oligomer, is required for outer segment localization. It is likely that the sorting signal in peripherin-2 is contained in its cytoplasmic C-terminus and requires tetramerization for recognition by the sorting machinery. Experiments are currently

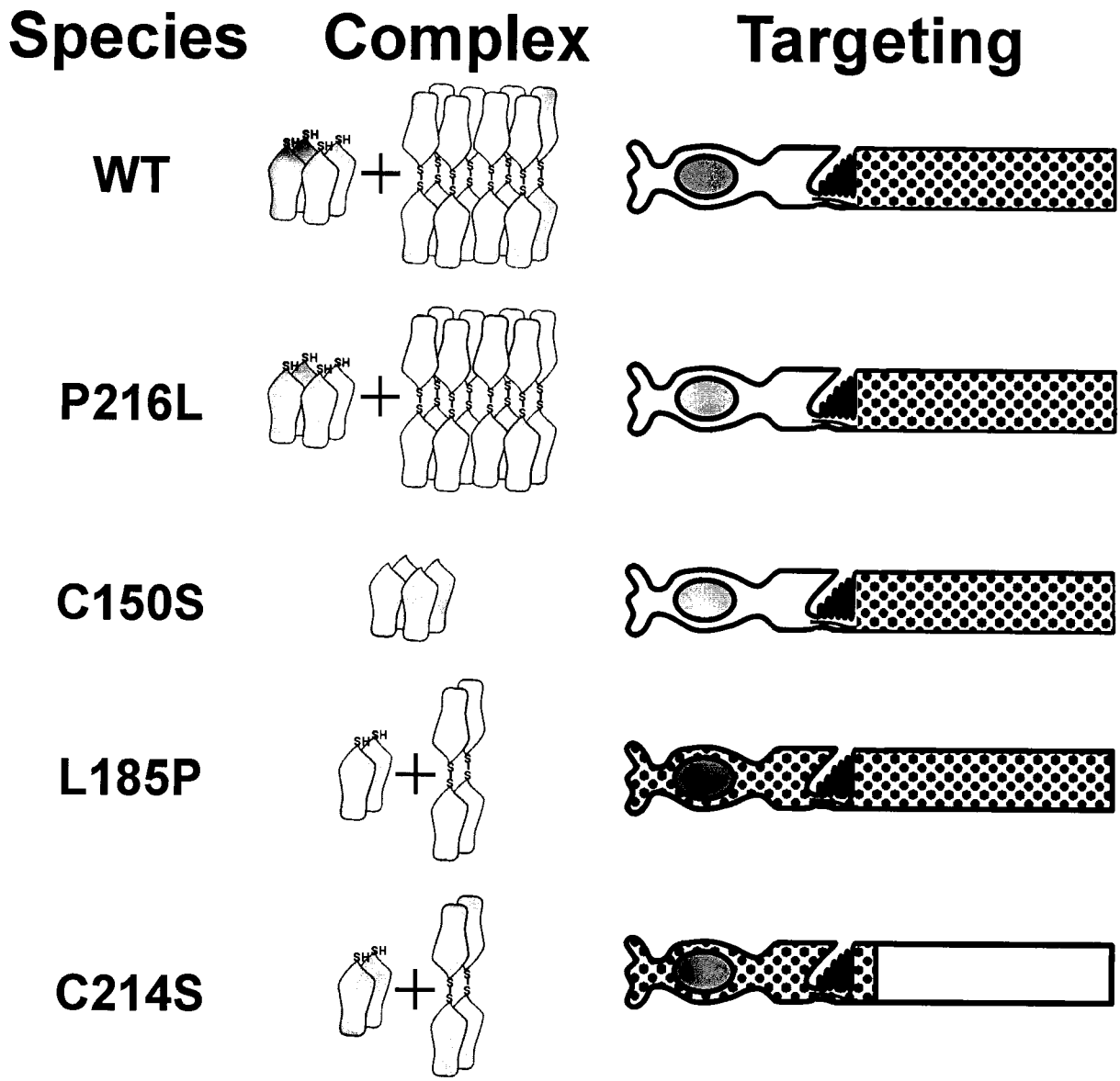

Fig 42. **Molecular rationale for targeting of peripherin-2 to ROS.** WT peripherin-2 forms core tetramers and disulfide-linked oligomers and targets specifically to ROS. The P216L mutation does not disrupt core or oligomer formation and does not disrupt targeting to ROS. The C150S mutation prevents disulfide-linked oligomerization but does not result in mistargeting to RIS. Therefore, disulfide-mediated oligomerization is not required for ROS targeting. The L185P mutation prevents core tetramer and oligomer formation in the absence of WT and results in mistargeting to RIS. A portion of L185P peripherin-2 forms core tetramers and oligomers with WT and targets to ROS. The C214S mutation prevents core tetramer and oligomer formation and does not interact with WT. C214S peripherin-2 mistargets to RIS. Therefore, the core tetramer is required for targeting of peripherin-2 to ROS. RP-causing mutations result in disease by (1) decreasing the level of peripherin-2 in ROS because of mistargeting, (2) exerting a dominant negative effect in ROS on rod function.

underway to identify this sequence.

Restoration of functional photoreceptor outer segments by gene therapy in the rds mouse has recently been accomplished by adding back WT peripherin-2 (Ali *et al.*, 2000). This technique may prove very useful in treating or curing blindness in people with defects in the gene encoding peripherin-2. However, it is essential to determine the molecular basis for how mutations in peripherin-2 cause photoreceptor degeneration in order to develop effective gene therapy treatment strategies. We have shown that, like RP-causing rhodopsin mutations (Sung & Tai, 2000), mutations in peripherin-2 cause RP through mistargeting of mutant protein to the inner segment. Therefore, RP that results from decreased total levels of peripherin-2 in the outer segment (like the C214S and L185P mutations, and probably the C165S mutation) should be treatable by increasing the level of WT peripherin-2. RP resulting from the P216L mutation and other dominant negative mutations, may require additional strategies to inactivate or decrease the level of the mutant protein.

CHAPTER 6 - CONCLUSION

6.1 SUMMARY

The results of this investigation have provided valuable new insight into the structural features of peripherin-2 and rom-1 complexes, and what functions they serve in photoreceptor outer segment development – a process that is absolutely required for photoreceptor viability and for vision. Without this intricate architecture, we would find no use for inventions like the light bulb or the printing press, and we would take no pleasure in the sights of paintings, photographs, a spring flower, a snow capped mountain, or of those dearest to us. As such, peripherin-2 plays a dominant role in photoreceptor development and creates the scaffold through which we see the world.

Disulfide bond formation within the intradiscal loop region of peripherin-2 is critical for folding and subunit assembly of the core tetrameric complex. Six of the seven conserved cysteines within the loop region are likely involved in forming intramolecular disulfide bonds, although these have yet to be demonstrated. One unique cysteine, *C150*, is solely responsible for intermolecular disulfide bond formation. We have demonstrated that instead of forming disulfide dimers within the core complex, C150 residues actually link tetramers into octamers and other higher-order oligomeric forms through intermolecular disulfide bond formation. This disulfide bond is readily reduced when subjected to only

mildly reducing conditions and facilitates dissociation of oligomers into core tetrameric complexes. This result and the fact that noncovalent core tetramers are also present in ROS, implies that a level of plasticity exists in oligomer formation, size and stability, and suggests a dynamic role for these complexes in the rims of discs. We have shown that core tetramer formation is required for oligomerization but not disulfide dimerization, and that formation of higher-order oligomers, therefore, involves both covalent (disulfide bonds) and noncovalent interactions. We propose that the core tetramer has two-fold symmetry and exists as a dimer-of-dimers. Experiments in transgenic frogs have revealed that the core tetramer is required for targeting to photoreceptor outer segments.

We have demonstrated a role for rom-1 in inhibition or regulation of higher-order oligomer formation. Peripherin-2 complexes from ROS that contain rom-1 are incompletely disulfide bonded and are limited in size to octamers. Rom-1 in the absence of peripherin-2 has a decreased ability to form disulfide-linked octamers, and when reconstituted with peripherin-2 in a heterologous system, limits the size of peripherin-2 complexes to octamers. Therefore, it is likely that association with rom-1 prevents the conformational change required to produce higher-order oligomers upon disulfide linking of C150 residues. These results are consistent with the dominant role for peripherin-2 in disc morphogenesis as demonstrated by the drastic phenotype associated with the *rds* mouse

and a regulatory role for rom-1 as demonstrated by the very mild phenotype of the rom-1 knockout mouse.

By examining the effects of disease-causing mutations in peripherin-2 on its oligomeric structure and targeting in rod photoreceptors, we have developed a molecular rationale describing how misfolding and mistargetting result in overall decreased levels of oligomeric complexes in ROS and photoreceptor degeneration. The important finding that some mutations (C165Y, C214S, L185P) prevent disulfide-mediated oligomerization provides further evidence for the functional significance of these oligomers in ROS. Another mutant, P216L, targets to ROS and appears structurally normal, but exerts a dominant negative effect on photoreceptor morphology and results in photoreceptor degeneration. This mutant is clearly behaving differently than the others. This finding suggests that either subtle undetected structural abnormalities lead to photoreceptor degeneration, or that another critical function or interaction has been disrupted. In any case, the inherent complexity and heterogeneity of disease phenotypes associated with mutations in peripherin-2 has been demonstrated.

Out of necessity, through the course of this work we have developed new methods to study the structure and function of membrane proteins. The 2-dimensional method which combines velocity sedimentation and non-reducing SDS-PAGE for determining the

contribution of intermolecular disulfide bonds to oligomeric protein structures is applicable to other membrane proteins. We have also developed an SDS-denaturation-immunopurification method to quantitate the absolute amount of a given protein subunit from a tissue. This technique is currently being used to determine the subunit stoichiometry of the cGMP-gated channel complex. Lastly, we have demonstrated for the first time, that transgenic *Xenopus laevis* can be used as a model system to study the effects of disease-causing mutations in photoreceptor genes on protein trafficking, photoreceptor morphology, and viability.

6.2 ORGANIZATION OF PERIPHERIN-2 COMPLEXES IN THE DISC RIM

We have proposed two models for how peripherin-2 oligomers are situated in the disc rim based on whether disulfide bonding of tetramers occurs laterally within one membrane (**Fig 43A**) or in a head-to-head manner across two membranes (**Fig 43B**). We assume that the subunits of the core tetramer exist in a single membrane because the smallest complex we can isolate from bovine ROS is the tetramer.

The *shell* model predicts that laterally disulfide-bonded tetramers will make an oligomeric ring or coil depending on whether the tetramers are perfectly aligned or off-set when they are linked. These rings then may associate noncovalently and circumscribe the disc rim. Peripherin-2

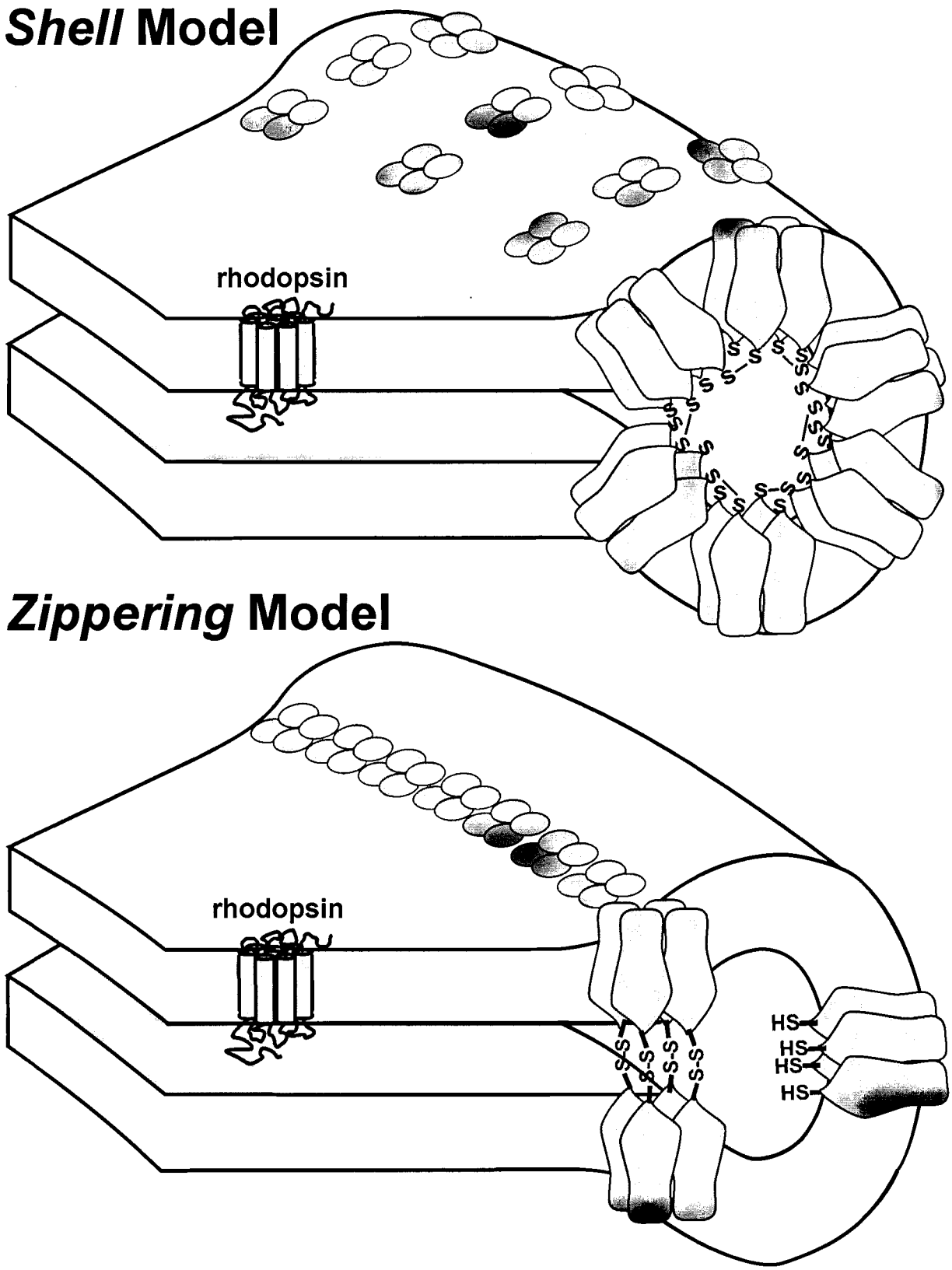

Fig 43. **Organization of peripherin-2 in the disc rim.** Two possible models are shown for how peripherin-2 oligomers create and stabilize the disc rim. For details, see the text.

oligomers that do not contain rom-1 need to be perfectly disulfide-linked, whereas those containing rom-1 do not (Loewen & Molday, 2000). Tetramers that do not align properly are not disulfide linked. The potential role of the intermediate oligomer or octamer is not as clearly defined in this model as in the *zippering* model. Support for the *shell* model comes from evidence of disulfide-mediated oligomerization of tetramers in the heterologous COS-1 cell system, which can likely accommodate linking of tetramers within the same membrane (Loewen & Molday, 2000). However, a direct role for oligomers in binding of adjacent membranes is not as obvious in this model and does not agree as well with recent studies showing peripherin-2-induced flattening of microsomal membranes (Wrigley *et al.*, 2000). Although, coils of oligomers could possibly induce "kinking" of the vesicles which might result in the observed vesicle morphology.

The *zippering* model predicts that core tetramers from opposing membranes at the lamellar-rim border align head-to-head to form octamers which bind the membranes. Octamerization facilitates higher-order oligomer formation which proceeds around the disc driving rim formation and circumscribing it. Tetramers that do not align with the correct geometry are not linked. This model emphasizes the octamer as a discrete structural and functional element and is supported by the existence of these complexes in both ROS and transfected COS-1 cells.

The ability of peripherin-2 complexes to flatten microsomal vesicles in a disulfide-dependent manner, and the existence of the myelin stabilizing protein Po which binds opposing myelin membranes across the extracellular space (Shapiro *et al.*, 1996) further support this model. A potential problem for the *zippering* model comes from COS-1 cell expression studies where disulfide-linked oligomerization does occur. If tetramers are linking across membranes in COS-1 cells, then pinching or flattening of these membranes must be occuring there also. It is unclear if these types of membrane and vesicle morphologies are present in transfected COS-1 cells.

6.3 CONSIDERATIONS FOR THE MOLECULAR BASIS FOR DISC MORPHOGENESIS

A model for disc morphogenesis involving the action of peripherin-2 oligomers is shown in **Fig 44**. Although the role for peripherin-2 and the mechanism of disc morphogenesis has yet to be unequivocally determined, enough evidence has accumulated that we can begin to build a simple molecular model for how this process occurs. Based on our results expressing peripherin-2 and peripherin-2 mutants in transgenic frogs, and the results of others examining the expression of rhodopsin mutants in transgenic photoreceptors (Green *et al.*, 2000; Moritz *et al.*, 2001; Sung *et al.*, 1994), it is clear that proteins destined for the rod

Fig 44. **Zippering model for disc morphogenesis in rods.** In normal disc morphogenesis, (1) core tetramers assembled in the ER and Golgi are packaged into transport vesicles and migrate to the connecting cilium (2) where they encounter a checkpoint. (3) Vesicles containing properly assembled tetramers are actively targeted to the disc rim forming region where they fuse with membranes of the growing rim. (4) Non-covalent tetramers in opposing membranes are linked together through intermolecular disulfide bonds by PDI to form disulfide-linked octamers which bind and stabilize the adjacent membranes. (5) Disulfide bonding of tetramers facilitates a conformational change that allows association of adjacent octamers into higher-order oligomeric complexes which (6) drives elongation of the disc rim. (7) Membrane fusion catalyzed by the C-terminal region of peripherin results in closed intact discs which are separate from the plasma membrane. (8) Fusion activity is capped by association with another protein (GARP) and mature discs migrate axially towards the distal tip of the rod. (9) Dissociation of GARP in the distal tip region allows fusion between disc and plasma membranes and phagocytosis by the RPE. Abnormal core tetramer formation (as in RP) results in mistargeting of peripherin-2 to the inner segment. (i) Mutant dimers assembled in the ER and Golgi are packaged into transport vesicles and migrate to the connecting cilium where they encounter the checkpoint (ii) and are refused entry into the OS. (iii) Vesicles containing mutant proteins are targeted for degradation and may affect photoreceptor fitness.

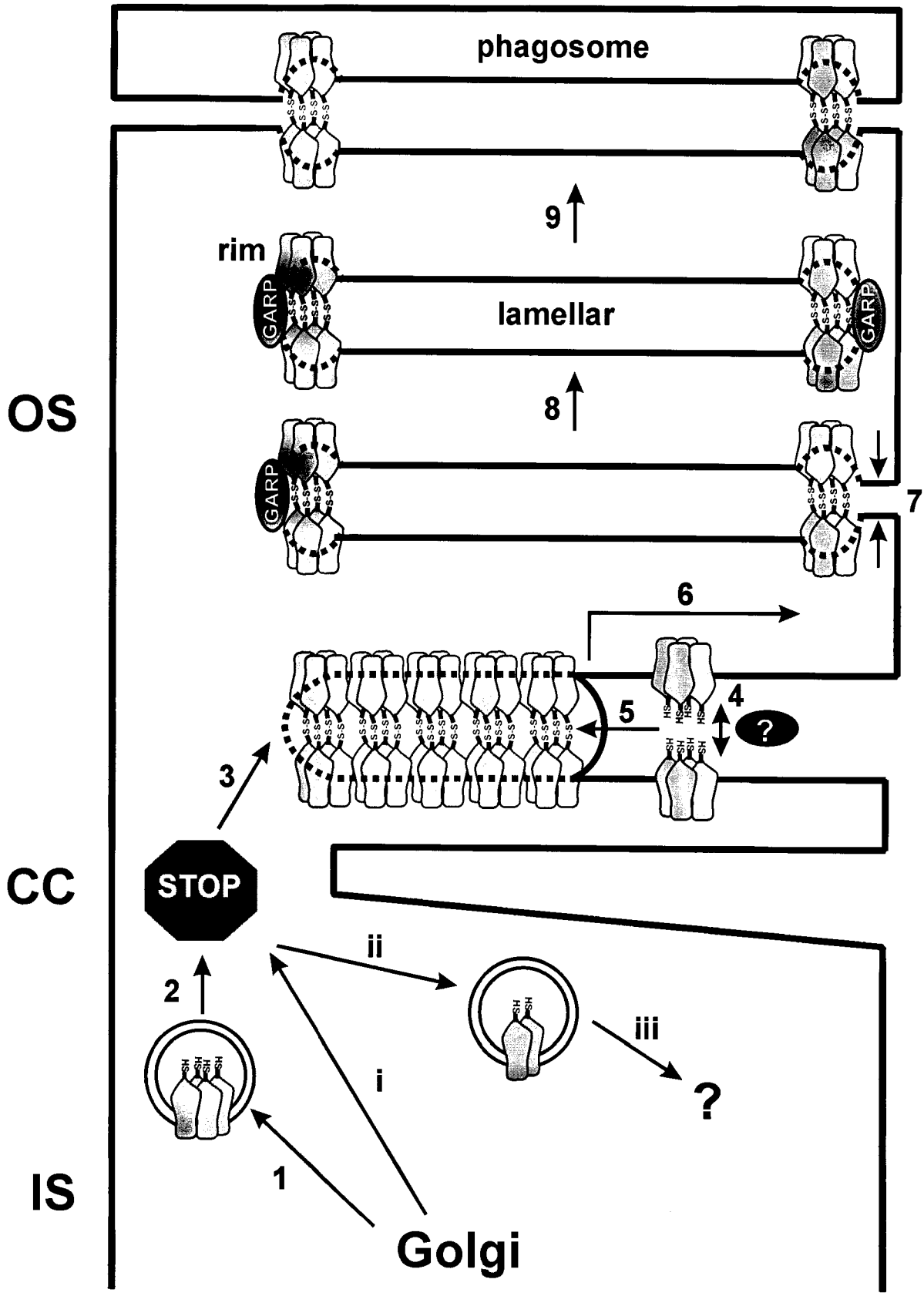
phagosome
9
rim
GARP
lamellar
GARP
8
GARP
7
6
5
4
?
3
OS
CC
IS
STOP
2
ii
iii
?
i
1
Golgi

outer segment are actively transported and must pass a checkpoint at the connecting cilium. In the case of rhodopsin, mutations that either interfere with the C-terminal OS targeting signal or those that result in a misfolded protein are detained and accumulate in vesicles of the inner segment. We have found with peripherin-2, that if core tetramers are not assembled correctly, they also are turned back at the connecting cilium and accumulate in vesicles in the inner segment.

From the rod cell's perspective, preventing nontetrameric core complexes from entering the outer segment must be a protective measure. It must be advantageous to have slightly decreased overall levels of peripherin-2 in ROS than to allow defective core complexes to interfere with the dynamic and sensitive process of disc morphogenesis. This sensitivity is demonstrated in frogs expressing P216L peripherin-2-GFP. This mutation causes no detectable defect in oligomerization and is presumably not caught by the checkpoint, but its presence in ROS interferes with some aspect of disc stability that results in photoreceptor degeneration. It is possible that if the photoreceptor could have recognized a defect in this protein and prevented trafficking to the outer segment, it could have lessened the damaging effects and increased its chances for survival.

The model in **Fig 44** predicts disulfide-mediated oligomerization to occur at the disc rim-forming region in the outer segment and not in the

ER of the cell. We have evidence that the ER proteins calnexin and protein disulfide isomerase (PDI) are present in ROS discs (C. Loewen and R. Molday, unpublished results). This suggests that protein folding and disulfide bond formation can occur in discs. It is possible that calnexin or another photoreceptor specific protein associates with the core tetramer in the ER and prevents it from disulfide bonding until it reaches the rim forming region, where PDI then catalyzes disulfide-linking of tetramers and rim formation. Alternatively, the geometric requirements for proper disulfide-linking of tetramers may not be met in the ER thereby preventing oligomerization. A unique feature of peripherin-2 oligomeric complexes isolated from ROS membranes is the presence of noncovalent tetramers in addition to disulfide-linked oligomers. This is very unusual since disulfide bonding is generally thought to be an all-or-none process as the tertiary and quaternary structure of the protein critically depends on it.

Further evidence for disulfide-mediated oligomerization at the disc rim comes from analysis of transgenic frogs expressing the C150S variant. In these frogs, defective disulfide-mediated oligomerization does not result in mislocalization of C150S peripherin-2-GFP complexes to the inner segment. A simple explanation for this observation is that non-disulfide bonded complexes are not detained at the connecting cilium

checkpoint because disulfide-mediated oligomerization normally occurs after it at the rim forming region.

It is possible however, that disulfide-mediated oligomerization occurs in the ER. Heterologous expression studies in COS-1 cells show that disulfide-mediated oligomerization of peripherin-2 occurs in a similar manner as observed in ROS. In these cells, both peripherin-2 noncovalent tetramers and disulfide-linked oligomers are observed. It is possible that the geometric requirements for complete disulfide-mediated oligomerization are not met in either the ER of COS-1 cells or the ER of photoreceptors. Improper alignment of tetramers in the ER would result in incomplete disulfide-mediated oligomerization and could explain the presence of noncovalent tetramers in ROS. An alternative explanation of the results observed in COS-1 cells is that disulfide-mediated oligomerization occurs outside of the ER in intracellular vesicles similarly to photoreceptors. These vesicles would mimic the rim forming region of photoreceptors and may contain PDI and calnexin.

Regulation of disc formation likely involves the inhibitory action of rom-1. Incorporation of rom-1 with peripherin-2 oligomers at the rim-forming region will decrease the extent of disulfide bonding and reduce the level and size of higher order oligomers. This likely modulates the stability of the rim region and also affects the rate of rim formation. Because rim formation occurs independently of membrane evagination

(Arikawa *et al.*, 1992; Steinberg, Fisher & Anderson, 1980), it is imperative that the photoreceptor regulate these processes. In rom-1 knockout mice, slightly larger discs are observed (Clarke *et al.*, 2000). This may be due either to increased rates of rim formation or to the production of more stable disc rims that allow for even larger disc diameter. In fact, the photoreceptor discs of *Xenopus laevis* can be ten times larger in diameter than mammalian discs and contain up to sixteen incisures which increase the rim surface area even greater. *Xenopus* rods do not appear to contain a rom-1 ortholog (Kedzierski *et al.*, 1996). Interestingly, we do not observe proper incisure formation in transgenic rods expressing C150S peripherin-2-GFP. This phenotype may be analogous to what is observed in mammalian rods which express the rom-1 gene and have few, or often only a single incisure.

Analysis of the photoreceptors of heterozygous *rds* mice which should contain only half the amount of peripherin-2 as WT reveals that disc rim formation is incomplete and large whorls of evaginating membranes are present adjacent to the connecting cilium (Sanyal & Jansen, 1981). It appears, therefore, that insufficient amounts of peripherin-2 result in the lack of rim formation, but do not affect the process of membrane evagination. This provides more evidence that peripherin-2 creates the disc rim and that rom-1 cannot compensate for its activity.

A membrane fusion event is required upon meeting of the two sides of the growing disc rim to seal the disc and create the plasma membrane. A role for the C-terminal region of peripherin-2 in membrane fusion has been proposed, but has not been confirmed in vivo (Boesze-Battaglia *et al.*, 1998). If peripherin-2 catalyzes this fusion event in rods, then its fusion activity must be inhibited in the mature disc while it migrates distally towards the tip of the rod. A glutamic acid rich protein (GARP), has been found to interact with the cytoplasmic region of only disulfide-linked peripherin-2 complexes in rods (A. Poetsch and R. Molday, unpublished results). GARP may function to cap the fusion activity by binding to peripherin-2 as disulfide-mediated oligomerization and rim formation are occurring. GARP may also mediate interactions between disc rims and between rims and the plasma membrane through interactions between peripherin-2 and the β–subunit of the cGMP gated channel.

As the discs reach the distal tip of the rod, a signaling event initiated by the RPE (or possibly another photoreceptor) may release GARP from the rim and allow peripherin-2-catalyzed fusion to occur again. This would result in fusion between the disc rim and the plasma membrane and release of a packet of discs (see Fig 5 in the introduction). Penetration of the outer segment by pseudopodia of the RPE and

ingestion may increase the local reducing potential and initiate the process of rim and disc collapse.

The differences observed between discs of rod and cone outer segments might also be due to differential regulation of oligomerization of peripherin-2. It has been proposed that rim formation in cones occurs more slowly and therefore is not often complete until the discs near the distal tip of the photoreceptor (Arikawa *et al.*, 1992). The result is that the majority of cone discs remain open to the extracellular space. Peripherin-2 has been found to extend along the discs only as far as the rim in cones. If cones synthesize less total peripherin-2, or if the ratio of peripherin-2 to rom-1 is decreased compared to rods (where it is 2:1 (Loewen & Molday, 2000)), the size and abundance of disulfide-linked oligomers of peripherin-2 will be decreased and a slower rate of rim formation may result - this being somehow advantageous to the cone cell.

6.4 FUTURE DIRECTIONS

Many questions remain unanswered – both structurally and functionally. The importance of peripherin-2 in maintaining healthy photoreceptor cells is obvious. It plays an intriguing role in modeling membranes and has a number of unique structural features that imply a mechanism for its action. A crystal structure of the complex is at the top

of the list of priorities. With current advances in X-ray crystallography technology, crystallization of whole membrane protein complexes is possible (Moffat, 1997; Pebay-Peyroula *et al.*, 1997). The high abundance of peripherin-2 in bovine photoreceptors and the availability of large amounts of bovine retinal tissue make it possible to purify enough complex for these types of studies. Also, expression of the intradiscal loop region in a bacterial system and structural analysis including X-ray crystallography and NMR techniques would be very informative. More structural studies include: electron microscopic analysis of oligomeric complexes in the detergent solubilized and reconstituted states; effect of reductant on the shape and stability of photoreceptor discs; isolation and characterization of peripherin-2-containing vesicles from transfected cells by immuno-EM; mapping of the proposed intramolecular disulfide bonds within the loop region by proteolysis and HPLC analysis.

Experiments can be designed also to address the role of disulfide-mediated oligomerization in disc formation. The use of membrane-impermeable sulfhydryl reagents in conjunction with labeling dyes like Lucifer yellow to study disc formation in photoreceptors in eyecups should determine the importance of disulfide bonding at the disc-forming region and identify the proteins involved. Preliminary experiments have revealed the presence of proteins with free sulfhydryl groups in this region (C. Loewen and R. Molday, unpublished). Antibodies generated to

the intradiscal region of peripherin-2 may also be useful in this type of study. Since a natural knockout is available, transgenic studies in mice adding-back C150S peripherin-2 or other chimeras would be extremely informative in determining the mechanisms of disc morphogenesis. Certain research groups are also using inducible promoters to begin to study this role for peripherin-2.

Studies in transgenic *Xenopus* examining the requirements for outer segment targeting are currently underway. This system can also be used to test the role of the C-terminus of peripherin-2 in membrane fusion in vivo. Interestingly, we did not find any serious defects in disc morphogenesis due to the presence of GFP at the C-terminus, and another group has found no serious problems in frogs that express peripherin-2 with a truncated C-terminus (Lee, Burnside & Flannery, 2001). Also, more disease causing mutations can be examined in the frog system to obtain a more comprehensive understanding of the molecular basis for retinal dystrophies. Lastly, the role of GARP and the interaction of peripherin-2 with other proteins, possibly cytoskeletal, will tell us more about the organization of photoreceptor outer segments.

REFERENCES

Ali, R. R., Sarra, G. M., Stephens, C., Alwis, M. D., Bainbridge, J. W., Munro, P. M., Fauser, S., Reichel, M. B., Kinnon, C., Hunt, D. M., Bhattacharya, S. S. & Thrasher, A. J. (2000). Restoration of photoreceptor ultrastructure and function in retinal degeneration slow mice by gene therapy [see comments]. *Nat Genet* **25,** 306-10.

Allikmets, R., Shroyer, N. F., Singh, N., Seddon, J. M., Lewis, R. A., Bernstein, P. S., Peiffer, A., Zabriskie, N. A., Li, Y., Hutchinson, A., Dean, M., Lupski, J. R. & Leppert, M. (1997a). Mutation of the Stargardt disease gene (ABCR) in age-related macular degeneration. *Science* **277,** 1805-7.

Allikmets, R., Singh, N., Sun, H., Shroyer, N. F., Hutchinson, A., Chidambaram, A., Gerrard, B., Baird, L., Stauffer, D., Peiffer, A., Rattner, A., Smallwood, P., Li, Y., Anderson, K. L., Lewis, R. A., Nathans, J., Leppert, M., Dean, M. & Lupski, J. R. (1997b). A photoreceptor cell-specific ATP-binding transporter gene (ABCR) is mutated in recessive Stargardt macular dystrophy. *Nat Genet* **15,** 236-46.

Amaya, E. & Kroll, K. L. (1999). A method for generating transgenic frog embryos. *Methods Mol Biol* **97,** 393-414.

Arikawa, K., Molday, L. L., Molday, R. S. & Williams, D. S. (1992). Localization of peripherin/rds in the disk membranes of cone and rod photoreceptors: relationship to disk membrane morphogenesis and retinal degeneration. *J Cell Biol* **116,** 659-67.

Atkinson, B., Ernst, C. S., Ghrist, B. F., Herlyn, M., Blaszczyk, M., Ross, A. H., Herlyn, D., Steplewski, Z. & Koprowski, H. (1984). Identification of melanoma-associated antigens using fixed tissue screening of antibodies. *Cancer Res* **44,** 2577-81.

Bareil, C., Delague, V., Arnaud, B., Demaille, J., Hamel, C. & Claustres, M. (2000). W179R: a novel missense mutation in the peripherin/RDS gene in a family with autosomal dominant retinitis pigmentosa. *Hum Mutat* **15,** 583-4.

Bascom, R. A., Garcia-Heras, J., Hsieh, C. L., Gerhard, D. S., Jones, C., Francke, U., Willard, H. F., Ledbetter, D. H. & McInnes, R. R. (1992a). Localization of the photoreceptor gene ROM1 to human chromosome 11 and mouse chromosome 19: sublocalization to human 11q13 between PGA and PYGM. *Am J Hum Genet* **51,** 1028-35.

Bascom, R. A., Liu, L., Humphries, P., Fishman, G. A., Murray, J. C. & McInnes, R. R. (1993). Polymorphisms and rare sequence variants at the ROM1 locus. *Hum Mol Genet* **2,** 1975-7.

Bascom, R. A., Manara, S., Collins, L., Molday, R. S., Kalnins, V. I. & McInnes, R. R. (1992b). Cloning of the cDNA for a novel photoreceptor membrane protein (rom-1) identifies a disk rim protein family implicated in human retinopathies. *Neuron* **8,** 1171-84.

Bascom, R. A., Schappert, K. & McInnes, R. R. (1993). Cloning of the human and murine ROM1 genes: genomic organization and sequence conservation. *Hum Mol Genet* **2,** 385-91.

Beard, L. M., Estes, P. A., Lyon, M. K. & Garcea, R. L. (1998). *J. Virol.* **72,** 2160–2167.

Begy, C. & Bridges, C. D. (1990). Nucleotide and predicted protein sequence of rat retinal degeneration slow (rds). *Nucleic Acids Res* **18,** 3058.

Berditchevski, F. & Odintsova, E. (1999). Characterization of integrin-tetraspanin adhesion complexes: role of tetraspanins in integrin signaling. *J Cell Biol* **146,** 477-92.

Besharse, J. C. & Defoe, D. M. (1998). Role of the pigment epithelium in photoreceptor membrane turnover. In *The Retinal Pigment Epithelium* (ed. M. M. F. and W. T. J.), pp. 152-172. Oxford University Press, Oxford.

Besharse, J. C., Hollyfield, J. G. & Rayborn, M. E. (1977). Turnover of rod photoreceptor outer segments. II. Membrane addition and loss in relationship to light. *J Cell Biol* **75,** 507-27.

Boesze-Battaglia, K., Kong, F., Lamba, O. P., Stefano, F. P. & Williams, D. S. (1997). Purification and light-dependent phosphorylation of a candidate fusion protein, the photoreceptor cell peripherin/rds. *Biochemistry* **36,** 6835-46.

Boesze-Battaglia, K., Lamba, O. P., Napoli, A. A., Jr., Sinha, S. & Guo, Y. (1998). Fusion between retinal rod outer segment membranes and model membranes: a role for photoreceptor peripherin/rds. *Biochemistry* **37,** 9477-87.

Boughman, J. A., Conneally, P. M. & Nance, W. E. (1980). Population genetic studies of retinitis pigmentosa. *Am J Hum Genet* **32,** 223-35.

Boyle, D., Tien, L. F., Cooper, N. G., Shepherd, V. & McLaughlin, B. J. (1991). A mannose receptor is involved in retinal phagocytosis. *Invest Ophthalmol Vis Sci* **32,** 1464-70.

Bressler, N. M., Bressler, S. B. & Fine, S. L. (1988). Age-related macular degeneration. *Surv Ophthalmol* **32,** 375-413.

Cascio, M., Kumar, N. M., Safarik, R. & Gilula, N. B. (1995). Physical characterization of gap junction membrane connexons (hemi-channels) isolated from rat liver. *J Biol Chem* **270,** 18643-8.

Chen, C. & Okayama, H. (1987). High-efficiency transformation of mammalian cells by plasmid DNA. *Mol Cell Biol* **7,** 2745-52.

Cheng, T., Peachey, N. S., Li, S., Goto, Y., Cao, Y. & Naash, M. I. (1997). The effect of peripherin/rds haploinsufficiency on rod and cone photoreceptors. *J Neurosci* **17,** 8118-28.

Chuang, J. Z. & Sung, C. H. (1998). The cytoplasmic tail of rhodopsin acts as a novel apical sorting signal in polarized MDCK cells. *J Cell Biol* **142,** 1245-56.

Clarke, G., Goldberg, A. F., Vidgen, D., Collins, L., Ploder, L., Schwarz, L., Molday, L. L., Rossant, J., Szel, A., Molday, R. S., Birch, D. G. & McInnes, R. R. (2000). Rom-1 is required for rod photoreceptor viability and the regulation of disk morphogenesis. *Nat Genet* **25,** 67-73.

Clarke, S. & Smigel, M. D. (1989). Size and shape of membrane protein-detergent complexes: hydrodynamic studies. *Methods Enzymol* **172,** 696-709.

Connell, G., Bascom, R., Molday, L., Reid, D., McInnes, R. R. & Molday, R. S. (1991). Photoreceptor peripherin is the normal product of the gene responsible for retinal degeneration in the rds mouse. *Proc Natl Acad Sci U S A* **88,** 723-6.

Connell, G. J. & Molday, R. S. (1990). Molecular cloning, primary structure, and orientation of the vertebrate photoreceptor cell protein peripherin in the rod outer segment disk membrane. *Biochemistry* **29,** 4691-8.

Cruickshanks, K. J., Klein, R. & Klein, B. E. (1993). Sunlight and age-related macular degeneration. The Beaver Dam Eye Study. *Arch Ophthalmol* **111,** 514-8.

Dose, A. (1995). Molecular characterization of the cyclic nucleotide-gated cation channel of bovine rod outer segments. PhD thesis, University of British Columbia.

Dryja, T. P., Hahn, L. B., Kajiwara, K. & Berson, E. L. (1997). Dominant and digenic mutations in the peripherin/RDS and ROM1 genes in retinitis pigmentosa. *Invest Ophthalmol Vis Sci* **38,** 1972-82.

Duke-Elder, S. (1954). Injuries. In *Text-Book of Ophthalmology*, vol. VI (ed. C. V. Mosby), pp. 6494-6517, St. Louis, MO.

Ekstrom, U., Ponjavic, V., Andreasson, S., Ehinger, B., Nilsson-Ehle, P. & Abrahamson, M. (1998). Detection of alterations in all three exons of the peripherin/RDS gene in Swedish patients with retinitis pigmentosa using an efficient DGGE system. *Mol Pathol* **51,** 287-91.

Elner, V. M., Schaffner, T., Taylor, K. & Glagov, S. (1981). Immunophagocytic properties of retinal pigment epithelium cells. *Science* **211,** 74-6.

Farrar, G. J., Jordan, S. A., Kenna, P., Humphries, M. M., Kumar-Singh, R., McWilliam, P., Allamand, V., Sharp, E. & Humphries, P. (1991a). Autosomal dominant retinitis pigmentosa: localization of a disease gene (RP6) to the short arm of chromosome 6 [published erratum appears in Genomics 1992 Aug;13(4):1384]. *Genomics* **11,** 870-4.

Farrar, G. J., Kenna, P., Jordan, S. A., Kumar-Singh, R., Humphries, M. M., Sharp, E. M., Sheils, D. & Humphries, P. (1992). Autosomal dominant retinitis pigmentosa: a novel mutation at the peripherin/RDS locus in the original 6p-linked pedigree [published erratum appears in Genomics 1993 Feb;15(2):466]. *Genomics* **14,** 805-7.

Farrar, G. J., Kenna, P., Jordan, S. A., Kumar-Singh, R., Humphries, M. M., Sharp, E. M., Sheils, D. M. & Humphries, P. (1991b). A three-base-pair deletion in the peripherin-RDS gene in one form of retinitis pigmentosa. *Nature* **354,** 478-80.

Fasman, G. D. & Chemical Rubber Company. (1975). *Handbook of biochemistry and molecular biology*, 3d edition. CRC Press, Cleveland.

Fishman, G. A., Stone, E., Gilbert, L. D., Vandenburgh, K., Sheffield, V. C. & Heckenlively, J. R. (1994). Clinical features of a previously undescribed codon 216 (proline to serine) mutation in the peripherin/retinal degeneration slow gene in autosomal dominant retinitis pigmentosa. *Ophthalmology* **101,** 1409-21.

Fishman, G. A., Stone, E. M., Alexander, K. R., Gilbert, L. D., Derlacki, D. J. & Butler, N. S. (1997). Serine-27-phenylalanine mutation within the peripherin/RDS gene in a family with cone dystrophy. *Ophthalmology* **104,** 299-306.

Goldberg, A. F., Loewen, C. J. & Molday, R. S. (1998). Cysteine residues of photoreceptor peripherin/rds: role in subunit assembly and autosomal dominant retinitis pigmentosa. *Biochemistry* **37,** 680-5.

Goldberg, A. F. & Molday, R. S. (1996a). Defective subunit assembly underlies a digenic form of retinitis pigmentosa linked to mutations in peripherin/rds and rom-1. *Proc Natl Acad Sci U S A* **93,** 13726-30.

Goldberg, A. F. & Molday, R. S. (1996b). Subunit composition of the peripherin/rds-rom-1 disk rim complex from rod photoreceptors: hydrodynamic evidence for a tetrameric quaternary structure. *Biochemistry* **35,** 6144-9.

Goldberg, A. F., Moritz, O. L. & Molday, R. S. (1995). Heterologous expression of photoreceptor peripherin/rds and Rom-1 in COS-1 cells: assembly, interactions, and localization of multisubunit complexes. *Biochemistry* **34,** 14213-9.

Gorin, M. B., Jackson, K. E., Ferrell, R. E., Sheffield, V. C., Jacobson, S. G., Gass, J. D., Mitchell, E. & Stone, E. M. (1995). A peripherin/retinal degeneration slow mutation (Pro-210-Arg) associated with macular and peripheral retinal degeneration. *Ophthalmology* **102,** 246-55.

Gorin, M. B., Snyder, S., To, A., Narfstrom, K. & Curtis, R. (1993). The cat RDS transcript: candidate gene analysis and phylogenetic sequence analysis. *Mamm Genome* **4,** 544-8.

Gray-Keller, M. P., Biernbaum, M. S. & Bownds, M. D. (1990). Transducin activation in electropermeabilized frog rod outer segments is highly amplified, and a portion equivalent to phosphodiesterase remains membrane-bound. *J Biol Chem* **265,** 15323-32.

Green, E. S., Menz, M. D., LaVail, M. M. & Flannery, J. G. (2000). Characterization of rhodopsin mis-sorting and constitutive activation in a transgenic rat model of retinitis pigmentosa. *Invest Ophthalmol Vis Sci* **41,** 1546-53.

Gruning, G., Millan, J. M., Meins, M., Beneyto, M., Caballero, M., Apfelstedt-Sylla, E., Bosch, R., Zrenner, E., Prieto, F. & Gal, A. (1994). Mutations in the human peripherin/RDS gene associated with autosomal dominant retinitis pigmentosa. *Hum Mutat* **3,** 321-3.

Hale, I. L., Fisher, S. K. & Matsumoto, B. (1991). Effects of retinal detachment on rod disc membrane assembly in cultured frog retinas. *Invest Ophthalmol Vis Sci* **32,** 2873-81.

Hale, I. L., Fisher, S. K. & Matsumoto, B. (1996). The actin network in the ciliary stalk of photoreceptors functions in the generation of new outer segment discs. *J Comp Neurol* **376,** 128-42.

Hawkins, R. K., Jansen, H. G. & Sanyal, S. (1985). Development and degeneration of retina in rds mutant mice: photoreceptor abnormalities in the heterozygotes. *Exp Eye Res* **41,** 701-20.

Henkenlively, J. R. (1988). *Retinitis Pigmentosa*. J.B. Lippincott Company.

Hollyfield, J. G. (1971). Differential growth of the neural retina in Xenopus laevis larvae. *Dev Biol* **24,** 264-86.

Hoyng, C. B., Heutink, P., Testers, L., Pinckers, A., Deutman, A. F. & Oostra, B. A. (1996). Autosomal dominant central areolar choroidal dystrophy caused by a mutation in codon 142 in the peripherin/RDS gene. *Am J Ophthalmol* **121,** 623-9.

Hsu, Y. T. & Molday, R. S. (1993). Modulation of the cGMP-gated channel of rod photoreceptor cells by calmodulin. *Nature* **361,** 76-9.

Ishida, T., Narita, M., Nozaki, M. & Horiike, K. (1996). Selective cleavage and modification of the intersubunit disulfide bonds of bovine dopamine beta-monooxygenase: conversion of tetramer to active dimer. *J Biochem (Tokyo)* **120,** 346-52.

Jacobson, S. G., Kemp, C. M., Cideciyan, A. V., Sun, X. K., Vandenburgh, K., Sheffield, V. C. & Stone, E. M. (1994). Spectrum of functional phenotypes in rds gene mutations. *Invest. Ophthalmol. Vis. Sci.* **35,** 1479.

Jansen, H. G. & Sanyal, S. (1984). Development and degeneration of retina in rds mutant mice: electron microscopy. *J Comp Neurol* **224,** 71-84.

Kajiwara, K., Berson, E. L. & Dryja, T. P. (1994). Digenic retinitis pigmentosa due to mutations at the unlinked peripherin/RDS and ROM1 loci. *Science* **264,** 1604-8.

Kajiwara, K., Hahn, L. B., Mukai, S., Berson, E. L. & T.P., D. (1992). Mutations in the human rds gene in patients with autosomal dominant Retinitis Pigmentosa. *Invest. Ophthalmol. Vis. Sci.* **33,** 1396.

Kajiwara, K., Hahn, L. B., Mukai, S., Travis, G. H., Berson, E. L. & Dryja, T. P. (1991). Mutations in the human retinal degeneration slow gene in autosomal dominant retinitis pigmentosa. *Nature* **354,** 480-3.

Kajiwara, K., Sandberg, M. A., Berson, E. L. & Dryja, T. P. (1993). A null mutation in the human peripherin/RDS gene in a family with autosomal dominant retinitis punctata albescens [see comments]. *Nat Genet* **3,** 208-12.

Kammerer, R. A. (1997). Alpha-helical coiled-coil oligomerization domains in extracellular proteins. *Matrix Biol* **15,** 555-65; discussion 567-8.

Kaplan, M. W. (1998). Disk membrane initiation and insertion are not required for axial disk displacement in Xenopus laevis rod outer segments. *Curr Eye Res* **17,** 73-8.

Kaplan, M. W., Iwata, R. T. & Sterrett, C. B. (1990). Retinal detachment prevents normal assembly of disk membranes in vitro. *Invest Ophthalmol Vis Sci* **31,** 1-8.

Kaplan, R. S. & Pedersen, P. L. (1985). Determination of microgram quantities of protein in the presence of milligram levels of lipid with amido black 10B. *Anal Biochem* **150,** 97-104.

Karnik, S. S. & Khorana, H. G. (1990). Assembly of functional rhodopsin requires a disulfide bond between cysteine residues 110 and 187. *J Biol Chem* **265,** 17520-4.

Kazmi, M. A., Sakmar, T. P. & Ostrer, H. (1997). Mutation of a conserved cysteine in the X-linked cone opsins causes color vision deficiencies by disrupting protein folding and stability. *Invest Ophthalmol Vis Sci* **38,** 1074-81.

Kedzierski, W., Lloyd, M., Birch, D. G., Bok, D. & Travis, G. H. (1997). Generation and analysis of transgenic mice expressing P216L-substituted rds/peripherin in rod photoreceptors. *Invest Ophthalmol Vis Sci* **38,** 498-509.

Kedzierski, W., Moghrabi, W. N., Allen, A. C., Jablonski-Stiemke, M. M., Azarian, S. M., Bok, D. & Travis, G. H. (1996). Three homologs of rds/peripherin in Xenopus laevis photoreceptors that exhibit covalent and non-covalent interactions. *J Cell Sci* **109,** 2551-60.

Kedzierski, W., Weng, J. & Travis, G. H. (1999). Analysis of the rds/peripherin.rom1 complex in transgenic photoreceptors that express a chimeric protein. *J Biol Chem* **274,** 29181-7.

Keen, T. J., Inglehearn, C. F., Kim, R., Bird, A. C. & Bhattacharya, S. (1994). Retinal pattern dystrophy associated with a 4 bp insertion at codon 140 in the RDS-peripherin gene. *Hum Mol Genet* **3,** 367-8.

Kemp, C. M., Jacobson, S. G., Cideciyan, A. V., Kimura, A. E., Sheffield, V. C. & Stone, E. M. (1994). RDS gene mutations causing retinitis pigmentosa or macular degeneration lead to the same abnormality in photoreceptor function. *Invest Ophthalmol Vis Sci* **35,** 3154-62.

Kikawa, E., Nakazawa, M., Chida, Y., Shiono, T. & Tamai, M. (1994). A novel mutation (Asn244Lys) in the peripherin/RDS gene causing autosomal dominant retinitis pigmentosa associated with bull's-eye maculopathy detected by nonradioisotopic SSCP. *Genomics* **20,** 137-9.

Kim, R. Y., Dollfus, H., Keen, T. J., Fitzke, F. W., Arden, G. B., Bhattacharya, S. S. & Bird, A. C. (1995). Autosomal dominant pattern dystrophy of the retina associated with a 4- base pair insertion at codon 140 in the peripherin/RDS gene. *Arch Ophthalmol* **113,** 451-5.

Koch, K. W. (1995). Control of photoreceptor proteins by Ca2+. *Cell Calcium* **18,** 314-21.

Kolb, H. (1994). The architecture of functional neural circuits in the vertebrate retina. The Proctor Lecture. *Invest Ophthalmol Vis Sci* **35,** 2385-404.

Kopczynski, C. C., Davis, G. W. & Goodman, C. S. (1996). A neural tetraspanin, encoded by late bloomer, that facilitates synapse formation. *Science* **271,** 1867-70.

Kroll, K. L. & Amaya, E. (1996). Transgenic Xenopus embryos from sperm nuclear transplantations reveal FGF signaling requirements during gastrulation. *Development* **122,** 3173-83.

Kunishima, N., Shimada, Y., Tsuji, Y., Sato, T., Yamamoto, M., Kumasaka, T., Nakanishi, S., Jingami, H. & Morikawa, K. (2000). Structural basis of glutamate recognition by a dimeric metabotropic glutamate receptor [In Process Citation]. *Nature* **407,** 971-7.

Laird, D. W. & Molday, R. S. (1988). Evidence against the role of rhodopsin in rod outer segment binding to RPE cells. *Invest Ophthalmol Vis Sci* **29,** 419-28.

Lanum, J. (1978). The damaging effects of light on the retina. Empirical findings, theoretical and practical implications. *Surv Ophthalmol* **22,** 221-49.

Lee, E. S., Burnside, B. & Flannery, J. G. (2001). Trafficking of C-terminal truncated peripherin/rds in transgenic *Xenopus leavis*. *Invest Ophthalmol Vis Sci* **42,** s366.

Li, Y. & Rubin, C. S. (1995). Mutagenesis of the regulatory subunit (RII beta) of cAMP-dependent protein kinase II beta reveals hydrophobic amino acids that are essential for RII beta dimerization and/or anchoring RII beta to the cytoskeleton. *J Biol Chem* **270,** 1935-44.

Locker, J. K. & Griffiths, G. (1999). An unconventional role for cytoplasmic disulfide bonds in vaccinia virus proteins. *J Cell Biol* **144,** 267-79.

Loewen, C. J. & Molday, R. S. (2000). Disulfide-mediated oligomerization of Peripherin/Rds and Rom-1 in photoreceptor disk membranes. Implications for photoreceptor outer segment morphogenesis and degeneration. *J Biol Chem* **275,** 5370-8.

Loewen, C. J., Moritz, O. L. & Molday, R. S. (2001). Molecular characterization of peripherin-2 and rom-1 mutants responsible for digenic retinitis pigmentosa. *J Biol Chem* **276,** 22388-96.

Luczak, J. A., Redick, S. D. & Schwarzbauer, J. E. (1998). A single cysteine, Cys-64, is essential for assembly of tenascin-C hexabrachions. *J Biol Chem* **273,** 2073-7.

MacKenzie, D., Arendt, A., Hargrave, P., McDowell, J. H. & Molday, R. S. (1984). Localization of binding sites for carboxyl terminal specific anti- rhodopsin monoclonal antibodies using synthetic peptides. *Biochemistry* **23,** 6544-9.

MacKenzie, D. & Molday, R. S. (1982). Organization of rhodopsin and a high molecular weight glycoprotein in rod photoreceptor disc membranes using monoclonal antibodies. *J Biol Chem* **257,** 7100-5.

MacKenzie, K. R., Prestegard, J. H. & Engelman, D. M. (1997). A transmembrane helix dimer: structure and implications. *Science* **276,** 131-3.

Martin, R. G. & Ames, B. N. (1961). *J. Biol. Chem.* **236,** 1372–1379.

Massey, S. C. & Maguire, G. (1995). The role of glutamate in retinal circuitry. Excitatory amino acids and synaptic transmission., pp. 201-221. Academic Press Ltd.

Matsumoto, B. & Besharse, J. C. (1985). Light and temperature modulated staining of the rod outer segment distal tips with Lucifer yellow. *Invest Ophthalmol Vis Sci* **26,** 628-35.

Matsumoto, B., Defoe, D. M. & Besharse, J. C. (1987). Membrane turnover in rod photoreceptors: ensheathment and phagocytosis of outer segment distal tips by pseudopodia of the retinal pigment epithelium. *Proc R Soc Lond B Biol Sci* **230,** 339-54.

Meins, M., Gruning, G., Blankenagel, A., Krastel, H., Reck, B., Fuchs, S., Schwinger, E. & Gal, A. (1993). Heterozygous 'null allele' mutation in the human peripherin/RDS gene. *Hum Mol Genet* **2,** 2181-2.

Moffat, A. S. (1997). Opening the door to more membrane protein structures. *Science* **277,** 1607-8.

Moghrabi, W. N., Kedzierski, W. & Travis, G. H. (1995). Canine homolog and exclusion of retinal degeneration slow (rds) as the gene for early retinal degeneration (erd) in the dog. *Exp Eye Res* **61,** 641-3.

Molday, R. S. (1994). Peripherin/rds and Rom-1: Molecular properties and role in photoreceptor cell degeneration. *Prog. Ret. Eye Res.* **13,** 271-299.

Molday, R. S. (1998). Photoreceptor membrane proteins, phototransduction, and retinal degenerative diseases. The Friedenwald Lecture. *Invest Ophthalmol Vis Sci* **39,** 2491-513.

Molday, R. S., Hicks, D. & Molday, L. (1987). Peripherin. A rim-specific membrane protein of rod outer segment discs. *Invest Ophthalmol Vis Sci* **28,** 50-61.

Moritz, O. L. & Molday, R. S. (1996). Molecular cloning, membrane topology, and localization of bovine rom-1 in rod and cone photoreceptor cells. *Invest Ophthalmol Vis Sci* **37,** 352-62.

Moritz, O. L., Tam, B. M., Knox, B. E. & Papermaster, D. S. (1999). Fluorescent photoreceptors of transgenic Xenopus laevis imaged in vivo by two microscopy techniques. *Invest Ophthalmol Vis Sci* **40,** 3276-80.

Moritz, O. L., Tam, B. M., Papermaster, D. S. & Nakayama, T. (2001). A functional rhodopsin-GFP fusion protein localizes correctly in transgenic Xenopus laevis retinal rods and is expressed in a time-dependent pattern. *J Biol Chem* **11,** 11.

Nakazawa, M., Kikawa, E., Chida, Y. & Tamai, M. (1994). Asn244His mutation of the peripherin/RDS gene causing autosomal dominant cone-rod degeneration. *Hum Mol Genet* **3,** 1195-6.

Nakazawa, M., Naoi, N., Wada, Y., Nakazaki, S., Maruiwa, F., Sawada, A. & Tamai, M. (1996). Autosomal dominant cone-rod dystrophy associated with a Val200Glu mutation of the peripherin/RDS gene. *Retina* **16,** 405-10.

Nelson, R. M. & Long, G. L. (1989). A general method of site-specific mutagenesis using a modification of the Thermus aquaticus polymerase chain reaction. *Anal Biochem* **180,** 147-51.

Nichols, B. E., Drack, A. V., Vandenburgh, K., Kimura, A. E., Sheffield, V. C. & Stone, E. M. (1993a). A 2 base pair deletion in the RDS gene associated with butterfly-shaped pigment dystrophy of the fovea [published erratum appears in Hum Mol Genet 1993 Aug;2(8):1347]. *Hum Mol Genet* **2,** 601-3.

Nichols, B. E., Sheffield, V. C., Vandenburgh, K., Drack, A. V., Kimura, A. E. & Stone, E. M. (1993b). Butterfly-shaped pigment dystrophy of the fovea caused by a point mutation in codon 167 of the RDS gene [see comments]. *Nat Genet* **3,** 202-7.

Nieuwkoop, P. D. & Faber, J. (1994). *Normal table of Xenopus laevis (Daudin): A systematical and chronological survey of the development from the fetilized egg till the end of metamorph.* Garland Publishing Inc., New York.

Oranisciak, D. T. & Winkler, B. S. (1994). *Prog. Retinal Eye Res.* **13,** 1-29.

Oren, R., Takahashi, S., Doss, C., Levy, R. & Levy, S. (1990). TAPA-1, the target of an antiproliferative antibody, defines a new family of transmembrane proteins. *Mol Cell Biol* **10,** 4007-15.

O'Shea, E. K., Klemm, J. D., Kim, P. S. & Alber, T. (1991). X-ray structure of the GCN4 leucine zipper, a two-stranded, parallel coiled coil. *Science* **254,** 539-44.

Osterberg, G. (1935). Topography of the layer of rods and cones in the human retina. *Acta. Ophthalmol.* **6.**

Palczewski, K. (1994). Is vertebrate phototransduction solved? New insights into the molecular mechanism of phototransduction. *Invest Ophthalmol Vis Sci* **35,** 3577-81.

Papermaster, D. S., Schneider, B. G., Zorn, M. A. & Kraehenbuhl, J. P. (1978). Immunocytochemical localization of a large intrinsic membrane protein to the incisures and margins of frog rod outer segment disks. *J Cell Biol* **78,** 415-25.

Pebay-Peyroula, E., Rummel, G., Rosenbusch, J. P. & Landau, E. M. (1997). X-ray structure of bacteriorhodopsin at 2.5 angstroms from microcrystals grown in lipidic cubic phases. *Science* **277,** 1676-81.

Polans, A., Baehr, W. & Palczewski, K. (1996). Turned on by Ca2+! The physiology and pathology of Ca(2+)-binding proteins in the retina. *Trends Neurosci* **19,** 547-54.

Pugh, E. N., Jr. & Lamb, T. D. (1993). Amplification and kinetics of the activation steps in phototransduction. *Biochim Biophys Acta* **1141,** 111-49.

Ray, K., Acland, G. M. & Aguirre, G. D. (1996). Nonallelism of erd and prcd and exclusion of the canine RDS/peripherin gene as a candidate for both retinal degeneration loci. *Invest Ophthalmol Vis Sci* **37,** 783-94.

Reme, C. E., Hafezi, F., Marti, A., Munz, K. & Reinboth, J. J. (1998). . In *The Retinal Pigment Epithelium* (ed. M. F. Marmor and T. J. Wolfensberger), pp. 563-586. Oxford University Press, Oxford.

Reznik, G. O., Vajda, S., Smith, C. L., Cantor, C. R. & Sano, T. (1996). Streptavidins with intersubunit crosslinks have enhanced stability. *Nat Biotechnol* **14,** 1007-11.

Ryeom, S. W., Sparrow, J. R. & Silverstein, R. L. (1996). CD36 participates in the phagocytosis of rod outer segments by retinal pigment epithelium. *J Cell Sci* **109,** 387-95.

Saga, M., Mashima, Y., Akeo, K., Oguchi, Y., Kudoh, J. & Shimizu, N. (1993). A novel Cys-214-Ser mutation in the peripherin/RDS gene in a Japanese family with autosomal dominant retinitis pigmentosa. *Hum Genet* **92,** 519-21.

Sanyal, S. & Jansen, H. G. (1981). Absence of receptor outer segments in the retina of rds mutant mice. *Neurosci Lett* **21,** 23-6.

Shapiro, L., Doyle, J. P., Hensley, P., Colman, D. R. & Hendrickson, W. A. (1996). Crystal structure of the extracellular domain from P0, the major structural protein of peripheral nerve myelin. *Neuron* **17,** 435-49.

Siegel, L. M. & Monty, K. J. (1966). Determination of molecular weights and frictional ratios of proteins in impure systems by use of gel filtration and density gradient centrifugation. Application to crude preparations of sulfite and hydroxylamine reductases. *Biochim Biophys Acta* **112,** 346-62.

Sohocki, M. M., Daiger, S. P., Bowne, S. J., Rodriquez, J. A., Northrup, H., Heckenlively, J. R., Birch, D. G., Mintz-Hittner, H., Ruiz, R. S., Lewis, R. A., Saperstein, D. A. & Sullivan, L. S. (2001). Prevalence of mutations causing retinitis pigmentosa and other inherited retinopathies. *Hum Mutat* **17,** 42-51.

Souied, E. H., Rozet, J. M., Gerber, S., Dufier, J. L., Soubrane, G., Coscas, G., Munnich, A. & Kaplan, J. (1998). Two novel missense mutations in the peripherin/RDS gene in two unrelated French patients with autosomal dominant retinitis pigmentosa. *Eur J Ophthalmol* **8,** 98-101.

Spalton, D. J., Hitchings, R. A. & Hunter, P. A. (1994). *Atlas of clinical ophthalmology*, 2d edition. Wolfe [Mosby-Year Book Europe Ltd.], London.

Steinberg, R. H., Fisher, S. K. & Anderson, D. H. (1980). Disc morphogenesis in vertebrate photoreceptors. *J Comp Neurol* **190,** 501-8.

Sun, H. & Nathans, J. (2001). ABCR, the ATP-binding cassette transporter responsible for Stargardt macular dystrophy, is an efficient target of all-trans-retinal-mediated photooxidative damage in vitro. Implications for retinal disease. *J Biol Chem* **276,** 11766-74.

Sung, C. H., Makino, C., Baylor, D. & Nathans, J. (1994). A rhodopsin gene mutation responsible for autosomal dominant retinitis pigmentosa results in a protein that is defective in localization to the photoreceptor outer segment. *J Neurosci* **14,** 5818-33.

Sung, C. H. & Tai, A. W. (2000). Rhodopsin trafficking and its role in retinal dystrophies. *Int Rev Cytol* **195,** 215-67.

Tam, B. M., Moritz, O. L., Hurd, L. B. & Papermaster, D. S. (2000). Identification of an outer segment targeting signal in the COOH terminus of rhodopsin using transgenic Xenopus laevis. *J Cell Biol* **151,** 1369-80.

Taylor, H. R., Munoz, B., West, S., Bressler, N. M., Bressler, S. B. & Rosenthal, F. S. (1990). Visible light and risk of age-related macular degeneration. *Trans Am Ophthalmol Soc* **88,** 163-73.

Taylor, H. R., West, S., Munoz, B., Rosenthal, F. S., Bressler, S. B. & Bressler, N. M. (1992). The long-term effects of visible light on the eye. *Arch Ophthalmol* **110,** 99-104.

Townes-Anderson, E., MacLeish, P. R. & Raviola, E. (1985). Rod cells dissociated from mature salamander retina: ultrastructure and uptake of horseradish peroxidase. *J Cell Biol* **100,** 175-88.

Travis, G. H., Brennan, M. B., Danielson, P. E., Kozak, C. A. & Sutcliffe, J. G. (1989). Identification of a photoreceptor-specific mRNA encoded by the gene responsible for retinal degeneration slow (rds). *Nature* **338,** 70-3.

Travis, G. H., Christerson, L., Danielson, P. E., Klisak, I., Sparkes, R. S., Hahn, L. B., Dryja, T. P. & Sutcliffe, J. G. (1991). The human retinal degeneration slow (RDS) gene: chromosome assignment and structure of the mRNA. *Genomics* **10,** 733-9.

Travis, G. H., Groshan, K. R., Lloyd, M. & Bok, D. (1992). Complete rescue of photoreceptor dysplasia and degeneration in transgenic retinal degeneration slow (rds) mice. *Neuron* **9,** 113-9.

Travis, G. H., Sutcliffe, J. G. & Bok, D. (1991). The retinal degeneration slow (rds) gene product is a photoreceptor disc membrane-associated glycoprotein. *Neuron* **6,** 61-70.

Trujillo, M. J., Bueno, J., Osorio, A., Sanz, R., Garcia-Sandoval, B., Ramos, C. & Ayuso, C. (1998). Three novel RDS-peripherin mutations (689delT, 857del17, G208D) in Spanish families affected with autosomal dominant retinal degenerations. Mutations in brief no. 147. Online. *Hum Mutat* **12,** 70.

Trujillo, M. J., Martinez-Gimeno, M., Gimenez, A., Lorda, I., Bueno, J., Garcia-Sandoval, B., Ramos, C., Carballo, M. & Ayuso, C. (2001). Two novel mutations (Y141H; C214Y) and previously published mutation (R142W) in the RDS-peripherin gene in autosomal dominant macular dystrophies in Spanish families. *Hum Mutat* **17,** 80.

Uehara, F., Ohba, N., Nakashima, Y., Yanagita, T., Ozawa, M. & Muramatsu, T. (1993). Distribution of peripherin/rds mRNA in cone-dominant squirrel retina [letter]. *Exp Eye Res* **56,** 611-3.

Wada, Y., Nakazawa, M., Kikawa, E., Chida, Y., Shiono, T. & Tamai, M. (1995). Phenotypes of patients with autosomal dominant retinal degeneration associated with Tyr184Ser and Arg172Trp mutations of the peripherin/rds gene. *Invest. Ophthalmol. Vis. Sci.* **36,** s890.

Weleber, R. G., Carr, R. E., Murphey, W. H., Sheffield, V. C. & Stone, E. M. (1993). Phenotypic variation including retinitis pigmentosa, pattern dystrophy, and fundus flavimaculatus in a single family with a deletion of codon 153 or 154 of the peripherin/RDS gene. *Arch Ophthalmol* **111,** 1531-42.

Wells, J., Wroblewski, J., Keen, J., Inglehearn, C., Jubb, C., Eckstein, A., Jay, M., Arden, G., Bhattacharya, S., Fitzke, F. & et al. (1993). Mutations in the human retinal degeneration slow (RDS) gene can cause either retinitis pigmentosa or macular dystrophy [see comments]. *Nat Genet* **3,** 213-8.

Wetzel, M. G., Parsons, S. E. & Besharse, J. C. (1994). The effect of sulfhydryl reagents on the morphogenesis of rod discs. *Invest. Ophthalmol. Vis. Sci.* **35,** 1519.

Worthington, B. C. (1993). *Worthington Enzyme Manual*, Freehold, NJ.

Wright, M. D. & Tomlinson, M. G. (1994). The ins and outs of the transmembrane 4 superfamily. *Immunol Today* **15,** 588-94.

Wrigley, J. D., Ahmed, T., Nevett, C. L. & Findlay, J. B. (2000). Peripherin/rds influences membrane vesicle morphology. Implications for retinopathies. *J Biol Chem* **275,** 13191-4.

Wu, M. & Gerhart, J. (1991). Raising Xenopus in the laboratory. *Methods Cell Biol* **36,** 3-18.

Yauch, R. L. & Hemler, M. E. (2000). Specific interactions among transmembrane 4 superfamily (TM4SF) proteins and phosphoinositide 4-kinase. *Biochem J* **351 Pt 3,** 629-37.

Yee, R. & Liebman, P. A. (1978). Light-activated phosphodiesterase of the rod outer segment. Kinetics and parameters of activation and deactivation. *J Biol Chem* **253,** 8902-9.

Young, R. W. (1976). Visual cells and the concept of renewal. *Invest Ophthalmol Vis Sci* **15,** 700-25.

Zottola, R. J., Cloherty, E. K., Coderre, P. E., Hansen, A., Hebert, D. N. & Carruthers, A. (1995). Glucose transporter function is controlled by transporter oligomeric structure. A single, intramolecular disulfide promotes GLUT1 tetramerization. *Biochemistry* **34,** 9734-47.